Title

Synthesis, Characterization, and Analysis of Molecular and Ionic Gold(I) Dimers with Diphosphine Ligands

Author

Costa, Sarah

Publication Date

2025

Peer reviewed|Thesis/dissertation

Synthesis, Characterization, and Analysis of Molecular and Ionic Gold(I) Dimers with Diphosphine Ligands

by

SARAH COSTA

DISSERTATION

Submitted in partial satisfaction of the requirements for the degree of

DOCTOR OF PHILOSOPHY

in

Chemistry

in the

OFFICE OF GRADUATE STUDIES

of the

UNIVERSITY OF CALIFORNIA

DAVIS

Approved:

_____

Alan L. Balch, Chair

_____

Philip P. Power

_____

Marie Heffern

Committee in Charge

2025

Dedication

To Sonya Costa, whose inspiration guided me into the world of science and whose unwavering support has been my constant companion. Te amo

Table of Contents

Acknowledgements

I would like to begin by expressing my deepest gratitude to my advisor, Dr. Alan L. Balch. Without your encouragement and mentorship, I would not be where I am today. Through every challenge, you have been there to guide me, instilling confidence in both my work and my worth. Whether addressing academic concerns or personal issues, you have always been there to trouble shoot with me. Your influence has profoundly shaped my approach to life. You have become such an integral part of my journey that it's hard to imagine a reality without the ability to walk to your office and share a conversation with you.

I want to extend my deepest gratitude to Dr. Marilyn Olmstead, whose stories inspire me daily. I cherish the brief moments we shared and am deeply saddened that we didn't have the chance to work more closely together. It's difficult to express my feelings without breaking into tears. Dr. Olmstead is fondly remembered as a joyful, brilliant teacher and friend. My greatest wish is to embody even a fraction of the remarkable person she was.

I would like to extend my sincere thanks to my dissertation committee, Dr. Phillip Power and Dr. Marie Heffern. Both of you were always willing to discuss chemistry and life whenever I knocked on your office doors. Dr. Power, your ability to brighten my day and encourage me to work harder was invaluable. Dr. Heffern, you demonstrated how to overcome adversity and be a supportive friend and mentor to others. I am deeply grateful for your kindness and support over the years.

To Dr. James C. Fettinger, thank you for the time you put into teaching me about crystallography and offering valuable insight in research and in learning. But in a larger capacity

you gave me valuable insight on how I work and learn from others. Working with you will always be a cherished memory.

To Dr. Bronte Charette, you inspired me profoundly at a pivotal moment in my academic journey. I will always remember the first day we met, when I asked, “How do you deal with conflict in academia?” Your refreshing response—suggesting that meetings should end with actionable steps for both parties—instilled hope in me for the future. I am deeply grateful for the opportunity to be your TA and for your support in my career, including offering me a GSR position during one of my final quarters at Davis. Your impact on my life and career is immeasurable.

I was fortunate to have worked with some great people in the Balch lab and within the department. Thank you to former and present Balch lab graduate students and undergraduates. Thank you to Lilia for being an awesome coworker and friend. You made every moment in lab better. You gave me honest feedback since the day we met on my visitation and you were one of the main reasons I joined the Balch Lab. You are one of my best friends and have been there for me without judgment. Te Amo! To Sarah Chui and Katelyn Espinoza who have inspired me in my last years here in Davis. I has been a pleasure to teach you and become your friends. You both have taught me so much.

Thank you to my dearest friend Skyler Gillette. You are one of the smartest and bravest people I know, and I strive every day to be a better friend to you. Just knowing you connected me to my partner Nate Harder, whose positivity and unconditional love made me a better person. I am incredibly excited to begin this new chapter of our lives out of grad school with our four-legged children.

I would like to thank my whole family, to all nine of us in that crazy house. To my mother whose hard work and sacrifices got me here. To Sonya my sister aunt, you inspire me every day because no matter what has been thrown your way you have been so strong. To my grandparents thank you for helping raise me to the person I have become.

Finally, I would like to acknowledge the funding agencies that have supported me through my dissertation work: the Department of Chemistry and Office of Graduate Studies at UC Davis for various fellowships and travel grants; The US National Science Foundation (Grant CHE-1807637 to A.L.B. and M.M.O.) for laboratory research and salary funding.

Abstract

This dissertation focuses on three main areas of study: (1) investigating the effects of 3-coordinate gold (I)-centered dimers with aurophilic interactions, (2) comparing these with 2-coordinate gold (I)-centered dimers in terms of their emission properties, and (3) exploring the impact of changes in the bridging ligand chain length (n), where $n \leq 3$, across different solvates and non-coordinating anions.

Chapter 1 reports that crystals of the dimer $Au_2(\mu\text{-dppe})_2I_2$ (dppe is 1,2-bis-(diphenylphosphino)ethane) have different separations between the three-coordinate gold ions, that are related to the solvent system used for crystallization. In the different solvates of $Au_2(\mu\text{-dppe})_2I_2$, the Au···Au separation varied from 3.192(1) to 3.7866(3) Å. Computational studies undertaken to understand the flexible nature of these dimers indicated that the structural differences were primarily a result of crystal packing effects with aurophillic interactions having a minimal effect.

Chapter 2 reports six salts containing the dication, $[Au_2(\mu\text{-dppe})_2]^{2+}$. The structure of the helical dication, $[Au_2(\mu\text{-dppe})_2]$, in the salts with non-coordinating anions is remarkably consistent with the Au···Au separation falling in the narrow range 2.9593(5) Å to 2.8787(9) Å. In the solid state, the six crystals display a green luminescence at room temperature and at 77 K, which has been assigned as phosphorescence. However, solutions of the dication are not luminescent. The other reported crystals are salts containing the analogous dication, $[Au_2(\mu\text{-dppp})_2]^{+2}$ (dppp is bis-(diphenylphosphine)propane). None of these crystals are luminescent, but all contain two nearly

parallel, linear P-Au-P groups and a long separation between the gold ions that varies from 5.6613(6) to 5.3409(4) Å.

Chapter 3 reports five new crystalline gold(I) complexes $Au_2(\mu\text{-dppm})_2X_n$•solvate, where dppm is bis-(diphenylphosphino)methane) and X=Br or Cl, that have been prepared and structurally characterized by single crystal X-ray diffraction. Colorless crystals of β-$Au_2(\mu\text{-dppm})_2Br_2$•$2CH_2Cl_2$ have a centrosymmetric structure with two three-coordinate gold(I) ions held in close proximity by the dppm ligands. Crystals of $[Au_2(\mu\text{-dppm})_2Br]Br$•$2CH_2Cl_2$, $[Au_2(\mu\text{-dppm})_2Br](PF_6)$, and $[Au_2(\mu\text{-dppm})_2Cl](BPh_4)$•$3CH_2Cl_2$ anion each have a cation with an unusual arrangement that binds a two-coordinate gold(I) ion to a three-coordinate gold(I) ion through an aurophilic interaction, or has an ion paired chloride ion that is symmetrically disposed between the two gold ions at a rather long distance. Each complex displays luminescence under UV irradiation.

Chapter 4 reports four that the new crystalline gold(I) complexes $[Au_2(\mu\text{-dppm})_2(\mu\text{-I})]X$ and $[Au_2(\mu\text{-dppm})_2](X)_2$, where dppm is bis-(diphenylphosphino)methane) and X^- is I^-, PF_6^-, or AsF_6^-, have been prepared and structurally characterized by single crystal X-ray diffraction and nuclear magnetic resonance. Yellow crystals of $[Au_2(\mu\text{-dppm})_2(\mu\text{-I})]X$ have a structure with two three-coordinate gold(I) ions held in close proximity by the dppm and bridging iodide ligands Yellow crystals of $[Au_2(\mu\text{-dppm})_2(\mu\text{-I})]I$•$2CH_2Cl_2$ and $[Au_2(\mu\text{-dppm})_2(\mu\text{-I})](PF_6)$•$CH_2Cl_2$ have a structure with two three-coordinate gold(I) ions held in close proximity by the dppm and bridging iodide ligands. Crystals of $[Au_2(\mu\text{-dppm})_2I][Au_2(\mu\text{-dppm})_2(\mu\text{-I})](AsF_6)_4$•$4CH_2Cl_2$ have two different cations: one similar to the preceding complexes and the other cation with a terminal iodide ligand in an unusual arrangement that binds a two-coordinate gold(I) ion to a three-coordinate gold(I) ion through an aurophilic interaction. In contrast, $[Au_2(\mu\text{-}$

dppm)$_2$](AsF_6)$_2$•CH_2Cl_2 has no anion bound and only has the gold ions as two-coordinate centers. Each complex displays luminescence under UV irradiation in solid and solution state. The NMR spectra of solutions of the iodide complexes suggest that the iodide ion is bound to the [Au_2(μ-dppm)$_2$]$^{2+}$ core but is able to circulate around this core.

Introduction

Gold (I) complexes have been investigated for their biological, biochemical, electronic, catalytic, and optical uses.[1] One of the key reasons for their study is the phenomenon of aurophilic interactions—weak, yet significant, attractive forces between gold(I) atoms arising from relativistic and correlation effects.[2–4] Relativistic effects are the result of the velocity of electrons approaching the speed of light, which leads to the contraction of the radial size.[5] In gold (I) atoms relativistic effects cause the s and p orbital contraction, spin-orbit coupling, and d orbital expansion.

Figure 1 shows a molecular orbital (MO) diagram for the association of two 2-coordinate gold(I) complexes along the z axis. The MO diagram shows that the association of two gold (I) complexes leads to the stabilization of the filled d_z^2 and empty p_z orbitals along the Au(I)···Au(I) interaction.[6,7] This interaction stabilizes the self-association between two gold (I) complexes at distances ranging from 2.8 to 3.6 Å.[2,3,8–11] These interactions are stronger than hydrogen bonding but weaker than a covalent bond. Under excitation, the promotion of an electron into the empty p_z orbital, followed by relaxation into a triplet state leads to the release of a photon, as seen in Figure 1B. [6,9,13–20] The relaxation mode correlated to the complexes mentioned in this dissertation and model in Figure 1B are phosphorescence with lifetimes within the microsecond scale.[21]

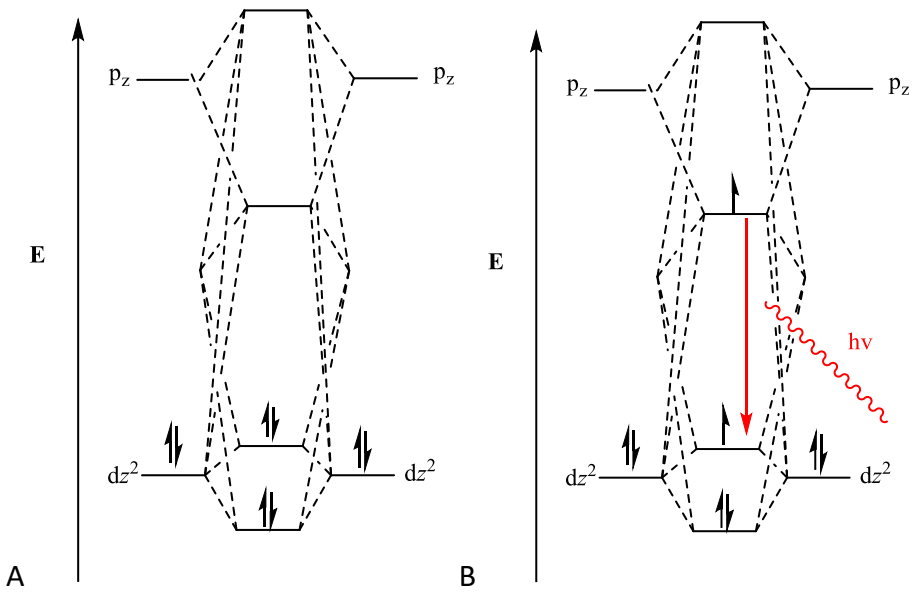

Figure 1: A, Molecular orbital diagram of Au(I)···Au(I) with relativistic effects. B, Molecular orbital diagram showing the emissive first excited triplet

Short bidentate phosphine ligand have commonly reacted with Au (I), leading to a variety of unique structures.[2] Gold (I) complexes prefer a 1:1 ratio of gold atoms to these bidentate ligands.[2] One of the most notable structures is the $[M_2((C_6H_5)_2P(CH_2)_nP(C_6H_5)_2)]^{2+}$, as seen in figure 2A, with Au(I) can contain an aurophilic interaction.[2,10,21–23] These 2-coordinate gold (I) dimers typically prefer inter- vs intra- molecular interactions between gold(I) ions, due to the bulky phenyl substituents that protrude from the dimer.[2] The conjunction of inter-molecular and aurophilic interactions leads to a host of luminescent properties dependent on solvates, gases, and non-coordinating anions.[10,21,22,24–27]

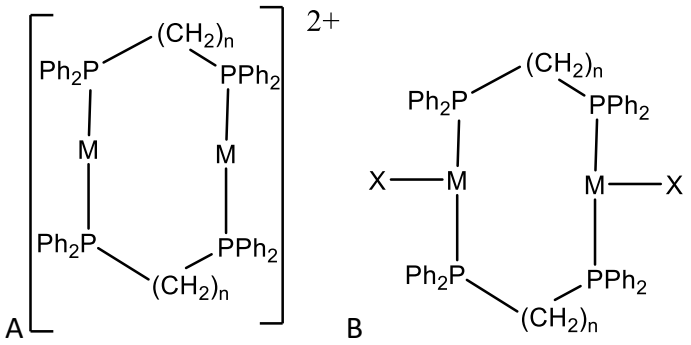

Figure 2: A, A drawing of a short bridging phosphine ligand connecting two 2-coordinate metal ions a dimeric form, $[M_2((C_6H_5)_2P(CH_2)_nP(C_6H_5)_2)]^{2+}$. B, A drawing of a short bridging phosphine ligand connecting two 3-coordinate metal ions into a dimeric form, $[M_2((C_6H_5)_2P(CH_2)_nP(C_6H_5)_2)X_2]$.

There is an alternative to the cationic structure, the molecular dimer with coordinating anions bonded to the metal centers shown in Figure 2B. For $Au_2(\mu\text{-}Ph_2P(CH_2)_nPPh_2)_2I_2$ where *n* =3 or greater, there are no aurophilic interactions present; however, all the complexes are emissive.[28] This luminescence is due to the three coordinate metal center excitation process involves a transition from $d_{x^2\text{-}y^2}$ and d_{xy} orbital to an empty p_z orbital.[7,10,20,29–32]

Three coordinate gold (I) complexes with aurophilic interactions have more interesting luminescence due to the dual excitation pathways.[22,23,33] Typically the 3-coordinate dimers have Au(1)···Au(I) distances that range from 3.2 to 3.8 Å and are heavily dependent on solvate or anion interactions.[7,10,20,29–32] Many 3-coordinate Au(I) dimers have the gold(I) ions widely spaced as seen in the dppp (diphenylphospinopropane) modelPThe reported structure of polymorphs α- and β- $Au_2(\mu\text{-dppe})_2I_2\bullet(CH_3)_2CO$ contains an aurophilic interaction between two three-coordinate centers.[23] These polymorphs have vapochromic properties allowing a reversible exchange between the polymorphs, cataloged by changes in emission.

An analogous compound, $Au_2(\mu\text{-}Ph_2P(CH_2)_nPPh_2)_2X_2$ (X = Cl, Br), where n = 1, has been reported in various crystal forms containing a three-coordinate gold(I) center with an aurophilic interaction. A notable example is $Au_2(\mu\text{-}dppm)_2Br_2{\bullet}CH_2Cl_2$ (dppm = diphenylphosphinomethane), where the aurophilic interaction is particularly short, at 3.015(2) Å. However, there has been minimal discussion on the impact of this bonding on emission properties. This gap in the field highlights the need for further investigations to better understand how 3-coordinate gold(I) centers with aurophilic interactions affect excitation pathways.

Another interesting and unique property of $M_2(\mu\text{-}dppm)_2^{+2}$ cations is the production of A-frames.[37–42] A-frames are binuclear complexes contain two bridging bidentate ligands and a single-atom bridge between metal atoms. Most metal centers undergoing A-frame conformations are square-planar metal centers Rh, Ir, Ni, Pd, Pt, and Au.[43] This A-frame structure with both aurophilic and three coordination could lead to novel emission and properties. Previous work encountering a similar Au(I) A-frame structure has provided limited information on luminescent properties.[44–48]

The $Au_2(dppm)_2^{2+}$ cation has major four coordination types, seen in Figure 3: the first completely molecular, next the A-frame, following the A-frame like, and lastly the completely ionic structures.[32,44–64] Only one of these studies reports luminescence due to aurophilicity or three coordinate gold centers which are not bonded to another metal. The Konno et al. group analyzed trigonal-planar di-gold(I) centers systems, $[Au_2(dppm)_3]^{2+}$, and the two coordinate di-gold(I) centers system $[Au_2(dppm)_2]^{2+}$.[53] These structures had unique emission in the solid state undergoing; thermochromic, solvachromic, and mechanochromic changes.

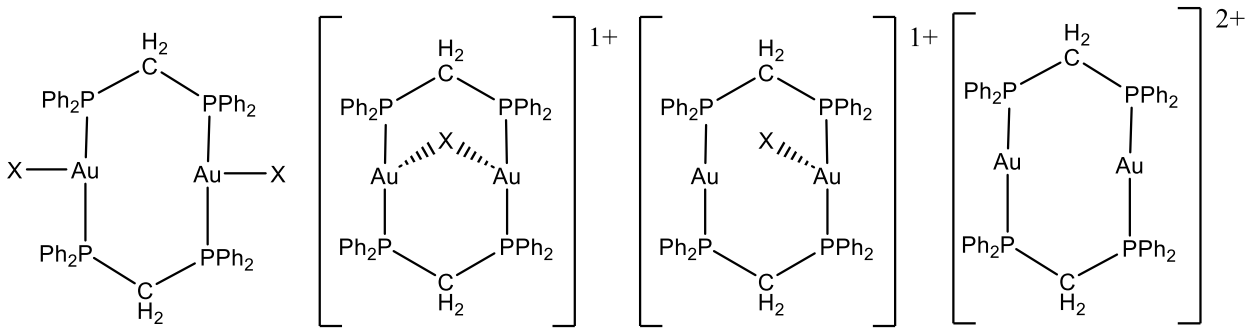

Figure 3: Types of bonding dimers with the dppm ligands ranging from molecular to cationic structures. The first ionic structure is the A-frame structure, the next is the A-frame like, and the last is the completely ionic complex with no coordinating halide.

This dissertation aims to investigate the effects of 3-coordinate dimers with aurophilic interactions compared to 2-coordinate dimers on emission properties, exploring various solvates, non-coordinating anions, and changes in *n* when less than or equal to 3.

References

(1) Hristova, Y. R.; Kemper, B.; Besenius, P. Water-Soluble Au(I) Complexes, Their Synthesis and Applications. *Tetrahedron* **2013**, *69* (49), 10525–10533.

(2) Schmidbaur, H.; Schier, A. A Briefing on Aurophilicity. *Chem. Soc. Rev.* **2008**, *37* (9), 1931–1951.

(3) Balch, A. L. Dynamic Crystals: Visually Detected Mechanochemical Changes in the Luminescence of Gold and Other Transition-Metal Complexes. *Angew. Chemie Int. Ed.* **2009**, *48* (15), 2641–2644.

(4) Pyykkö, P. Theoretical Chemistry of Gold. *Angew. Chem. Int. Ed. Engl.* **2004**, *43* (34), 4412–4456.

(5) Schmidbaur, H. The Fascinating Implications of New Results in Gold Chemistry. *Gold Bull.* **1990**, *23* (1), 11–21.

(6) Balch, A. L. Remarkable Luminescence Behaviors and Structural Variations of Two-CoordinateGold(I) Complexes BT - Photofunctional Transition Metal Complexes; Yam, V. W. W., Ed.; Springer Berlin Heidelberg: Berlin, Heidelberg, 2007; pp 1–40.

(7) Barakat, K. A.; Cundari, T. R.; Omary, M. A. Jahn-Teller Distortion in the Phosphorescent Excited State of Three-Coordinate Au(I) Phosphine Complexes. *J. Am. Chem. Soc.* **2003**, *125* (47), 14228–14229.

(8) Schmidbaur, H. Ludwig Mond Lecture. High-Carat Gold Compounds. *Chem. Soc. Rev.* **1995**, *24* (6), 391–400.

(9) He, X.; Yam, V. W. W. Luminescent Gold(I) Complexes for Chemosensing. *Coord. Chem. Rev.* **2011**, *255* (17–18), 2111–2123.

(10) Costa, S.; Walters, D. T.; McNamara, L. E.; Olmstead, M. M.; Fettinger, J. C.; Balch, A. L. Structure and Luminescence Studies of Salts of the Helical Dication, $[Au_2(\mu\text{-Bis(Diphenylphosphine)Ethane})_2]^{2+}$ and Comparison with Salts of $[Au_2(\mu\text{-Bis(Diphenylphosphine)Propane})_2]^{2+}$. *Inorg. Chem.* **2023**, *62* (39), 15902–15911.

(11) Olmstead, M. M.; Jiang, F.; Attar, S.; Balch, A. L. Alteration of the Aurophilic Interactions in Trimeric Gold(I) Compounds through Charge Transfer. Behavior of Solvoluminescent Au3(MeN=COMe)3 in the Presence of Electron Acceptors. *J. Am. Chem. Soc.* **2001**, *123* (14),

3260–3267.

(12) Pawlędzio, S.; Malinska, M.; Kleemiss, F.; Grabowsky, S.; Woźniak, K. Aurophilic Interactions Studied by Quantum Crystallography. *Inorg. Chem.* **2022**, *61* (10), 4235–4239.

(13) Mirzadeh, N.; Privér, S. H.; Blake, A. J.; Schmidbaur, H.; Bhargava, S. K. Innovative Molecular Design Strategies in Materials Science Following the Aurophilicity Concept. *Chem. Rev.* **2020**, *120* (15), 7551–7591.

(14) Pyykkö, P. Strong Closed-Shell Interactions in Inorganic Chemistry. *Chem. Rev.* **1997**, *97* (3), 597–636.

(15) Pyykkö, P.; Li, J.; Runeberg, N. Predicted Ligand Dependence of the Au(I)…Au(I) Attraction in (XAuPH3)2. *Chem. Phys. Lett.* **1994**, *218* (1–2), 133–138.

(16) Schmidbaur, H.; Schier, A. Aurophilic Interactions as a Subject of Current Research: An up-Date. *Chem. Soc. Rev.* **2011**, *41* (1), 370–412.

(17) Lin, J. C. Y.; Tang, S. S.; Sekhar Vasam, C.; You, W. C.; Ho, T. W.; Huang, C. H.; Sun, B. J.; Huang, C. Y.; Lee, C. S.; Hwang, W. S.; Chang, A. H. H.; Lin, I. J. B. Structural, Photophysical, and Catalytic Properties of Au(I) Complexes with 4-Substituted Pyridines. *Inorg. Chem.* **2008**, *47* (7), 2543–2551.

(18) Yam, V. W. W.; Au, V. K. M.; Leung, S. Y. L. Light-Emitting Self-Assembled Materials Based on d^8 and d^{10} Transition Metal Complexes. *Chem. Rev.* **2015**, *115* (15), 7589–7728.

(19) White-Morris, R. L.; Olmstead, M. M.; Balch, A. L.; Elbjeirami, O.; Omary, M. A. Orange Luminescence and Structural Properties of Three Isostructural Halocyclohexylisonitrilegold(I) Complexes. *Inorg. Chem.* **2003**, *42* (21), 6741–6748.

(20) Walters, D. T.; England, K. R.; Ghiassi, K. B.; Semma, F. Z.; Olmstead, M. M.; Balch, A. L. Steric Effects and Aurophilic Interactions in Crystals of Au_2(μ-1,2-Bis(Diphenylphosphino)Ethane)X_2 and Au_2(μ-1,2-Bis(Dicyclohexylphosphino)Ethane)X_2 (X = Cl, Br, I). *Polyhedron* **2016**, *117*, 535–541.

(21) Costa, S.; Aristov, M. M.; Lim, S. H.; Chui, S. M.; Espinoza, K. A.; Olmstead, M. M.; Fettinger, J. C.; Berry, J. F.; Balch, A. L. Molecular Flexibility in Solvated Crystals of the Dimer, Au_2(μ-1,2-Bis(Diphenylphosphino)Ethane)$_2I_2$, with Three-Coordinate Gold(I). *Inorg. Chem.* **2024**, *21*, 4.

(22) Lim, S. H.; Olmstead, M. M.; Balch, A. L. Inorganic Topochemistry. Vapor-Induced Solid State

Transformations of Luminescent, Three-Coordinate Gold(I) Complexes. *Chem. Sci.* **2012**, *4* (1), 311–318.

(23) Lim, S. H.; Olmstead, M. M.; Balch, A. L. Molecular Accordion: Vapoluminescence and Molecular Flexibility in the Orange and Green Luminescent Crystals of the Dimer, Au_2(μ-Bis-(Diphenylphosphino)Ethane)$_2Br_2$. *J. Am. Chem. Soc.* **2011**, *133* (26), 10229–10238.

(24) Walters, D. T.; Aristov, M. M.; Babadi Aghakhanpour, R.; SantaLucia, D. J.; Costa, S.; McNamara, L. E.; Olmstead, M. M.; Berry, J. F.; Balch, A. L. Self-Assembled Encapsulation of CuX^{2-} (X = Br, Cl) in a Gold Phosphine Box-like Cavity with Metallophilic Au-Cu Interactions. *Inorg. Chem.* **2023**, *62* (11), 4467–4475.

(25) Luong, L. M. C.; Olmstead, M. M.; Balch, A. L. A Non-Luminescent Polymorph of [(Cyclohexyl Isocyanide)$_2$Au]PF_6 That Becomes Luminescent upon Grinding or Exposure to Dichloromethane Vapor. *Chem. Commun.* **2021**, *57* (6), 793–796.

(26) Luong, L. M. C.; Malwitz, M. A.; Moshayedi, V.; Olmstead, M. M.; Balch, A. L. Role of Anions and Mixtures of Anions on the Thermochromism, Vapochromism, and Polymorph Formation of Luminescent Crystals of a Single Cation, $[(C_6H_{11}NC)_2Au]^+$. *J. Am. Chem. Soc.* **2020**, *142* (12), 5689–5701.

(27) Luong, L. M. C.; Lowe, C. D.; Adams, A. V.; Moshayedi, V.; Olmstead, M. M.; Balch, A. L. Seeing Luminescence Appear as Crystals Crumble. Isolation and Subsequent Self-Association of Individual $[(C_6H_{11}NC)_2Au]^+$ Ions in Crystals. *Chem. Sci.* **2020**, *11* (43), 11705–11713.

(28) Lim, S. H.; Schmitt, J. C.; Shearer, J.; Jia, J.; Olmstead, M. M.; Fettinger, J. C.; Balch, A. L. Crystallographic and Computational Studies of Luminescent, Binuclear Gold(I) Complexes, $AuI_2(Ph_2P(CH_2)NPPh_2)_2I_2$ (n = 3-6). *Inorg. Chem.* **2013**, *52* (2), 823–831.

(29) Sinha, P.; Wilson, A. K.; Omary, M. A. Beyond a T-Shape. *J. Am. Chem. Soc.* **2005**, *127* (36), 12488–12489.

(30) Schmidbaur, H. Gold Chemistry Is Different. **1992**, *17* (3), 213–220.

(31) Assefa, Z.; McBurnett, B. G.; Staples, R. J.; Fackler, J. P.; Assmann, B.; Angermaier, K.; Schmidbaur, H. Syntheses, Structures, and Spectroscopic Properties of Gold(I) Complexes of 1,3,5-Triaza-7-Phosphaadamantane (TPA). Correlation of the Supramolecular Au.Cntdot. .Cntdot. .Cntdot.Au Interaction and Photoluminescence for the Species (TPA)AuCl and [(TPA-HCl). *Inorg. Chem.* **1995**, *34* (1), 75–83.

(32) McCleskey, T. M.; Winkler, J. R.; Gray, H. B. Bimolecular Electron Transfer at High Driving Forces. Photoreactions of Gold(I) and Iridium(I) Complexes with Pyridinium Derivatives. *Inorganica Chim. Acta* **1994**, *225* (1–2), 319–322.

(33) Walters, D. T.; Powers, X. B.; Olmstead, M. M.; Balch, A. L. The Preparation of Luminescent, Mechanochromic Molecular Containers from Non-Emissive Components: The Box Cations, $[Au_6(Triphos)_4Br]^{5+}$ and $[Au_6(Triphos)_4Br_2]^{4+}$. *Chem. – A Eur. J.* **2019**, *25* (15), 3849–3857.

(34) SHAIN, J.; FACKLER, J. P. J. First Example of a Gold Bis(Diphenylphosphino)Methane Cationic Dimer with a Bridging Iodide. X-Ray Crystal Structures of $(\mu\text{-I})(Au(Dppm))_2(I)$ and $(Au(Dppm)Br)_2$. *ChemInform* **1987**, *18* (51).

(35) Wang, J. C.; Khan, M. N. I.; Fackler Jnr, J. P. Structure of Bis(Tetraphenyldiphosphinomethane)Digold(I) Dinitrate. *0108-2701* **1989**, *45* (10), 1482–1485.

(36) Chen, X.-Y.; Zhou, X.; Wang, J.; Dong, G. FMPhos: Expanding the Catalytic Capacity of Small-Bite-Angle Bisphosphine Ligands in Regioselective Alkene Hydrofunctionalizations. **2020**, *10*, 14349–14358.

(37) Olmstead, M. M.; Hope, H.; Balch, A. L. Insertion of Isocyanides and Carbon Monoxide into Metal-Metal Bonds. Preparation and Structure of $[Pd_2(CNCH_3)_3[(C_6H_5)_2PCH_2P(C_6H_5)_2]_2][PF_6]_2$. *J. Am. Chem. Soc.* **1977**, *99* (16), 5502–5503.

(38) Bo, C.; Costas, M.; Poblet, J. M.; Rohmer, M. M.; Benard, M. Electronic Structure of $Rh_2(MCO)(CO)_2(H_2PCH_2Ph_2)_2$. An Example of a Non-a-Frame Structure. *Inorg. Chem.* **1996**, *35* (11), 3298–3306.

(39) Hoffman, D. M.; Hoffmann, R. A-Frames. *Inorg. Chem.* **1981**, *20* (10), 3543–3555.

(40) Kubiak, C. P.; Eisenberg, R. Binuclear Rhodium(I) Complexes. Molecular A Frames. *J. Am. Chem. Soc.* **1977**, *99* (18), 6129–6131.

(41) Puddephatt, R. J.; Azam, K. A.; Hill, R. H.; Brown, M. P.; Charles Nelson, lb D.; Roger Moulding, lb P.; Seddon, K. R.; Grosselld, M. C.; J Chem Soc, M. A. Mechanisms of "A"-Frame Inversion for Binuclear Platinum(II) Complexes with Bis(Diphenylphosphino)Methane Ligands. *Homog. Catal. with Met. Phosphine Complexes* **1983**, *105* (3), 1374.

(42) Puddephatt, R. J. Chemistry of Bis(Dipheny1phosphino)Methane.

(43) Billig, E.; Williams, R.; Bernal, I.; Waters, J. H.; Gray, H. B. The Electronic Structures of Square-

Planar Metal Complexes. II. The Complexes of Maleonitriledithiolate with Copper(II), Nickel(II), Palladium(II), and Platinum(II). *Inorg. Chem.* **1964**, *3* (5), 663–666.

(44) Liou, L.-S.; Liu, C.-P.; Wang, J.-C. The Monoclinic Phase [Au2(C25H22P2)2]Cl2.2CH3CN. *0108-2701* **1994**, *50* (4), 538–540..

(45) Bauer, A.; Schmidbaur, H. Bis- and Tris-(Trichlorogermyl)Gold(I) Anions in Their Salts with Cyclic Dications $[Au_2(Ph_2PCH_2PPh_2)_2]^{2+}$ and $[Au_2(Ph_2PCH_2CH_2PPh_2)_2]^{2+}$. *J. Chem. Soc. Dalt. Trans.* **1997**, *0* (7), 1115–1116.

(46) Paul, M.; Schmidbaur, H. Coordination Chemistry of Dimethylgold Halides with Bidentate Phosphorus and Arsenic Ligands – Revisited. *Chem. Ber.* **1996**, *129* (1), 77–83.

(47) Bruce, M. I.; Jevric, M.; Skelton, B. W.; Smith, M. E.; White, A. H.; Zaitseva, N. N. Syntheses and Molecular Structures of Some Phosphine–Gold(I) Derivatives of 1,3-Diynes. *J. Organomet. Chem.* **2006**, *691* (3), 361–370.

(48) Khan, M. N. I.; King, C.; Heinrich, D. D.; Fackler, J. P.; Porter, L. C. Syntheses and Crystal Structures (No Au-H Interactions) of Luminescent $[Au_2(Dppm)_2][BH_3CN]_2$and of $[Au_2(Dppm)_2(I)][Au(CN)_2]$ and $[Au_2(Dppm)_2(S_2CNEt_2)][BH_3CN]$. *Inorg. Chem.* **1989**, *28* (11), 2150–2154.

(49) Kaub, C.; Augenstein, T.; Bauer, T. O.; Rothe, E.; Esmezjan, L.; Schünemann, V.; Roesky, P. W. High-Coordinate Gold(I) Complexes with Dithiocarboxylate Ligands. *Inorg. Chem.* **2014**, *53* (9), 4491–4499.

(50) Liou, L.-S.; Liu, C.-P.; Wang, J.-C. The Monoclinic Phase $[Au_2(C_{25}H_{22}P_2)_2]Cl_2{\cdot}2CH_3CN$. *0108-2701* **1994**, *50* (4), 538–540.

(51) Wu, M.; Zhang, L.; Chen, Z. Bis[μ-Bis(Diphenylphosphino)Methane]-Digold(I) Bis(Hexafluorophosphate) Dichloromethane Disolvate. *Acta Crystallogr. Sect. E Struct. Reports Online* **2003**, *59* (2), m72–m73.

(52) Cao, Q. Y.; Yin, B.; Liu, J. H. Bis[μ-Bis(Diphenylphosphino)Methane-K2P:P′] -Digold(I) Bis(Perchlorate). *Acta Crystallogr. Sect. E Struct. Reports Online* **2006**, *62* (10), m2730–m2731.

(53) Igawa, K.; Yoshinari, N.; Okumura, M.; Ohtsu, H.; Kawano, M.; Konno, T. Crystalline-Amorphous-Crystalline Transformation in a Highly Brilliant Luminescent System with Trigonal-Planar Gold(I) Centers. *Sci. Reports 2016 61* **2016**, *6* (1), 1–8.

(54) King, C.; Wang, J. chun; Khan, M. N. I.; Fackler, J. P. Luminescence and Metal-Metal Interactions in Binuclear Gold Compounds. *Inorg. Chem.* **1989**, *28* (11), 2145–2149.

(55) Schmidbaur, H.; Wohlleben, A.; Schubert, U.; Frank, A.; Huttner, G. Gold-Komplexe von Diphosphinomethanen, II. Synthese Und Kristallstruktur Achtgliedriger Ringverbindungen von Gold(I) Mit Au–Au-Wechselwirkung. *Chem. Ber.* **1977**, *110* (8), 2751–2757.

(56) Bauer, A.; Schmidbaur, H. Bis- and Tris-(Trichlorogermyl)Gold(I) Anions in Their Salts with Cyclic Dications$[Au_2(Ph_2PCH_2PPh_2)_2]^{2+}$ and$[Au_2(Ph_2PCH_2CH_2PPh_2)_2]^{2+}$. *J. Chem. Soc. Dalt. Trans.* **1997**, *8* (7), 1115–1116.

(57) Gruber, F.; Jansen, M. Salt-like Structures of Oligomeric Gold Complexes and Polyoxometalates. *Zeitschrift fur Anorg. und Allg. Chemie* **2010**, *636* (13–14), 2352–2356.

(58) Maspero, A.; Kani, I.; Mohamed, A. A.; Omary, M. A.; Staples, R. J.; Fackler, J. P. Syntheses and Structures of Dinuclear Gold(I) Dithiophosphonate Complexes and the Reaction of the Dithiophosphonate Complexes with Phosphines: Diverse Coordination Types. *Inorg. Chem.* **2003**, *42* (17), 5311–5319.

(59) Kobayashi, R.; Yumura, T.; Imoto, H.; Naka, K.; Li, R. Homo- and Hetero-Metallophilicity-Driven Synthesis of Highly Emissive and Stimuli-Responsive Au(I)–Cu(I) Double Salts. *Chem. Commun.* **2021**, *57* (44), 5382–5385.

(60) Yeo, C. I.; Tan, Y. S.; Tiekink, E. R. T. Crystal Structure of Bis[μ-Bis(Diphenylphosphanyl)-Methane-$\supseteq_2$P:P']Digold(I) Dichloride Acetone Monosolvate Monohydrate. *Acta Crystallogr. Sect. E Crystallogr. Commun.* **2015**, *71* (8), 937–940.

(61) Costa, S.; Chui, S. M.; Espinoza, K. A.; Olmstead, M. M.; Fettinger, J. C.; Balch, A. L. Bridging 1,2-Bis-(diphenylphosphino)methane Ligands Facilitate the Formation of Binuclear Complexes with Both Two-Coordinate and Three-Coordinate Gold(I) Ions. *Inorg. Chem.* **2024**, *63* (52), 24563–24572.

(62) Costa, S.; Chui, S. M.; Espinoza, K. A.; Olmstead, M. M.; Fettinger, J. C.; Balch, A. L. A Molecular Planetarium: Evidence for an Iodide Ligand Orbiting two Gold (I) Ions in $[Au_2$(μ-1,2 Bis-(diphenylphosphino)methane$)_2I]^+$. *In Submission.* **2025.**

(63) Wang, J.-C.; Liu, L.-K. $[Au_2(C_6H_5CS_2)$(μ-Dppm$)_2]$Cl.:*0108-2701* **1994**, *50* (5), 704–706.

(64) Porter, L. C.; Khan, M. N. I.; King, C.; Fackler, J. P. Structure of the

Bis[Bis(Diphenylphosphino)Methane]Digold(I) Cation in $[Au_2(Dppm)_2](BF_4)_2$. *0108-2701* **1989**, *45* (6), 947–949.

Chapter 1

Molecular Flexibility in Solvated Crystals of the Dimer, Au_2 (μ-1,2-bis-(diphenylphosphino)ethane)$_2I_2$, with Three-Coordinate Gold(I) †

† Reprinted in part with permission from (1) Costa, S.; Aristov, M. M.; Lim, S. H.; Chui, S. M.; Espinoza, K. A.; Olmstead, M. M.; Fettinger, J. C.; Berry, J. F.; Balch, A. L. Molecular Flexibility in Solvated Crystals of the Dimer, Au2(μ-1,2-Bis(Diphenylphosphino)Ethane)$_2I_2$, with Three-Coordinate Gold(I). Inorg. Chem. 2024, 21, 4. https://pubs.acs.org/doi/full/10.1021/acs.inorgchem.4c00783.

Abstract

We report the ability to trap the dimer $Au_2(\mu\text{-dppe})_2I_2$ (dppe is 1,2-bis-(diphenylphosphino)ethane) with different separations between the three-coordinate gold ions in crystalline solvates. All of these solvates ($(Au_2(\mu\text{-dppe})_2I_2\bullet 4(CH_2Cl_2)$ (**1**), $Au_2(\mu\text{-dppe})_2I_2\bullet 2(CH_2Cl_2)$ (**2**) the polymorphs $\alpha\text{-}Au_2(\mu\text{-dppe})_2I_2\cdot 2(HC(O)NMe_2)$ (**3**) and $\beta\text{-}Au_2(\mu\text{-dppe})_2I_2\cdot 2(HC(O)NMe_2)$ (**4**) and $Au_2(\mu\text{-dppe})_2I_2\cdot 4(CHCl_3)$ (**5**) along with polymeric $\{Au(\mu\text{-dppe})I\}_n\cdot n(CHCl_3)$ (**6**) originated from the same reaction, only the solvent system used for crystallization differed. In the different solvates of $Au_2(\mu\text{-dppe})_2I_2$, the Au···Au separation varied from 3.192(1) to 3.7866(3) Å. Computational studies undertaken to understand the flexible nature of these dimers indicated that the structural differences were primarily a result of crystal packing effects with aurophillic interactions having a minimal effect.

Introduction

Diphosphine ligands have been used to prepare a range of binuclear, polynuclear and polymeric metal complexes.[1,2] In particular, ligands of the type $R_2P(CH_2)_nPR_2$, have been used to form binuclear, macrocyclic complexes with an $M_2(\mu\text{-}R_2P(CH_2)_nR_2)_2$ core with varying distances between the metal ions. When n is 1, the ligand places the metal centers in close proximity and facilitates bonding between these metal centers.[3,4] When n is three or more, the metal centers are generally widely separated and not directly interacting with one another.[5-11] However, when n is 2 the bridging ligand can accommodate a range of separations between the metal centers.[9,12,13]

The remarkable flexibility of the bridging diphosphine ligand 1,2-bis(diphenyl)phosphinoethane (dppe) in the dimers $Au_2(\mu\text{-dppe})_2I_2$ and $Au_2(\mu\text{-dppe})_2Br_2$ produced solvated crystals with varying Au···Au separations and some unusual luminescent

properties.[12,13] Scheme 1 shows the behavior of crystals containing the dimer $Au_2(\mu\text{-dppe})_2I_2$ and related compounds.[13] The two polymorphs of the acetone solvate $Au_2(\mu\text{-dppe})_2I_2\cdot 2(OCMe_2)$ exhibit different luminescence and different separations between the planar, three-coordinate gold ions. Upon brief exposure to air, the orange luminescent α-polymorph with an Au···Au distance of 3.6720(2) Å was converted into the green luminescent β-polymorph with an Au···Au distance of 3.3955(3) Å. This process could be reversed by exposure of the crystals to acetone vapor. However, upon prolonged standing in air the β-polymorph lost acetone to form a green luminescent powder that was converted into orange luminescent $Au_2(\mu\text{-dppe})_2(\mu\text{-I})_2$ upon exposure to acetone vapor. Crystals containing the dimer $Au_2(\mu\text{-dppe})_2Br_2$ also displayed a range of Au···Au distances that extended from 3.0943(2) to 3.8479(3) Å and displayed varying luminescence: green when the Au···Au distance was less than 3.5 Å, orange when it was greater than 3.5 Å.[12] Even shorter Au···Au distances (in the range 2.8787(9) to 2.9593(5) Å) occur in the cationic dimers, $[Au_2(\mu\text{-dppe})_2]^{2+}$, which involve two-coordinate, rather than three-coordinate gold(I) ions.[11,14]

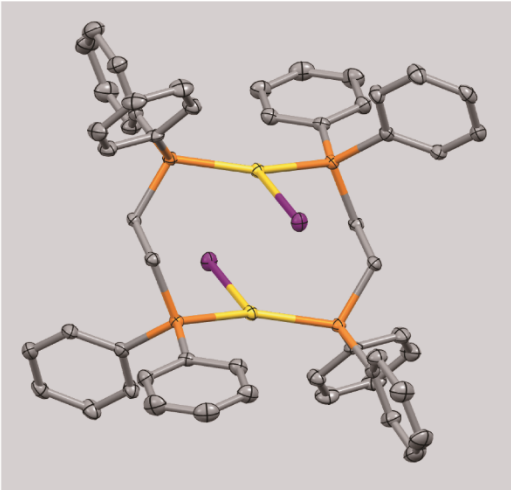

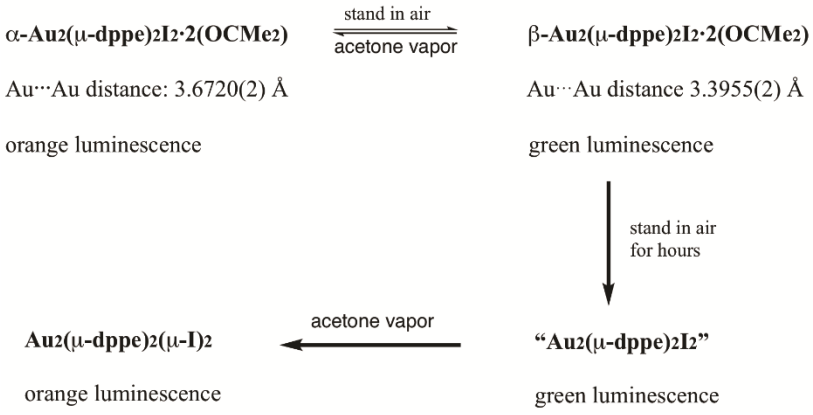

Scheme 1. Crystal transformations of the polymorphs of $Au_2(\mu\text{-dppe})_2I_2\cdot 2(OCMe_2)$ and related compounds from data in ref. 13.

The variation in the Au···Au distances in the solvates of $Au_2(\mu\text{-dppe})_2I_2$ and $Au_2(\mu\text{-dppe})_2Br_2$ suggested that aurophilic interactions between the two gold ions might influence the structure and luminescence of the crystals. Aurophilic interactions between closed shell d^{10} Au(I) ions occur when there are short distances between adjacent gold(I) ions and involve mixing of the filled 5d orbitals with the empty 6s and 6p gold orbitals.[15,16] Such interactions are particularly prevelant in two-coordinate gold(I) complexes[17] and are likely to occur when the Au···Au separation is shorter than the distance of about 3.6 Å expected from simple van der Waals factors.

Here we report the structures and luminescent behavior of new crystalline solvates of $Au_2(\mu\text{-dppe})_2I_2$ along with computational studies designed to understand the factors responsible for the variations in Au···Au distances in these crystals.

Results and Discussion

Preparation and Crystal Growth. Addition of dppe to a slurry of solid AuI in acetone or dichloromethane produced a colorless solution, which yielded a colorless solid upon evaporation. This colorless solid was crystallized from three different solvents to yield pairs of crystalline compounds as outlined below. Crystal data for the six compounds are set out in Table 1. Significant interatomic distances and angles are given in Table 2.

Table 1. Crystal Data and Data Collection Parameters

	$Au_2(\mu\text{-dppe})_2I_2 \cdot 4(CH_2Cl_2)$ (**1**)	$Au_2(\mu\text{-dppe})_2I_2 \cdot 2(CH_2Cl_2)$ (**2**)	$\alpha\text{-}Au_2(\mu\text{-dppe})_2I_2 \cdot 2(HC(O)NMe_2)$ (**3**)
Formula	$C_{56}H_{56}Au_2Cl_8I_2P_4$	$C_{54}H_{52}Au_2Cl_4I_2P_4$	$C_{58}H_{62}Au_2I_2NOP_4$
Formula weight	1784.22	1614.37	1590.72
T, K	100.15	100(2)	90(2) K
Color and Habit	Colorless block	Colorless block	Colorless plate
Crystal system	Monoclinic	Monoclinic	Triclinic
Space group	$P2_1/c$	$P2_1/c$	P-1
a, Å	13.539(4)	10.7304(4)	11.9418(5)
b, Å	22.002(7)	22.6930(8)	12.0967(5)
c, Å	10.801(4)	11.9931(4)	12.5362(5)
α, deg	90	90	63.892(2)
β, deg	110.057(14)	108.4470(10)	68.434(2)
χ, deg	90	90	64.039(2)
V, $Å^3$	3022.3(17)	2770.32(17)	1427.31(10)
Z	2	4	1
d_{calcd}, $g \cdot cm^{-3}$	1.961	3.148	1.816
μ, mm^{-1}	6.366	13.268	6.366
Unique data	6960	6370	6513
Restraints	0	0	0
Parameters.	325	309	318
R1[a]	0.0404	0.0267	0.0163
wR2[b]	0.1001	0.0602	0.0500

[a] For data with $I > 2\sigma I$ $R1 = \frac{\sum ||Fo| - |Fc||}{\sum |Fo|}$; [b] For all data. $wR2 = \sqrt{\frac{\sum \left[w\left(Fo^2 - Fc^2\right)^2\right]}{\sum \left[w\left(Fo^2\right)^2\right]}}$; $w = 1/\sigma^2 (F_o^2)$ + $(aP)^2$ + bP, where $P = [\max(0 \text{ or } F_o^2) + 2(F_c^2)]/3$

Table 1 continued. Crystal Data and Data Collection Parameters

	β-Au_2(μ-dppe)$_2I_2$ ·2(HC(O)NMe_2) (**4**)	Au_2(μ-dppe)$_2I_2$ ·4($CHCl_3$) (**5**)	{Au(μ-dppe)I}$_n$ ·*n*($CHCl_3$) (**6**)
Formula	$C_{58}H_{62}Au_2I_2N_2O_2P_4$	$C_{56}H_{52}Au_2Cl_{12}I_2P_4$	$C_{27}H_{25}AuCl_3IP_2$
Formula weight	1590.71	1921.99	841.63
T, K	90(2) K	100(2)	90(2) K
Color and Habit	Colorless plate	Colorless block	Colorless irregular plate
Crystal system	Triclinic	Triclinic	Triclinic
Space group	P-1	P-1	P-1
a, Å	11.9340(5)	10.5616(11)	10.0425(7)
b, Å	14.2277(6)	12.7861(13)	11.4032(8)
c, Å	18.4006(8)	13.0433(14)	13.7462(10)
α, deg	83.4850(10)	69.469(2)	76.248(10)
β, deg	89.3280(10)	83.592(2)	88.288(1)
χ, deg	66.3480(10)	88.929(2)	70.641(1)
V, $Å^3$	2841.4(2)	1638.8(3)	1440.53(18)
Z	2	1	2
d_{calcd}, g•cm^{-3}	1.859	1.947	1.939
μ, mm^{-1}	6.399	6.036	6.578
Unique data	13954	9479	6582
Restraints	0	0	0
Parameters	635	344	307
R1[a]	0.0399	0.0178	0.0411
wR2[b]	0.0745	0.0402	0.0680

[a] For data with $I > 2\sigma I$ $R1 = \frac{\sum ||Fo| - |Fc||}{\sum |Fo|}$; [b] For all data. $wR2 = \sqrt{\frac{\sum \left[w\left(Fo^2 - Fc^2\right)^2\right]}{\sum \left[w\left(Fo^2\right)^2\right]}}$; $w = 1/\sigma^2 (F_o^2)$ + $(aP)^2$ + bP, where $P = [\max(0 \text{ or } F_o^2) + 2(F_c^2)]/3$

Table 2. Selected Interatomic Distances (Å) and Angles (deg) for Gold Complexes**.**

Distances (Å)	$Au_2(\mu\text{-dppe})_2I_2 \cdot 4(CH_2Cl_2)$ (**1**)	$Au_2(\mu\text{-dppe})_2I_2 \cdot 2(CH_2Cl_2)$ (**2**)	$\alpha\text{-}Au_2(\mu\text{-dppe})_2I_2 \cdot 2(HC(O)NMe_2)$ (**3**)
Au1···Au1A	3.192(1)	3.5013(2)	3.4289(2)
P1···P2	4.025(2)	4.116(1)	4.0888(9)
Au1-I1	2.9173(9)	2.9045(3)	2.9699(2)
Au1-P1	2.315(2)	2.3182(9)	2.3170(7)
Au1-P2	2.326(2)	2.3126(8)	2.3156(8)
Angles (deg)			
P1···Au1···P2	148.24(6)	153.24(3)	152.91(2)
P1···Au1···I1	108.56(4)	103.40(2)	103.07(2)
P2···Au1···I1	102.65(4)	102.94(2)	103.55(2)
Σ Angles about Au1	359.45	359.58	359.53

Table 2. Continued

Distances (Å)	β-Au_2(μ-dppe)$_2I_2$ ·2(HC(O)NMe_2) (**4**) Site A	β-Au_2(μ-dppe)$_2I_2$ ·2(HC(O)NMe_2) (**4**) Site B	Au_2(μ-dppe)$_2I_2$ ·2($CHCl_3$) (**5**)	{Au(μ-dppe)I}$_n$ · *n*($CHCl_3$) (**6**)
Au1···Au1A	3.2366(3)	3.7866(3)	3.5959(5)	7.1910(7)
P1···P2	4.040(2)	4.202(2)	4.1251(8)	4.437(2)
Au1-I1	3.0044(4)	3.0055(4)	2.9296(4)	2.8499(4)
Au1-P1	2.301(2)	2.320(2)	2.3183(7)	2.316(2)
Au1-P2	2.310(2)	2.318(2)	2.3162(7)	2.300(2)
Angles (deg)				
P1···Au1···P2	155.43(6)	160.12(6)	153.92(2)	148.03(6)
P1···Au1···I1	102.52(4)	100.44(4)	102.45(2)	101.98(4)
P2···Au1···I1	99.22(4)	99.40(4)	103.45(2)	108.43(4)
Σ Angles about Au1	357.17	359.96	359.82	358.44

Crystallization from Dichloromethane: Formation of Solvates $Au_2(\mu\text{-dppe})_2I_2 \cdot 4(CH_2Cl_2)$ (1) and $Au_2(\mu\text{-dppe})_2I_2 \cdot 2(CH_2Cl_2)$ (2)

Crystals of the two solvates, $Au_2(\mu\text{-dppe})_2I_2 \bullet 4(CH_2Cl_2)$ (**1**) and $Au_2(\mu\text{-dppe})_2I_2 \bullet 2(CH_2Cl_2)$ (**2**), were obtained individually by diffusion of diethyl ether into a dichloromethane solution of the colorless solid mentioned above. Oddly, the sample of $Au_2(\mu\text{-dppe})_2I_2 \bullet 4(CH_2Cl_2)$ (**1**) was obtained during the summer, while sample of $Au_2(\mu\text{-dppe})_2I_2 \bullet 2(CH_2Cl_2)$ (**2**) was obtained during the winter. Based upon their luminescence and crystal morphology, each of the samples appeared to be homogenous. The structure of $Au_2(\mu\text{-dppe})_2I_2 \bullet 4(CH_2Cl_2)$ (**1**) is shown in Figure 1. The asymmetric unit of the gold complex consists of a gold ion, an iodide ion and a bridging dppe ligand with the rest of the molecule created by reflection through a center of symmetry. The distance between the two gold ions is 3.192(1) Å, which is the shortest such distance in the complexes reported here. Each gold ion exhibits planar, three-coordinate geometry. The P-Au-P angle is much wider than the two P-Au-I angles, but the sum of the three angles is close to 360°. This situation is characteristic of other molecules with two phosphine ligands and an iodide ligand as can be seen in Table 3. The four solvate molecules are rather far from the gold ions. The closest interaction is the 5.473 Å distance between a gold ion and a hydrogen atom of the nearest dichloromethane molecule.

The structure of $Au_2(\mu\text{-dppe})_2I_2 \bullet 2(CH_2Cl_2)$ (**2**) is similar to that of $Au_2(\mu\text{-dppe})_2I_2 \bullet 4(CH_2Cl_2)$ (**1**). In both solvates, the dimeric complexes are centrosymmetric. However, the separation between the two gold ions is longer in $Au_2(\mu\text{-dppe})_2I_2 \bullet 2(CH_2Cl_2)$ (**2**) (3.5013(2) Å) than in $Au_2(\mu\text{-dppe})_2I_2 \bullet 4(CH_2Cl_2)$ (**1**) (3.192(1) Å). Additionally, the distance between the two phosphorus atoms in the bridging dppe ligand is longer in $Au_2(\mu\text{-dppe})_2I_2 \bullet 2(CH_2Cl_2)$ (**2**) (4.116(1) Å) than in $Au_2(\mu\text{-dppe})_2I_2 \bullet 4(CH_2Cl_2)$ (**1**) (4.025(2) Å).

Colorless crystals of $Au_2(\mu\text{-dppe})_2I_2 \bullet 4(CH_2Cl_2)$ (**1**) and $Au_2(\mu\text{-dppe})_2I_2 \bullet 2(CH_2Cl_2)$ (**2**) are photoluminescent. Figure 2 shows the excitation and emission spectra for the two complexes at room temperature and at 77 K. These spectra and all other excitation and emission spectra reported here were obtained from crystalline samples that were handled to minimize the loss of solvate molecules, which could result in alteration of the spectroscopic properties as has been reported previously.[18,19] Information about the excitation and emission maxima for these and other crystals are shown in Table 4. At room temperature both complexes show a single excitation band at 380 – 384 nm and a single emission band at 556 nm for compound (**1**) or 594 nm for compound (**2**). At 77 K the emission bands shift to longer wavelengths without a significant change in the excitation spectrum. For $Au_2(\mu\text{-dppe})_2I_2 \bullet 2(CH_2Cl_2)$ (**2**), the emission lifetime at room temperature is 9 microseconds, while at 77 K it lengthens to 14 microseconds. These lifetimes suggest that the emission arises from phosphorescence.

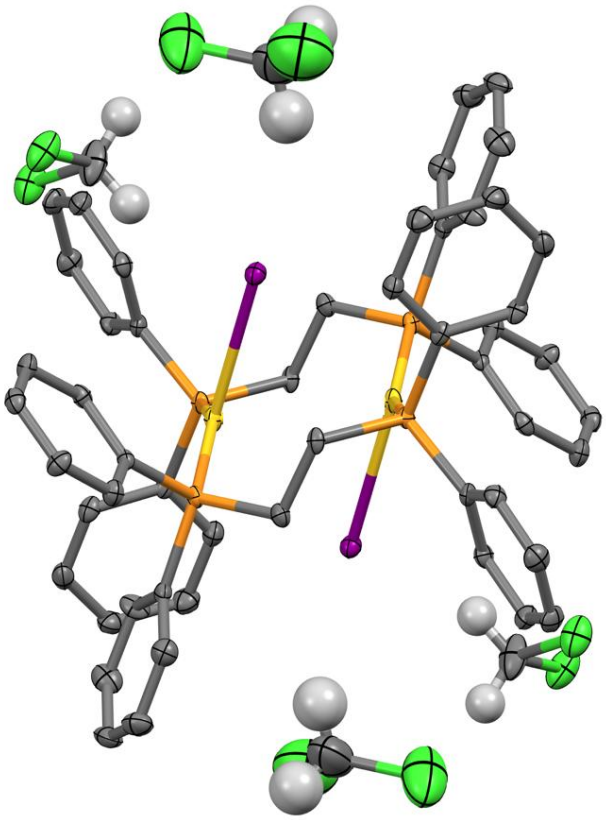

Figure 1. The molecular structure of $Au_2(\mu\text{-dppe})_2I_2 \bullet 4(CH_2Cl_2)$ (**1**) with the hydrogen atoms removed for clarity except for those on the dichloromethane molecules. Color code: gold, yellow; phosphorus, orange; iodine, purple; carbon, grey; chlorine, green; hydrogen, white.

Table 3. Selected Bond Distances (Å) and Angles (deg) for Three-Coordinate Gold Complexes**.**

	$Au(PCy_3)_2I$[a]	$Au(PCy_3)_2I \cdot PCy_3$[a]	$Au(PPh_3)_2I$[b]	$Au_2(\mu\text{-dcmp})_2I_2$[c]
Bond distances (Å)				
Au1-I1	2.895(2)	3.008(1)	2.7588(6)	2.9960(7)
Au1-P1	2.344(2)	2.315(3)	2.3331(1)	2.342(3)
Au1-P2	2.328(2)	2.310(3)	2.3331(1)	2.321(3)
Au···Au				3.0756(6)
Bond angles (deg)				
P1···Au1···P2	143.1(1)	159.1(1)	131.86(6)	157.93(7)
P1···Au1···I1	106.26(7)	98.69(7)	114.07(3)	94.40(6)
P2···Au1···Br1	110.45(7)	101.87(7)	114.07(3)	107.62(6)
Σ Angles about Au1	359.81	359.66	360.00	359.95

Data from: [a] PCy_3 = tricyclohexylphosphine. Bowmaker, G. A.; Brown, C. L.; Hart, R. D.; Healy, P. C.; Englehardt, L. M.; Rickard, C. E. F.; White, A. H. *J. Chem. Soc. Dalton Trans.* **1999**, 881-889. [b] Fränkel, R.; Kniczek, J.; Ponikwar, W.; Nöth, H.; Polborn, K.; Fehlhammer, W. P. *Inorg. Chim. Acta* **2001**, *312*, 23. [c] dcmp = bis-(dicyclohexylphosphino)methane, centrosymmetric dimer. Fu. W.-F.; Chan, K.-C.; Cheung, K.-K.; Che, C.-M. *Chem. Eur. J.* **2001**, *7*, 4656. [d]dmpe = bis-(dimethylphosphino)ethane. Jaw, H.-R. C.; Savas, M. M.; Rogers, R. D.; Mason, W. R. *Inorg. Chem.* **1989**, *28*, 1028-1037. [e] dpmp = bis(diphenylphosphinomethyl)phenylphosphine. Xiao, H.; Weng, Y.-X. Wong, W.-T.; Mak, T. C. W.; Che, C.-M. *Dalton Trans.*, ***1997***, 221–226.

Table 3. Continued Selected Bond Distances (Å) and Angles (deg) for Three-Coordinate Gold Complexes**.**

	[{Au_2(μ-dmpe)$_2$}$_2$μ-I][a] Au1	[{Au_2(μ-dmpe)$_2$}$_2$μ-I][a] Au2	[{Au_2(μ-dmpe)$_2$}$_2$μ-I][a] Au3	[{Au_2(μ-dmpe)$_2$}$_2$μ-I][a] Au4
Bond distances (Å)				
Au1-I1	3.267(2)	3.331(2)	3.151(2)	3.277(2)
Au1-P1	2.287(5)	2.285(5)	2.292(5)	2.297(2)
Au1-P2	2.294(5)	2.287(5)	2.291(5)	2.310(5)
Au···Au	2.971(2)	2.971(2)	2.976(1)	2.976(1)
Bond angles (deg)				
P1-Au1-P2	174.0(2)	176.0(2)	171.6(2)	178.6(2)
P1-Au1-I1	93.8(1)	87.8(1)	89.6(1)	93.8(1)
P2-Au1-I1	89.4(1)	89.2(1)	94.3(1)	84.8(1)
Σ Angles about Au1	357.2	353.0	355.5	357.2

Table 3. Continued Selected Bond Distances (Å) and Angles (deg) for Three-Coordinate Gold Complexes**.**

	$[Au_3(\mu\text{-dpmp})_2(\mu\text{-I})I]I^e$ Au1	$[Au_3(\mu\text{-dpmp})_2(\mu\text{-I})I]I^e$ Au2	$[Au_3(\mu\text{-dpmp})_2(\mu\text{-I})I]I^e$ Au3
Bond distances (Å)			
Au1-I1	3.008(1)	3.036(1)	3.191(1)
Au1-P1	2.306(3)	2.309(3)	2.313(3)
Au1-P2	2.316(3)	2.321(3)	2.315(3)
Au···Au	2.9525(9)	2.9525(9) 3.0202(9)	3.0202(9)
Bond angles (deg)			
P1-Au1-P2	173.0(1)	155.3(1)	170.4(1)
P1-Au1-I1	93.37(8)	103.46(8)	95.89(8)
P2-Au1-I1	93.44(8)	101.15(8)	91.42(8)
Σ Angles about Au1	359.81	359.91	357.71

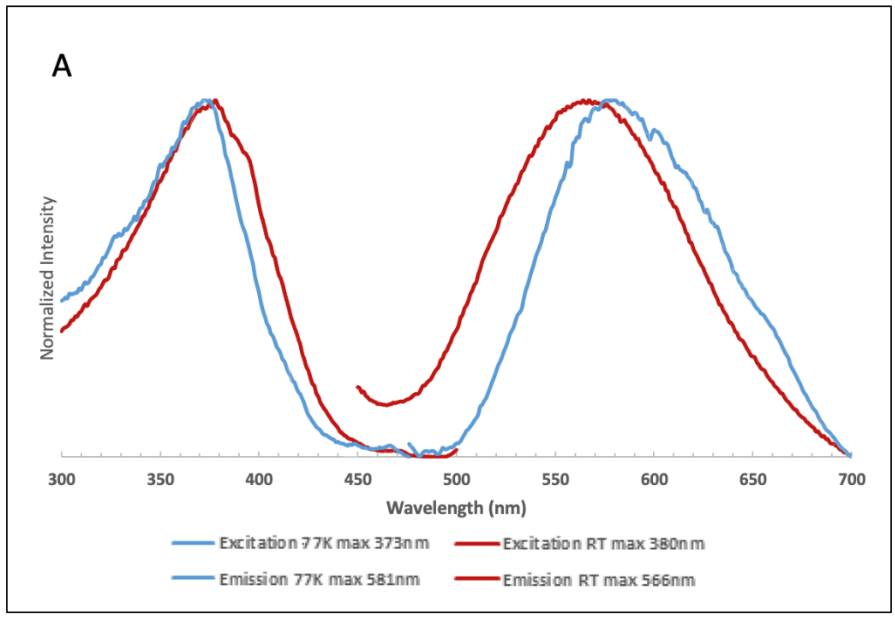

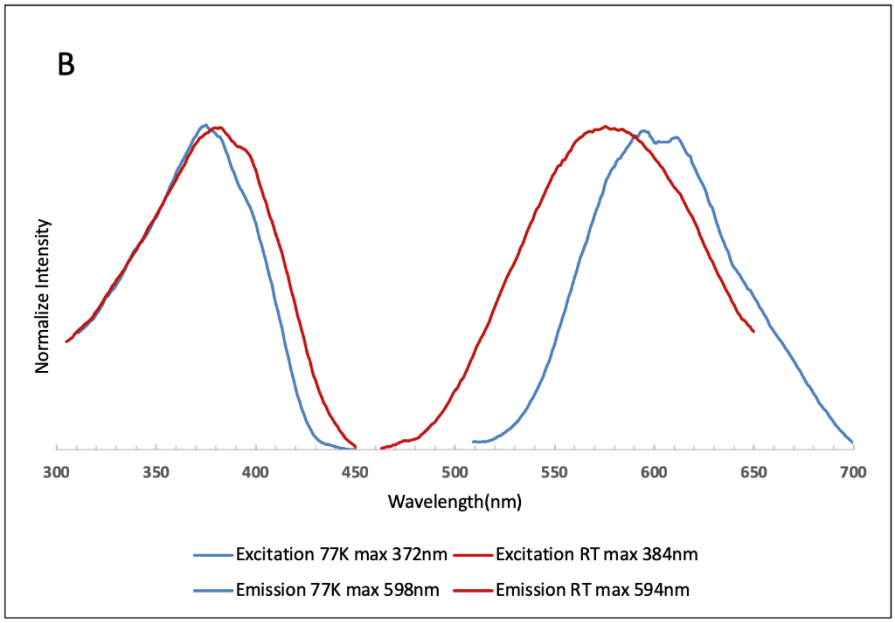

Figure 2. Excitation and emission spectra from crystalline solids of: A, $Au_2(\mu\text{-}dppe)_2I_2 \bullet 4(CH_2Cl_2)$ and B, $Au_2(\mu\text{-}dppe)_2I_2 \bullet 2(CH_2Cl_2)$ (**2**).

Table 4. Excitation and Emission Spectral Data

Compound	Temp. (K)	Excitation (nm)	Emission (nm)
$Au_2(\mu\text{-dppe})_2I_2\cdot 4(CH_2Cl_2)$ (**1**)	298 77	378 373	556 581
$Au_2(\mu\text{-dppe})_2I_2\cdot 2(CH_2Cl_2)$ (**2**)	298 77	384 372	594 598
$\alpha\text{-}Au_2(\mu\text{-dppe})_2I_2\cdot 2(HC(O)NMe_2)$ (**3**)	298	371	581
$\beta\text{-}Au_2(\mu\text{-dppe})_2I_2\cdot 2(HC(O)NMe_2)$ (**4**)	298 77	394 378	570 572
$Au_2(\mu\text{-dppe})_2I_2\cdot 2(CHCl_3)$ (**5**)	298 77	365 395	537 540
$\{Au(\mu\text{-dppe})I\}_n\cdot n(CHCl_3)$ (**6**)	298 77	None 300, 347	None 437

Polymorphs of $Au_2(\mu\text{-dppe})_2I_2\cdot 2(HC(O)NMe_2)$. Evaporation of an N,N-dimethylformamide solution of the colorless complex obtained from adding dppe to AuI in dichloromethane produced colorless crystals of the α-polymorph, which displayed a yellow-green luminescence along with colorless crystals of the β-polymorph that produced yellow emission. Figure 3 shows photographs of crystals of both $\alpha\text{-}Au_2(\mu\text{-dppe})_2I_2\cdot 2(HC(O)NMe_2)$ (**3**) and $\beta\text{-}Au_2(\mu\text{-dppe})_2I_2\cdot 2(HC(O)NMe_2)$ (**4**) under ambient and UV light. The crystals were separated manually based on their morphology and luminescence to provide samples for spectroscopic investigation. The excitation and emission maxima for the two different polymorphs are given in Table 4.

Crystals of $\alpha\text{-}Au_2(\mu\text{-dppe})_2I_2\cdot 2(HC(O)NMe_2)$ (**3**) contain a centrosymmetric $Au_2(\mu\text{-dppe})_2I_2$ molecule, whose structure is similar to the dimers in crystals of (**1**) and (**2**). In $\alpha\text{-}Au_2(\mu\text{-dppe})_2I_2\cdot 2(HC(O)NMe_2)$ (**3**) the separation between the two gold ions is 3.4289(2) Å. The other dimensions of this dimer are given in Table 2.

The β-polymorph contains two distinct centrosymmetric dimers with different distances between the gold ions: 3.7866(5) and 3.2366(5) Å. One of the dimers in this polymorph contains the longest Au···Au separation seen in this study. The structures of the two different dimers are compared in Figure 4. In addition to the variation in Au···Au distances, the orientations of the phenyl rings are different in the two molecules. In the molecule with the shorter separation between the gold ions, the two phenyl rings that protrude toward the viewer in Figure 4 are roughly perpendicular to one another, and the two phenyl rings that extend away from the viewer at the back of the dimer are also roughly perpendicular to one another. In contrast, in the molecule with the longer separation between the gold ions seen at the bottom of Figure 4, the two phenyl rings that protrude toward the viewer are roughly parallel to one another as are the two phenyl rings that extend away for the viewer on the backside of the molecule.

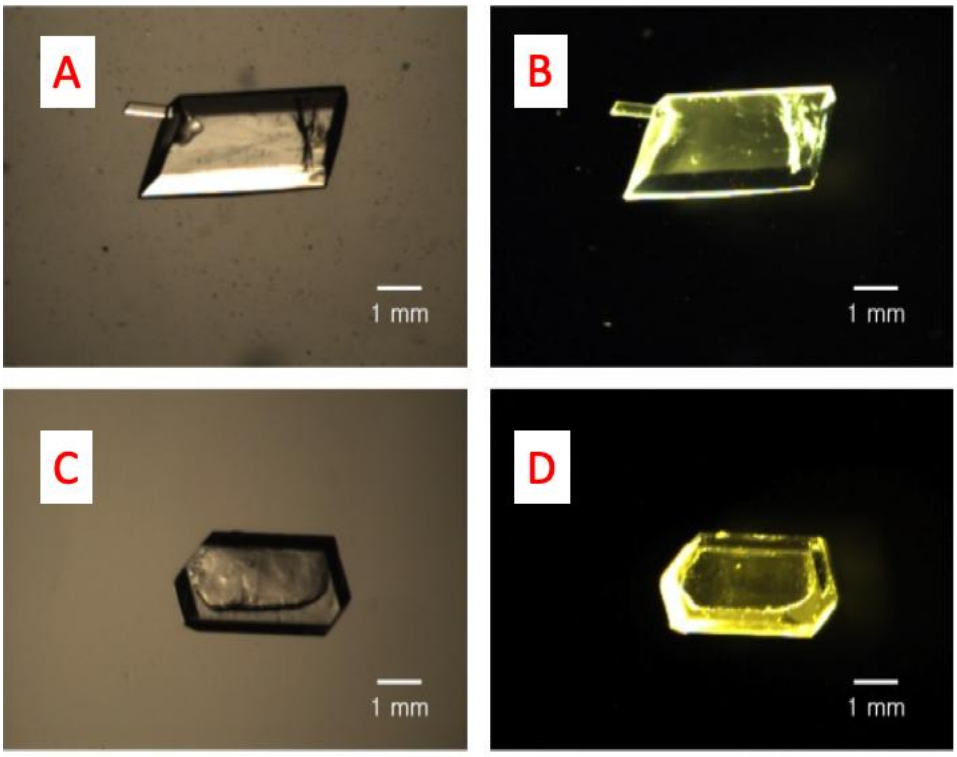

Figure 3. Photographs of crystals of α-Au_2(μ-dppe)$_2I_2$·2(HC(O)NMe_2) (**3**) under (A) ambient light and (B) under UV irradiation, and β-Au_2(μ-dppe)$_2I_2$·2(HC(O)NMe_2) (**4**) under (C) ambient light and (D) under UV irradiation

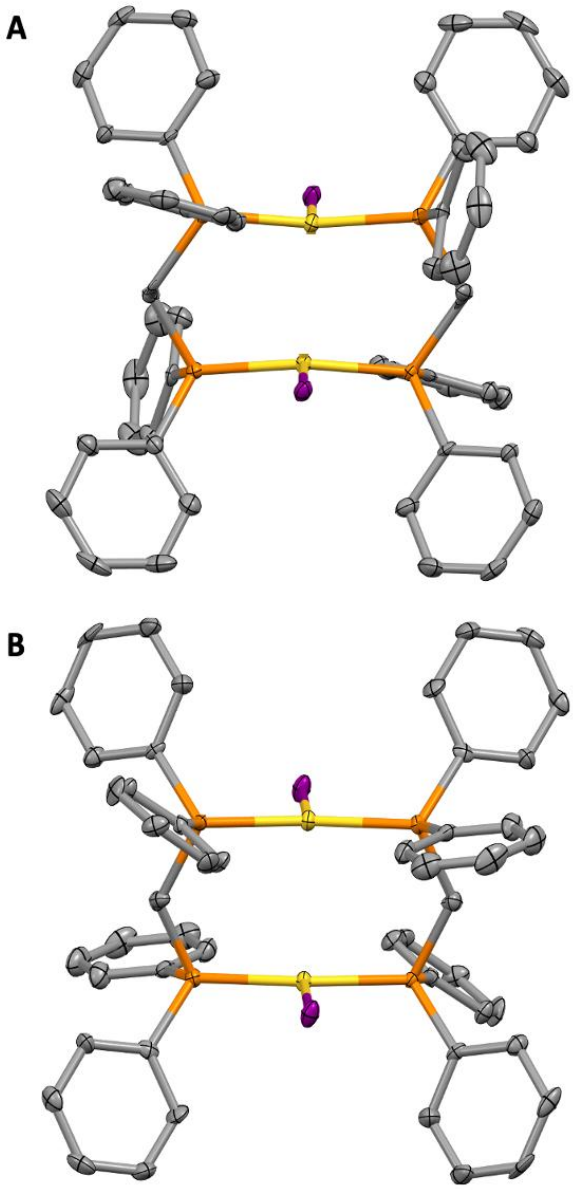

Figure 4. The structures of the two independent dimers in β-$Au_2(\mu\text{-dppe})_2I_2$•$2(HC(O)NMe_2)$ (**4**) with the hydrogen atoms and solvate molecules removed for clarity. The molecule with the shorter separation between the gold ions is shown in A. The molecule with the longer separation between the gold ions is shown in B. Color code: gold, yellow; phosphorus, orange; iodine, purple; carbon, grey.

Crystallization from Chloroform: Formation of dimeric $Au_2(\mu\text{-dppe})_2I_2\cdot 4(CHCl_3)$ (5) and Polymeric $\{Au(\mu\text{-dppe})I\}_n\cdot n(CHCl_3)$ (6). Layering diethyl ether over a chloroform solution of the product from the reaction between gold(I) iodide and dppe produced colorless blocks of $Au_2(\mu\text{-dppe})_2I_2\cdot 4(CHCl_3)$ (**5**), which displayed green luminescence under UV irradiation. Excitation and emission data are given in Table 4. The structure of the complex is similar the other gold dimers reported here. The separation between the gold ions is 3.5959(5) Å.

Colorless blocks of the polymer $\{Au(\mu\text{-dppe})I\}_n\cdot n(CHCl_3)$ (**6**) were obtained by layering pentane over a chloroform solution of the initial colorless product. A portion of the structure of the product is shown in Figure 5. The asymmetric unit consists of a chloroform molecule in a general position and a $CH_2Ph_2PAuIPPh_2CH_2$ unit with the rest of each dppe ligand formed by reflection through a center of inversion. Within the polymer, the gold center is planar and coordinated to a terminal iodide ligand and phosphorus atoms from two different bridging ligands. The gold ions are widely separated in these polymers. The closest contact between two gold centers is 6.7401(7) Å within a chain and 10.0425(7) Å between different chains. Clearly, there are no aurophilic interactions in these polymers. The structure of polymeric $\{Au(\mu\text{-dppe})I\}_n\cdot n(CHCl_3)$ (**6**) is similar to the structures of $\{Au(\mu\text{-dppe})Br\}_n\cdot(CH_2Cl_2)$ and$\{Au(\mu\text{-dppe})Br\}_n\cdot 0.5(C_4H_{10}O)$ reported previously,[12] but none of these crystals are isostructural.

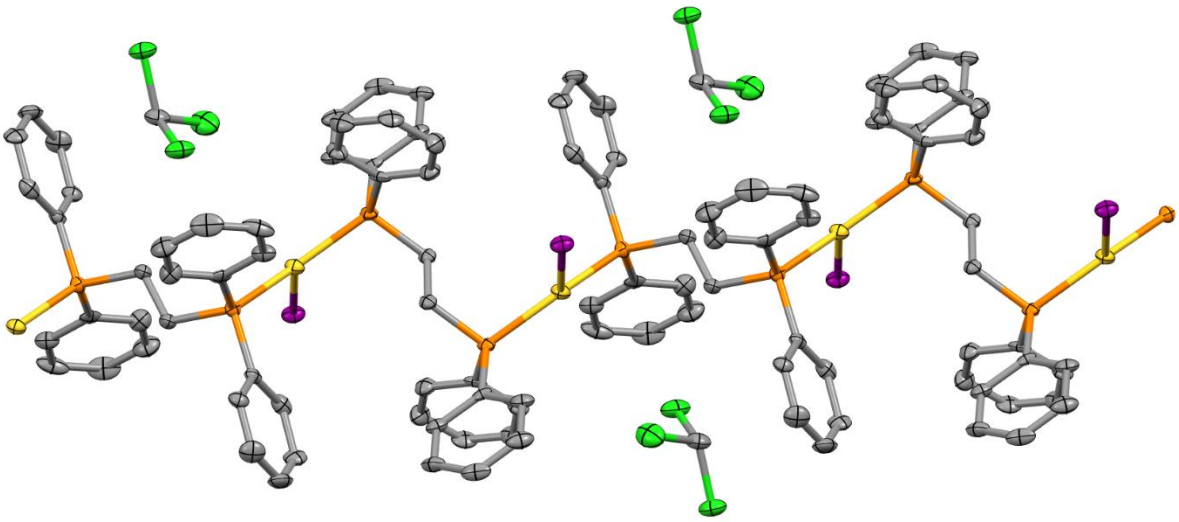

Figure 5. The structure of part of the polymeric chain in $\{Au(\mu\text{-dppe})I\}_n \cdot n(CHCl_3)$ (**6**) with the hydrogen atoms removed for clarity. Color code: gold, yellow; phosphorus, orange; iodine, purple; carbon, grey; chlorine, green.

The polymer is not luminescent at room temperature but becomes luminescent (λ_{max} for excitation, 300, 347nm; λ_{max} for emission 437 nm) when cooled to 77 K. The lack of luminescence at room temperature is somewhat unusual, particularly since the related polymers, $\{Au(\mu\text{-dppe})Br\}_n \cdot (CH_2Cl_2)$ and $\{Au(\mu\text{-dppe})Br\}_n \cdot 0.5(C_4H_{10}O)$, are luminescent at room temperature as are many other three-coordinate gold(I) complexes. [7,12]

Computational Analysis of Structural Differences: Computational methods were employed to better understand the energetics and the nature of the Au···Au interactions in structures of dimeric $Au_2(\mu\text{-dppe})_2I_2$. Au···Au distances in this family of compounds span an unusually large range, from 3.19 to 3.79 Å. In order to probe the factors controlling this distance, we have performed computational analysis on two structures that correspond to the two polymorphs of previously

reported $Au_2(\mu\text{-dppe})_2I_2 \bullet 2(OC(CH_3)_2)$:[13] **Geom(Short)** with an Au···Au distance of 3.3177(7) Å and **Geom(Long)** with an Au···Au distance of 3.6720(2) Å.

Geometry optimizations starting from crystallographic coordinates were used to locate energetic minima corresponding to these structures. To optimize geometries for these two structures, the Au···Au distances were constrained while all other distances were allowed to optimize. A third hypothetical structure, **Geom(Very_Short)**, with an Au–Au distance of 2.987 Å, well below the sum of the Au van der Waals radii, was obtained from a full geometry optimization (including the Au···Au distance) starting from the **Geom(Short)** structure. Selected measurements and comparisons between the computational structures and their experimental counterparts are noted in Table 1. A notable difference between **Geom(Short)** and **Geom(Long)** is the Au···I interaction between the gold center and the iodine atom bound to the other gold center. As the Au···Au distance shrinks, so does this Au···I interaction, and in the **Geom(Very_Short)** this distance is smaller than the sum of the van der Waals radii, 3.64 Å. No significant differences in other non-covalent interactions were observed between the three optimized structures. Frequency calculations confirm that all three structures occupy local energetic minima, and allow comparison of the Gibbs free energies, ΔG, of the structures. **Geom(Very_Short)** was found to be lowest in ΔG (at 298.15 K), followed by **Geom(Short)** (+9.2 kJ mol^{-1}), followed by **Geom(Long)** (+18.4 kJ mol^{-1}). The change in calculated energy between the Short and Long structures (< 10 kJ/mol) is within the associated range of crystal packing effects, which, for this system, are predominantly weak hydrogen-bonding interactions, namely solvent – aryl-proton (2-20 kJ/mol) and proton-to-phenyl π-stacking (>3 kcal/mol).[23-28] The <10 kJ/mol difference in energies between the two calculated structures and notable intermolecular forces in the packed structure strongly

suggest that the differences in Au···Au distances in the two polymorphs are primarily a result of crystal packing effects resulting from the incorporation of various solvate molecules.

Another factor that affects the Au – Au separation is the relative orientations of the phenyl rings within $Au_2(\mu\text{-dppe})_2I_2$. The Supporting Information contains two animations that show the output from the relaxed surface scan where the Au···Au distance was surveyed from 4.599 Å to 2.959 Å over the course of 50 steps. The animation shows a glitch at about 65% through the animation or at an Au – Au separation of ~3.5 Å where the orientation of the phenyl rings changes from that shown in Figure 4B with pairs of phenyl rings nearly parallel to each other and an Au…Au separation of 3.7866(3) Å to that shown in Figure 4A, where the same pairs of phenyl rings are nearly perpendicular to one another and the Au…Au separation is 3.2366(3) Å.

Table 5. Selected geometric features of $Au_2(\mu\text{-dppe})_2I_2$ from the experimental crystal structures and the computed systems.

	Au–Au, Å	Au–P Å	Au–I Au···I Å	I–Au–Au Angle	P–Au–P Angle	P–Au–I Angle	Origin
Geom(Short)	3.395 (fixed)	2.321	2.871 3.695	71.7°	146.0°	109.7° 104.3°	DFT
Au(Short)	3.3955(2)	2.316(2)	2.9759(2) 3.7143(2)	70.97(2)°	152.98(2)°	103.57(2)° 102.79(2)°	Crystal Ref. 13
Geom(Long)	3.6720 (fixed)	2.321	2.871 3.842	70.7°	146.1°	108.8° 104.8°	DFT
Au(Long)	3.6720(2)	2.314(1)	2.9106(2) 3.937(2)	72.43(2)°	154.33(2)°	103.34(2)° 102.27(2)°	Crystal Ref. 13
Geom(Very_Short)	2.987	2.327	2.865 3.576	75.3°	143.5°	111.5° 103.4°	DFT

Analysis of Au···Au Interactions: Single point calculations on the three gold structures were used to determine the nature of the interactions between the two Au atoms in each structure using the calculated Mayer bond orders (MBO).[20-22] The **Geom(Very_Short)** structure was calculated to have an Au–Au MBO of 0.11, indicating a weak but non-zero Au–Au bonding interaction. Both the **Geom(Short)** and **Geom(Long)** structures returned MBO values less than 0.10. Thus, Au–Au bonding interactions in these two structures are minimal. These bond order results agree with the comparison of the Au···Au distances to the sum of the Au van der Waals radii, described above.

Metal-metal bonding between the d^{10} Au(I) ions can occur at short Au–Au distances when the Au–Au antibonding highest filled molecular orbital (HFMO, consisting of an out-of-phase combination of 5d orbitals) is raised close enough in energy to mix significantly with the empty 6s and 6p orbitals.[23-28] This mixing, particularly with the 6p orbitals, causes the HFMO to have non-bonding, rather than antibonding, character, as the orbital lobes bulge out away from the Au–Au centroid. The structures **Geom(Very_Short)**, **Geom(Short)**, and **Geom(Long)**, provide snapshots of this effect, which is seen via analysis of the orbital compositions given in Table 6 and Figure 6. Starting with **Geom(Long)**, beyond the sum of the Au van der Waals radii, we see that the HFMO is essentially a hybrid of 5d and 6s orbitals with little 6p character (<3% of the metal contribution per Au atom). **Geom(Short)**, which is very close to the sum of the Au van der Waals radii, has ~5% 6p character, while **Geom(Very_Short)** has ~20% p character.

Table 6. Percentage contributions of atomic orbitals to the filled Au–Au σ and σ* molecular orbitals.

	System	Contributions (%)
Geom(Very_Short)		
Highest Occupied Metal		
Orbital	Au 1	d: 9.4; s: 2.4; p: 2.9
	Au 2	d: 9.4; s: 2.4; p: 2.9
	other	70.6
Geom(Short)		
Highest Occupied Metal		
Orbital	Au 1	d: 8.8; s: 4.2; p: 0.7
	Au 2	d: 8.8; s: 4.2; p: 0.7
	other	72.6
Geom(Long)		
Highest Occupied Metal		
Orbital	Au 1	d: 4.8; s: 2.8; p: 0.2
	Au 2	d: 4.8; s: 2.8; p: 0.2
	other	84.4

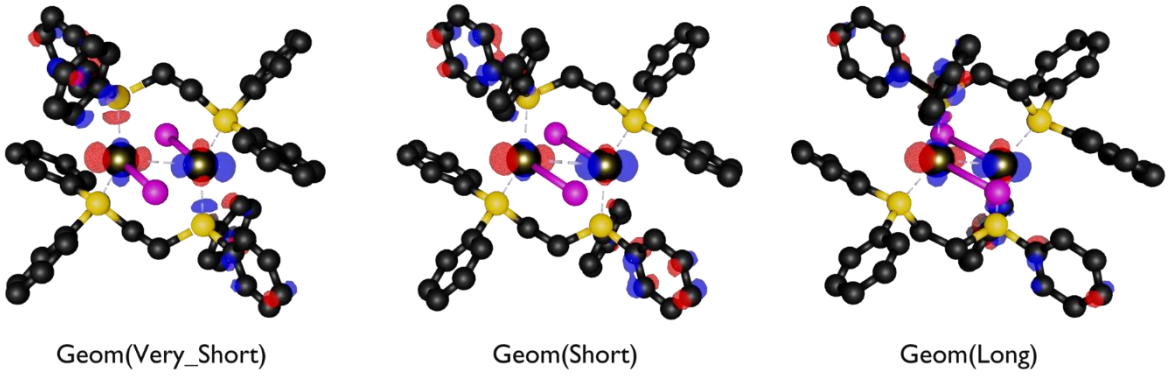

Figure 6. Isosurface plots (at 50%) of the highest filled metal orbitals for **Geom(Very_Short)**, **Geom(Short)**, and **Geom(Long)**, highlighting the increasing degree of Au–Au antibonding character across the series.

Conclusions Our results indicate that crystallization of materials containing the components Au^{+}, dppe, and I^{-} in a 1:1:1 ratio can produce solvates of the centrosymmetric dimer, $Au_2(\mu\text{-dppe})_2I_2$, as well as the polymer, $\{Au(\mu\text{-dppe})I\}_n \cdot n(CHCl_3)$ (**6**), and the iodide bridged dimer, $Au_2(\mu\text{-dppe})_2(\mu\text{-I})_2$, which was reported previously.[13] The centrosymmetric dimer, $Au_2(\mu\text{-dppe})_2I_2$, is quite flexible with Au···Au separations that range from 3.192(1) to 3.7866(3) Å. However, none of the compounds we have isolated have Au···Au separations that are as short as 2.987 Å, the distance that was computed for the hypothetical **Geom(Very_Short).** Only the cationic dimer, $[Au_2(\mu\text{-dppe})_2]^{2+}$, with two-coordinate gold(I) ions has an Au···Au separation that short.[11,14] Thus, at short Au···Au contacts, the formation of the dimeric dication, $[Au_2(\mu\text{-dppe})_2]^{2+}$, with two-coordinate gold(I) centers is preferable to retaining the iodide ligands to form the molecular dimer, $Au_2(\mu\text{-dppe})_2I_2$, with three-coordinate gold(I) centers.

The pair of polymorphs of $Au_2(\mu\text{-dppe})_2I_2 \cdot 2(OC(CH_3)_2)$ were investigated computationally to better understand the origin of their different Au···Au distances. These two

structures were computationally predicted to differ in energy by only ~ 10 kJ/mol, an energy that is small enough to be attributable to crystal packing forces. An analysis of Au···Au interactions highlighted the changes in electronic structure that occurred as the Au atoms were brought together from a non-bonding range into the aurophilic bonding range. Notably, an increase in 6p contribution to the Au–Au highest filled metal orbital (HFMO) changes the nature of this orbital from Au–Au antibonding to Au–Au non-bonding as the two Au atoms were brought together. However, this effect was minimal over the crystallographically observed Au···Au distances, and only became relevant at a hypothetical Au−Au distance of <3.2 Å. Overall, the structural differences between the Au dimers were found to originate primarily from crystal packing effects with minimal aurophilic influence.

The interplay of coordination number and aurophilic interactions is not clear cut. Two-coordinate gold(I) complexes frequently engage in aurophilic interactions, which are responsible for the self-association of some these compounds.[17] For three-coordinate gold(I) the issue is ambigous. As our computations have shown, aurophilic interactions are not significant at the distances found in our solvates of $Au_2(\mu\text{-dppe})_2I_2$. However, there are several three-coordinate gold(I) complexes involving AuP_2I coordination where shorter Au···Au distances may indicate aurophilic interactions. We have included relevant data about these complexes in Table 3. Finally, there are a least two cases of four-coordinate gold being involved in aurophilic interactions with other two-coordinate gold centers.[29,30]

The luminescence in the solvated crystals of $Au_2(\mu\text{-dppe})_2I_2$ is associated with the presence of planar, three-coordinate gold centers, which are usually luminescent without the need for aurophilic interactions.[31-34] For such complexes, the excitation process generally involves a

promotion of an electron from the doubly occupied, in-plane $d_{x^2-y^2}$,d_{xy} gold orbitals into an empty orbital, which can be the out-of-plane p_x gold orbital or a an empty ligand orbital.[28,29]

B3LYP density functional computations have been conducted on the related series of dimeric complexes, $Au_2(\mu\text{-}Ph_2P(CH_2)_nPPh_2)_2I_2$ (n = 3−6) and on mononuclear $Au(PPh_2Me)_2I$.[7] Those calculations indicated that for compounds with an AuP_2I core, the excitation involves metal-to-ligand charge-transfer (MLCT) from an orbital with Au-I antibonding character to an orbital that is largely composed of phosphine ligand π bonds. These computations also examined variations in the P-Au-P bond angles and the Au-I distances and found a correlation between the Au-I distances in these complexes and the emission wavelength.[7] That correlation is not observed in the crystals of $Au_2(\mu\text{-dppe})_2I_2$, where the variation in emission wavelength is small as seen in Table 4.

Experimental Section.

Preparation of Au(dppe)I. A 100mg (0.309 mmol) portion of AuI was suspended in 30 mL of dichloromethane and to this suspension was added 185mg (0.463mmol) of dppe. After stirring for 3hr, the suspension became a clear solution. The solution was filtered, and then the solvent was removed in a vacuum. The white solid was collected and washed with diethyl ether: yield, 195 mg (87.4%). This material was used to obtain crystalline samples of the following compounds.

$Au_2(\mu\text{-dppe})_2I_2\cdot 4(CH_2Cl_2)$ (1). Crystals suitable for X-ray structure determination were grown by slow diffusion of diethyl ether to a solution of the colorless solid in chloroform. Colorless, block-shaped crystals with yellow luminescence grew in the mixture in about three to four days.

Infrared spectrum: 3035w, 2933m, 2920m, 2849m, 1718w, 1441w, 1431s, 1433w, 1430w, 1377w, 1274m, 1177m, 1174m, 1096m, 1098m, 1027m, 999m, 995m, 727s, 699s cm^{-1}.

$Au_2(\mu\text{-dppe})_2I_2\cdot 2(CH_2Cl_2)$ (**2**). The suitable crystals for X-ray structure determination were grown by slow diffusion of diethyl ether to a saturated solution of the initial white solid in dichloromethane. The colorless blocks of $Au_2(\mu\text{-dppe})_2I_2\cdot 2(CH_2Cl_2)$ with a yellow luminescence formed over a 2-3 day period.

Infrared spectrum: 3048w, 2891w, 1480s, 1434m, 1415m, 1305w, 1264w, 1156w, 1098s, 1069m, 998w, 820m, 741m, 727m, 705m, 689s, 521m, 508s, 486m cm^{-1}

α-$Au_2(\mu\text{-dppe})_2I_2\cdot 2(HC(O)NMe_2)$ (3) and β-$Au_2(\mu\text{-dppe})_2I_2\cdot 2(HC(O)NMe_2)$ (4). The white solid was dissolved in a minimum volume of N,N-dimethylformamide and the colorless solution was filtered. After evaporation for a week, two different kinds of colorless blocks grew from in the solution. These crystals, which produced yellow-green and yellow-orange luminescence respectively, were separated manually and used for the spectroscopy and crystallography.

Infrared spectrum green emissive α-$Au_2(\mu\text{-dppe})_2I_2\cdot 2(HC(O)NMe_2)$ (**3**): 3053w, 2927w, 2893w, 1660s(ν C=O from $HC(O)NMe_2$), 1483m, 1433m, 1386m, 1098s, 1053m, 1024m, 952m, 822m, 741m, 721m, 705m, 688s, 659m, 519m, 507s, 488m, 478m cm^{-1}

Infrared spectrum yellow emissive β-$Au_2(\mu\text{-dppe})_2I_2\cdot 2(HC(O)NMe_2)$ (**4**): 3054w, 2929w, 2894w, 1662s(ν C=O from $HC(O)NMe_2$), 1483m, 1434m, 1414m, 1385m, 1097s, 1053m, 1023m, 951m, 822m, 742m, 721m, 705m, 688s, 659m,519m, 508s, 486m, 478m cm^{-1}

$Au_2(\mu\text{-dppe})_2I_2\cdot 2(CHCl_3)$ (5). Crystals suitable for X-ray structure determination were grown by slow diffusion of diethyl ether to a solution of the colorless solid in chloroform. Colorless, block-shaped crystals of $Au_2(\mu\text{-dppe})_2I_2\cdot 2(CHCl_3)$ appeared within two to three days.

Infrared spectrum: 2940m, 2922vs, 2852m, 2362w, 2332w, 1464m, 1435w, 1377w, 1260w, 1187w, 1171w, 1175m, 1099m,1072w, 1027w, 998w, 802w, 740s, 728s, 691vs cm^{-1}

Polymeric $\{Au(\mu\text{-dppe})I\}_n\cdot n(CHCl_3)$ (6). Crystals suitable for X-ray structure determination were grown by slow diffusion of diethyl ether to a solution of the colorless solid in chloroform. Colorless, irregular plates of $\{Au(\mu\text{-dppe})I\}_n\cdot n(CHCl_3)$ (**6**) appeared in three to four days.

Infrared spectrum: 3049w, 2975w, 2899w, 1481s, 1433s, 1412m, 1315m, 1099s, 1072m, 950m, 750m, 726s, 692s, 521m, 509s, 486m, 477m

X-ray Crystallography and Data Collection. The crystals were removed from the glass tubes in which they were grown together with a small amount of mother liquor and immediately coated with a hydrocarbon oil on a microscope slide. A suitable crystal of each compound was mounted on a glass fiber with silicone grease and placed in the liquid nitrogen cold stream of a Bruker SMART CCD with graphite monochromated Mo Kα radiation at 90(2) K. Check reflections were stable throughout the data collection.

The structures were solved by direct methods and refined using all data (based on F^2) using the software SHELXTL 5.1. A semiempirical method utilizing equivalents was employed to correct for absorptions. Hydrogen atoms were added geometrically and refined with a riding model. [35]

Physical Measurements. Infrared spectra were recorded on a Bruker ALPHA FT-IR spectrometer. Fluorescence excitation and emission spectra were recorded on a Perkin-Elmer LS50B luminescence spectrophotometer.

Computational Methods: Geometry optimizations, frequency calculations, and single-point (SP), were carried out using ORCA version 5.0.1.[36,37] For the geometry optimizations and frequency calculations the BP86 exchange-correlation functional was used.[38,39,40,41] Crystallographic coordinates, excluding solvent molecules, were used as the starting point for all geometry optimizations. The two experimental crystal structures were used as a basis for two computational models, **Geom(Short)** and **Geom(Long)**, having Au···Au distances fixed to those of the two polymorphs.[13] All other geometric parameters were optimized. A third model, **Geom(Very_Short)**, with an even shorter Au–Au distance of 2.99 Å, resulted from a full geometry optimization without fixing the Au···Au distances. All calculations used the resolution of identity and correlation of spheres, RIJCOSX approximation.[42,43,44] The segmented all-electron relativistic contracted (SARC) basis set, SARC-DKH-TZVPP,[45, 46, 47] was used for the Au atoms. The SARC contracted Karlsruhe basis set, SARC-DKH-TZVP,[48] was used for I atoms, while def2-SVP[49] was used for all other atoms. The auxiliary coulomb basis set, def2/J,[50] was used for all atoms. Dispersion corrections to the calculations were accounted for with the atom pairwise dispersion correction employing the Becke-Johnson damping scheme (D3BJ).[51, 52] All molecules were calculated in their open shell singlet state using unrestricted Kohn Sham (UKS) theory. The radial grid of the Au atoms was set to 10, whereas the grids for all other atoms were set to 6. Frequency calculations were performed by numerical differentiation with a central-differences increment of

0.01. Visualizations of the orbitals from self-consistent field calculations were carried out with the UCSF Chimera package.[53] Structure comparisons were made using Mercury.[54]

Acknowledgments. We thank the Petroleum Research Fund (Grant 37056-AC to ALB) and U. S. National Science Foundation [CHE-0716843 and CHE-1807637 to ALB and MMO; CHE-2246913 to JFB] for support.

Supporting Information Available: X-ray crystallographic files in CIF format. This material is available free of charge via the Internet at http://pubs.acs.org. Tables of Cartesian coordinates from geometry optimizations (PDF). Two Gifs: These short animations display the output from the relaxed surface scan where the Au - Au distance was surveyed from 4.599 Å to 2.959 Å over the course of 50 steps.

Contribution to Work

SC synthesized, crystallized, and analyzed all the compounds in the paper from the preliminary results of SHL. Analysis included harvesting the crystals, solving, and collecting luminescence data. Additionally, contributed to writing, editing, figures, and tables that are in this table.

References

1 Paderina, A. V.; Koshevoy, I. O.; Grachova, E. V. Keep it tight: a crucial role of bridging phosphine ligands in the design and optical properties of multinuclear coinage metal complexes. *Dalton Trans*. **2021**, *50*, 6003–6033

2 Puddephatt, R. J. Macrocycles, catenanes, oligomers and polymers in gold chemistry. *Chem. Soc. Rev*. **2008**, *37*, 2012–2027.

3 Puddephatt, R. J. Chemistry of Bis(dipheny1phosphino)methane. ***Chem. Soc. Rev.*** **1983**,***12***, 99-127.

4 Chaudret, B.; Delavaux, B.; Poilblanc, R. Bisdiphenylphosphinomethane in Dinuclear Complexes. *Coord. Chem. Rev*. **1988**, *86*, 191-243.

5 Balch, A. L.; Tulyathan, B. Interactions between Rhodium(I) Centers in Dimeric Complexes. *Inorg. Chem*. **1997**, *16*, 2840-2845.

6 Haddow, M. F.; Middleton, A.J.; Orpen, A. G.; Pringle, P. G.; Papp, R. Stereoelectronic effects in a homologous series of bidentate cyclic phosphines. A clear correlation of hydroformylation catalyst activity with ring size. *Dalton Trans.* **2009**, 202–209.

7 Lim, S. H.; Schmitt, J. C.; Shearer, J.; Jia, J.; Olmstead, M. M.; Fettinger, J. C.; Balch, A. L. Crystallographic and Computational Studies of Luminescent, Binuclear Gold(I) Complexes, $Au^{I}_2(Ph_2P(CH_2)_nPPh_2)_2I_2$ (n = 3−6). *Inorg. Chem*. **2013**, *52*, 823−831.

8 Streitberger, M.; Schmied, A.; Hey-Hawkins, E. Selective Formation of Gold(I) Bis-Phospholane Macrocycles, Polymeric Chains, and Nanotubes. *Inorg. Chem*. **201**4, *53*, 6794−6804.

9 Boar, P. Lönnecke, P.; Hey-Hawkins, E. Silver(I) Complexes of Two Flexible Bis-phospholane Ligands: Metallamacrocycles, Polymeric Chains, and Metallacryptands *Z. Anorg. Allg. Chem.* **2020**, *646*, 915–922.

10 Boar, P.; Streitberger, M.; Lönnecke, P.; Hey-Hawkins, E. Copper(I) Complexes of a Flexible Bis-phospholane Ligand: Route to Paddle-Wheel- and Box-Type Macrocycles. *Inorg. Chem.* **2017**, *56*, 7285−7291.

11 Costa, S.; Walters, D. T.; McNamara, L. E.; Olmstead, M. M.; Fettinger, J. C.; Balch, A. L. Structure and Luminescence Studies of Salts of the Helical Dication, $[Au_2(\mu$-bis(diphenylphosphine)ethane$)_2]^{2+}$ and Comparison with Salts of $[Au_2(\mu$-bis(diphenylphosphine)propane$)_2]^{2+}$. *Inorg. Chem.* **2023**, *62*, 15902−15911.

12 Lim, S. H.; Olmstead, M. M.; Balch, A. L. Molecular Accordion: Vapoluminescence and Molecular Flexibility in the Orange and Green Luminescent Crystals of the Dimer, Au_2(μ-bis-(diphenylphosphino)ethane$)_2Br_2$. *J. Am. Chem. Soc.* **2011**, *133*, 10229-10238.

13 Lim, S. H.; Olmstead, M. M.; Balch, A. L., Inorganic topochemistry. Vapor-induced solid state transformations of luminescent, three-coordinate gold(I) complexes. *Chem. Sci.* **2013,** *4*, 311-318.

14 Schuh, W.; Kopacka, H.; Wurst, K.; Peringer, P. Observation of a P/M interconversion of a gold–phosphine helicate via ^{31}P NMR. *Chem. Commun*. **2001**, 2186–2187.

15 Schmidbaur, H.; Schier, A. Aurophilic Interactions In and Between Molecules as a Subject of Current Interest. *Chem. Soc. Rev*. **2012**, *41*, 370−412.

16 Mirzadeh, N.; Privér, S. H.; Blake, A. J.; Schmidbaur, H.; Bhargava, S. K. Innovative Molecular Design Strategies in Materials Science Following the Aurophilicity Concept. *Chem. Rev*. **2020**, *120*, 7551−7591.

17 Balch, A. L. Polymorphism and Luminescent Behavior of Linear, Two-Coordinate Gold(I) Complexes**.** *Gold Bull*. **2004**, *37*, 45-50.

18 England, K. R.; Lim, S. H.; Luong, L. M. C.; Olmstead, M. M.; Balch, A. L. Vapoluminescent Behavior and the Single-Crystal-to Single-Crystal Transformations of Chloroform Solvates of $[Au_2(\mu\text{-}1,2\text{-bis(diphenylarsino)ethane})_2](AsF_6)_2$. *Chem. Eur. J.* **2019**, *25*, 874 – 878.

19 Luong, L. M. C.; Lowe, C. D.; Adams, A. V.; Moshayedi, V.; Olmstead, M. M.; Balch, A. L. Seeing luminescence appear as crystals crumble. Isolation and subsequent self-association of individual $[(C_6H_{11}NC)_2Au]^+$ ions in crystals. *Chem. Sci*. **2020**, *11*, 11705–11713.

20 Bridgeman, A. J.; Cavigliasso, G.; Ireland, L. R.; Rothery, J., The Mayer bond order as a tool in inorganic chemistry. *Dalton Trans.* **2001,** (14), 2095-2108.

21 Mayer, I., Charge, bond order and valence in the AB initio SCF theory. *Chem. Phys. Lett.* **1983,** *97* (3), 270-274.

22 Mayer, I., Bond order and valence: Relations to Mulliken's population analysis. *Internat. J. Quantum Chem.* **1984,** *26* (1), 151-154.

23 Pyykkö, P., Relativistic quantum chemistry. In *Advances in quantum chemistry*, Elsevier: 1978; Vol. 11, pp 353-409.

24 Pyykko, P.; Desclaux, J. P., Relativity and the periodic system of elements. *Acc. Chem. Res.* **1979,** *12* (8), 276-281.

25 Pyykkö, P., Strong closed-shell interactions in inorganic chemistry. *Chem. Rev.* **1997,** *97*, 597-636.

26 Schmidbaur, H., The aurophilicity phenomenon: a decade of experimental findings, theoretical concepts and emerging applications. *Gold Bull.* **2000,** *33*, 3-10.

27 Hutchings, G. J.; Brust, M.; Schmidbaur, H., Gold—an introductory perspective. *Chem. Soc. Rev.* **2008,** *37*, 1759-1765.

28 Wang, S.-G.; Schwarz, W. H. E., Quasi-Relativistic Density Functional Study of Aurophilic Interactions. *J. Am. Chem. Soc.* **2004,** *126*, 1266-1276.

29 Schmidbaur, H.; Hartmann, C.; Reber, G.; Muller, G. Isovalent and Mixed-Valent Ylide Complexes of Gold: The Synthesis of Trinuclear Compounds Having Double Paddlewheel Structure. *Angew. Chem. Int. Ed.* **1987**, *26*, 1146-1148.

30 Zank, J.; Schier, A.; Schmidbaur, H. Gold and silver cations in the "Procrustean Bed" of the bis[2-(diphenylphosphino)phenyl]phenylphosphine ligand. Observations and conclusions. *J. Chem. Soc., Dalton Trans.* **1999**, 415-420.

31 Ziolo, R.; Lipton, S.; Z. Dori, Z. The Photoluminescence of Phosphine Complexes of d^{10} Metals. *Chem. Comm.* **1970**, 1124-1125.

32 King, C.; Khan, M. N. I.; Staples, R. J.; Fackler, Jr., J. P. Luminescent mononuclear gold(I) phosphines. *Inorg. Chem.* **1992**, *31,* 3236-3238.

33 Barakat, K. A.; Cundari, T. R.; Omary, M. A. Jahn−Teller Distortion in the Phosphorescent Excited State of Three-Coordinate Au(I) Phosphine Complexes. *J. Am. Chem. Soc*. **2003**, *125*, 14228-14229.

34 Sinha, P.; Wilson, A. K.; Omary, M. A. Beyond a T-Shape. *J. Am. Chem. Soc*. **2005**, *127*, 12488-12489.

35 Sheldrick, G. M. A short history of *SHELX*. *Acta Crystallogr., Sect. A*, **2008**, *64*, 112-122.

36 Neese, F., The ORCA program system. *WIREs Computational Molecular Science* **2012,** *2*, 73-78.

37 Neese, F., Software update: The ORCA program system—Version 5.0. *WIREs Computational Molecular Science* **2022**, e1606.

38 Becke, A. D., Density-functional exchange-energy approximation with correct asymptotic behavior. *Phys. Rev. A Gen. Phys.* **1988,** *38*, 3098-3100.

39 Stephens, P. J.; Devlin, F. J.; Chabalowski, C. F.; Frisch, M. J., Ab initio calculation of vibrational absorption and circular dichroism spectra using density functional force fields. *J. Phys. Chem.* **1994,** *98*, 45, 11623-11627.

40 Becke, A. D., Density-functional thermochemistry. III. The role of exact exchange. *J. Chem. Phys.* **1993,** *98*, 5648-5652.

41 Lee, C.; Yang, W.; Parr, R. G., Development of the Colle-Salvetti correlation-energy formula into a functional of the electron density. *Phys. Rev. B* **1988,** *37*, 785.

42 Guevara-Vela, J. M.; Rocha-Rinza, T.; Pendás, Á. M., Performance of the RI and RIJCOSX approximations in the topological analysis of the electron density. *Theor. Chem. Acc.* **2017,** *136*, 57.

43 Neese, F., An improvement of the resolution of the identity approximation for the formation of the Coulomb matrix. *J. Comput. Chem.* **2003,** *24*, 1740-1747.

44 Neese, F.; Wennmohs, F.; Hansen, A.; Becker, U., Efficient, approximate and parallel Hartree–Fock and hybrid DFT calculations. A 'chain-of-spheres' algorithm for the Hartree–Fock exchange. *Chem. Phys.* **2009,** *356*, 98-109.

45 Weigend, F., Accurate Coulomb-Fitting Basis Sets for H to Rn. *Phys. Chem. Chem. Phys.* **2006,** *8*, 1057-1065.

46 Pantazis, D. A.; Chen, X.-Y.; Landis, C. R.; Neese, F., All-Electron Scalar Relativistic Basis Sets for Third-Row Transition Metal Atoms. *J. Chem. Theory Comput.* **2008,** *4*, 908-919.

47 Peterson, K. A.; Puzzarini, C., Systematically Convergent Basis Sets for Transition Metals. II Pseudopotential-Based Correlation Consistent Basis Sets for the Group 11 (Cu, Ag, Au) and 12 (Zn, Cd, Hg) Elements. *Theor. Chem. Acc.* **2005,** *114*, 283-296.

48 Rolfes, J. D.; Neese, F.; Pantazis, D. A., All-electron scalar relativistic basis sets for the elements Rb–Xe. *J. Comput. Chem.* **2020,** *41*, 1842-1849.

49 Weigend, F.; Ahlrichs, R., Balanced Basis Sets of Split Valence, Triple Zeta Valence and Quadruple Zeta Valence Quality hor H To Rn: Design and Assessment of Accuracy. *Phys. Chem. Chem. Phys.* **2005,** *7*, 3297-3305.

50 Weigend, F., Accurate Coulomb-fitting basis sets for H to Rn. *Phys. Chem. Chem. Phys.* **2006,** *8*, 1057-1065.

51 Grimme, S.; Antony, J.; Ehrlich, S.; Krieg, H., A Consistent and Accurate ab initio Parametrization of Density Functional Dispersion Correction (DFT-D) for the 94 Elements H-Pu. *J. Chem. Phys.* **2010,** *132*, 154104.

52 Grimme, S.; Ehrlich, S.; Goerigk, L., Effect of the Damping Function in Dispersion Corrected Density Functional Theory. *J. Comput. Chem.* **2011,** *32*, 1456-1465.

53 Pettersen, E. F.; Goddard, T. D.; Huang, C. C.; Couch, G. S.; Greenblatt, D. M.; Meng, E. C.; Ferrin, T. E., UCSF Chimera—A Visualization System for Exploratory Research and Analysis. *J. Comput. Chem.* **2004,** *25*, 1605-1612.

54 Macrae, C. F.; Sovago, I.; Cottrell, S. J.; Galek, P. T. A.; McCabe, P.; Pidcock, E.; Platings, M.; Shields, G. P.; Stevens, J. S.; Towler, M.; Wood, P. A., Mercury 4.0: from visualization to analysis, design and prediction. *J. Appl. Crystallogr.* **2020,** *53*, 226-235.

TOC Image

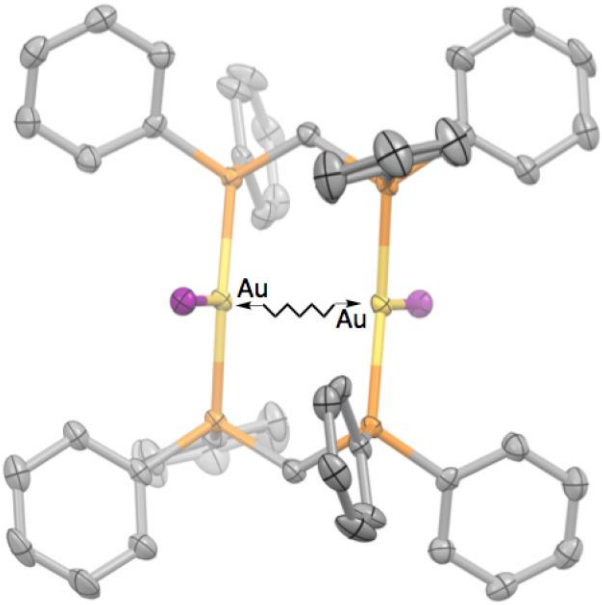

TOC Text:

The flexibility of the three-coordinate dimer, Au_2(μ-1,2-bis-(diphenylphosphino)ethane)$_2I_2$, with different separations between the gold ions in crystalline solvates has been examined crystallographically, spectroscopically and by computations.

Chapter 2

Structure and Luminescence Studies of Salts of the Helical Dication, $[Au_2(\mu\text{-bis(diphenylphosphine)ethane})_2]^{2+}$ and Comparison with Salts of $[Au_2(\mu\text{-bis(diphenylphosphine)propane})_2]^{2+}$ †

† Reprinted in part with permission from Costa, S.; Walters, D. T.; McNamara, L. E.; Olmstead, M. M.; Fettinger, J. C.; Balch, A. L. Structure and Luminescence Studies of Salts of the Helical Dication, $[Au_2(\mu\text{-Bis(Diphenylphosphine)Ethane})_2]^{2+}$ and Comparison with Salts of $[Au_2(\mu\text{-Bis(Diphenylphosphine)Propane})_2]^{2+}$. *Inorg. Chem.* **2023**, *62* (39), 15902–15911. https://pubs.acs.org/doi/full/10.1021/acs.inorgchem.3c01961.

Abstract

Six salts ($[Au_2(\mu\text{-dppe})_2](BF_4)_2 \bullet CHCl_3$, $[Au_2(\mu\text{-dppe})_2](BF_4)_2 \bullet 1,2\text{-}Cl_2C_2H_4$, $[Au_2(\mu\text{-dppe})_2](PF_6)_2 \bullet CHCl_3$, $[Au_2(\mu\text{-dppe})_2](PF_6)_2$, $[Au_2(\mu\text{-dppe})_2](SbF_6)_2$, and $[Au_2(\mu\text{-dppe})_2](OTf)_2 \bullet 2CHCl_3$, (dppe is bis-(diphenylphosphine)ethane) containing the dication, $[Au_2(\mu\text{-dppe})_2]^{2+}$, have been prepared and structurally characterized by single crystal X-ray crystallography. Unlike the three-coordinate dppe-bridged dimers, $Au_2X_2(\mu\text{-dppe})_2$ (X = Br, I), which show considerable variation in the distance between the gold(I) ions over the range 3.8479(3) to 3.0995(10) Å in various solvates, the structure of the helical dication, $[Au_2(\mu\text{-dppe})_2]$, in the new non-coordinating salts is remarkably consistent with the Au···Au separation falling in the narrow range 2.9593(5) Å to 2.8787(9) Å. In the solid state, the six crystals display a green luminescence at room temperature and at 77 K, which has been assigned as phosphorescence. However, solutions of the dication are not luminescent. Salts containing the analogous dication, $[Au_2(\mu\text{-dppp})_2](PF_6)_2$ (dppp is bis-(diphenylphosphine)propane), have been prepared to determine whether the longer bridging ligand might also twist into a helical shape. These salts include $[Au_2(\mu\text{-dppp})_2](OTf)_2$ (OTf is triflate) and three crystalline forms of $[Au_2(\mu\text{-dppp})_2](PF_6)_2$: the solvate, $[Au_2(\mu\text{-dppp})_2](PF_6)_2 \bullet (CHCl_3)$, and two polymorphs of the unsolvated salt. None of these crystals are luminescent but all contain a similar dication, $[Au_2(\mu\text{-dppp})_2]^{2+}$, that contains two nearly parallel, linear P-Au-P groups and a long separation between the gold ions that varies from 5.6613(6) to 5.3409(4) Å.

Introduction

Many gold(I) complexes display interesting luminescent properties that make them promising candidates for applications in sensing and electro-optic devices.[1-6] For example, three-coordinate, planar gold(I) complexes are generally luminescent both in the solid state and in solution.[7-11] For such trigonal planar complexes, the excitation process involves a transition from the filled, in-plane $d_{x^2-y^2}$,d_{xy} gold orbitals to an empty orbital that may be a ligand-based orbital or the p_z gold orbital and may cause significant distortion of the excited state.[10,11]

On the other hand, two-coordinate linear gold(I) complexes are frequently non-emissive but can become emissive through aurophilic interactions with another gold(I) center.[1,12-15] For example, salts containing the cations, $[(cyclohexylNC)_2Au]^+$, exhibit no luminescence when the cations are isolated from one another, but show vibrant emission when aggregation occurs due to the formation of close contacts between the gold(I) ions.[16-20]

Prior work has demonstrated that planar, three-coordinate, gold(I) complexes bridged by bis-(diphenylphosphine)ethane, (dppe), ligands show remarkable flexibility that is reflected in the Au···Au distance and in the luminescence of the complexes. For example, dimeric $Au_2(\mu\text{-dppe})_2Br_2$ crystallizes as a variety of different solvates in which the Au···Au separations range from 3.0995(10) to 3.8479(3)Å.[21] Figure 1 shows the structure of one such solvate, $Au_2(\mu\text{-dppe})_2Br_2\bullet 2(OSMe_2)$, which has the longest Au···Au separation, 3.8479(3) Å. The luminescence for different solvates of $Au_2(\mu\text{-dppe})_2Br_2$ varies. Crystals with Au···Au separations longer than 3.5 Å display orange luminescence, while those with Au···Au separations shorter than 3.5 Å produce green luminescence. While the presence of different solvate molecules in these crystals alters the molecular packing, no direct interactions of the solvate molecules with the gold ions have been identified.

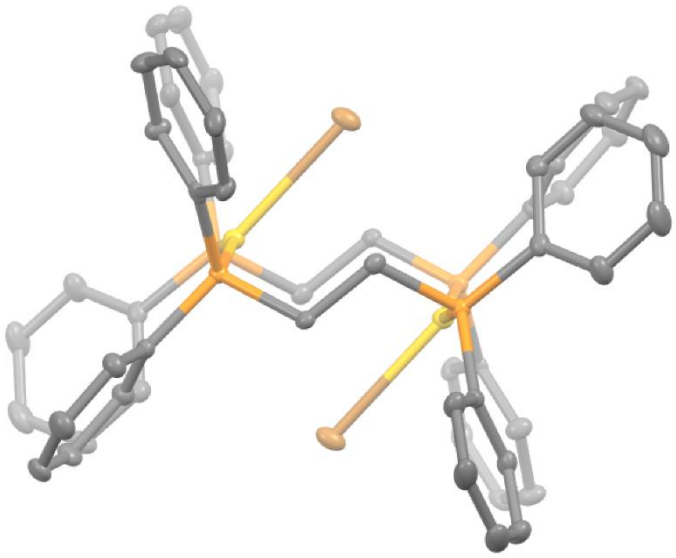

Figure 1. The structure of the centrosymmetric dimer, $Au_2(\mu\text{-dppe})_2Br_2$, in crystalline $Au_2(\mu\text{-dppe})_2Br_2\bullet 2(OSMe_2)$ where the Au···Au separation is 3.8479(3) Å drawn with thermal contours at the 30% probability level. For clarity hydrogen atoms and solvate molecules have been omitted. Color scheme: gold, yellow; phosphorus, orange; bromine, brown; carbon, grey.

The related three-coordinate dimer, $Au_2(\mu\text{-dppe})_2I_2$, crystallizes from acetone solution as two polymorphs that also show the flexibility of the bridging ligand. Crystals of $\alpha\text{-}Au_2(\mu\text{-dppe})_2I_2\cdot 2OCMe_2$ exhibit orange emission and an Au···Au distance of 3.6720(2) Å while colorless crystals of $\beta\text{-}Au_2(\mu\text{-dppe})_2I_2\cdot 2OCMe_2$ (2) display a green emission and a shorter Au···Au distance of 3.3955(2) Å.[22]

Most other two coordinate gold(I) complexes lack aurophilic interactions and luminescence. However, based on the previous work, we became interested in examining the luminescence and structure of the dimeric dication $[Au_2(\mu\text{-dppe})_2]^{2+}$.[23,24] Peringer and coworkers examined the structure of $[Au_2(\mu\text{-dppe})_2](OTf)_2\bullet 2CH_3OH$ and observed that it had a helical

structure with a short Au···Au distance of 2.9594(10) Å and two distinct environments for the phosphorus atoms.[1] Nevertheless, in solution only a single ^{31}P NMR resonance was detected, which the authors suggested came from rapid exchange. Awuah and coworkers found a similar structure for the dication in another salt, $[Au_2(\mu\text{-dppe})_2](ClO_4)_2 \bullet CH_3CN$.[26] However, they also reported a computed structure at the B3LYP level that produced a more symmetrical, non-helical structure with an Au···Au separation of 4.494 Å. Since solvate molecules and poorly coordinated anions can influence the structures of gold(I) complexes,[27-30] we have prepared and examined several other salts containing the dimeric dication, $[Au_2(\mu\text{-dppe})_2]^{2+}$, to examine their luminescence and the possibility that the cation structure might be flexible and readily altered. We have also prepared and examined the structure of the related dication, $[Au_2(\mu\text{-dppp})_2]^{2+}$ (dppp is bis-(diphenylphosphine)propane), with a longer bridging diphosphine ligand in order to see how the longer bridge affects structure and luminescence. In related cases, longer bridging diphosphines tend to create longer separations between gold(I) centers in dinuclear complexes.[31,32] It is also interesting to note that with only one bridging dppe ligand, the two-coordinate complex, AuCl(μ-dppp)AuCl, lacks intramolecular aurophilic interactions but dimerizes via two intermolecular aurophilic interactions in the solid state.[33,34]

Results and Discussion

Preparation of Salts of $[Au_2(\mu\text{-dppe})_2]^{2+}$. Salts containing $[Au_2(\mu\text{-dppe})_2]^{2+}$ were obtained by mixing dichloromethane solutions of equimolar amounts of thtAuCl and dppe followed by the addition of the appropriate anion from sodium tetrafluoroborate, ammonium hexafluoro-phosphate, sodium hexafluorostibonate, or potassium triflate in a mixture of dichloromethane and methanol. The resulting solutions were evaporated to dryness and the resulting solids were treated with dichloromethane to extract the gold salt. The dichloromethane solution was evaporated to dryness. Colorless crystals of $[Au_2(\mu\text{-dppe})_2](BF_4)_2\bullet CHCl_3$, $[Au_2(\mu\text{-dppe})_2](BF_4)_2\bullet 1,2\text{-}Cl_2C_2H_4$, $[Au_2(\mu\text{-dppe})_2](PF_6)_2\bullet CHCl_3$, $[Au_2(\mu\text{-dppe})_2](SbF_6)_2$, and $[Au_2(\mu\text{-dppe})_2](OTf)_2 \bullet 2(CHCl_3)$, each with a green luminescence, were grown by slow diffusion of a mixture of diethyl ether or toluene into a chloroform or 1,2-dichloroethane solution of the salt.

Crystallographic Characterization of Salts Containing $[Au_2(\mu\text{-dppe})_2]^{2+}$. The structure of the dication, $[Au_2(\mu\text{-dppe})_2]^{2+}$, changes only slightly in the six different crystalline salts examined here and is similar to that found earlier in $[Au_2(\mu\text{-dppe})_2](OTf)_2\bullet 2CH_3OH$ and $[Au_2(\mu\text{-dppe})_2](ClO_4)_2\bullet CH_3CN$.[25,26] Figure 2 shows two views of the dication in crystals of $Au_2(\mu\text{-dppe})_2](BF_4)_2\bullet(CHCl_3)$. The view labelled B of this figure shows, the cation has a helical geometry with the bridging diphosphine ligands twisting about the two gold ions. These diphosphine ligands are arranged so that two of the eight phenyl rings extend outward at one end of the dication on the left side of Figure 2 A, while four of the phenyl groups protrude outwardly at the opposite end of the dication on the right side of Figure 2 A. In the salts reported here, individual dications are chiral due to their helical shape. However, these salts form in the centrosymmetric space groups, $P2_1/c$ or $P\bar{1}$, and consequently each crystal contains a racemate of the dications.

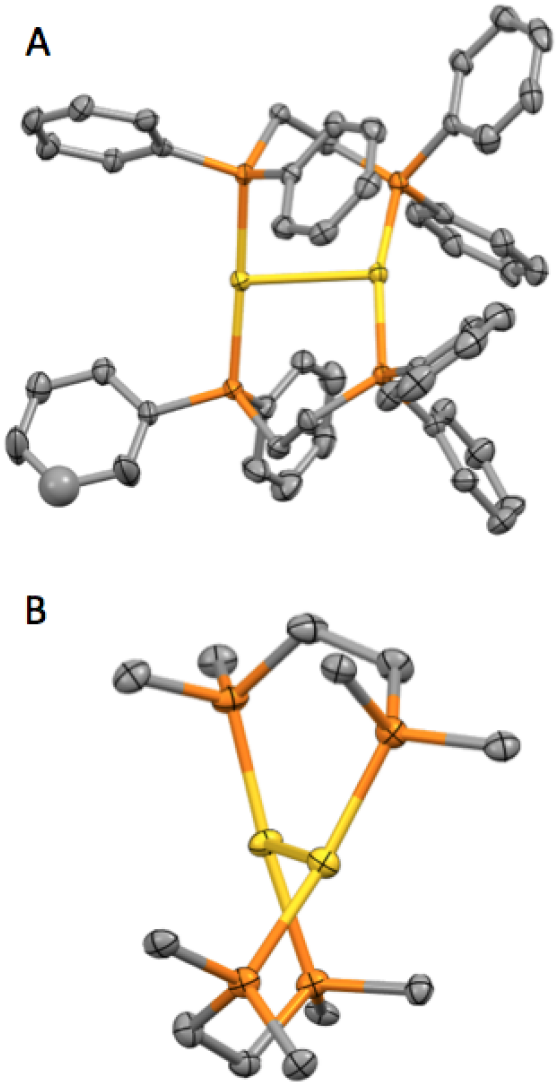

Figure 2. Two views of the structure of the dication, $[Au_2(\mu\text{-dppe})_2]^{2+}$, in crystalline $Au_2(\mu\text{-dppe})_2](BF_4)_2\bullet(CHCl_3)$ drawn with thermal contours at the 50% probability level. In B, only the ipso carbon atoms of each phenyl ring are shown for clarity. Color scheme: gold, yellow; phosphorus, orange; carbon, grey.

Figure 3 shows the numbering scheme of the dication. Table 1 presents bond distances, bond angles and torsional angles for the dication in the different salts. Each gold ion is bound to

two phosphorus atoms of the bridging dppe ligands and to the other gold ion. The Au···Au distance varies only slightly over the range, 2.8787(9) to 2.9593(5)Å. In contrast, the three coordinate, centrosymmetric dimer, $Au_2(\mu\text{-dppe})_2Br_2$, has a large variation in the Au···Au separation from 3.0943(2) to 3.8479(3)Å in different solvated crystals.[21,22] In $[Au_2(\mu\text{-dppe})_2]^{2+}$ the P1-Au1-P4 bond angles range from 164.82(3) to 171.37(3)° while the P2-Au2-P3 bond angles, which range from 174.14(3) to 179.21(7)°, are more nearly linear. The Au2 center is consistently near the anions with two phenyl rings pointed away from the cation. In comparison to these bond angles, the torsional angles, P2-Au2···Au1-P1 and P3-Au2···Au1-P4, are nearly equal in the hexafluorophosphate, hexafluoroantimonate and triflate salts. These torsional angles differ significantly only in the two solvated forms of the smallest anion, the tetrafluoroborate salts.

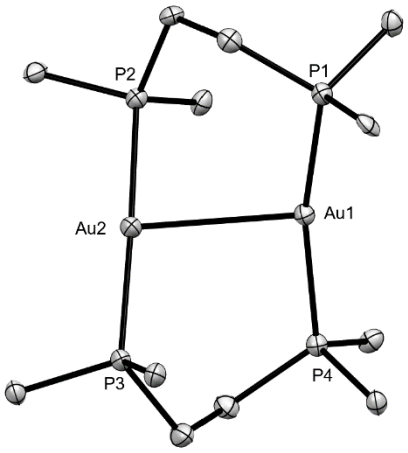

Figure 3. Numbering scheme for the dication $[Au_2(\mu\text{-dppe})_2]^{2+}$. Only the ipso carbon atom of each phenyl ring is shown for clarity. Anions and solvate molecules are not shown.

Table 1. Selected Bond Distances and Angles for $[Au_2(\mu\text{-dppe})_2]^{2+}$.

Complex	$[Au_2(\mu\text{-dppe})_2](BF_4)_2 \bullet CHCl_3$	$[Au_2(\mu\text{-dppe})_2](BF_4)_2 \bullet 1,2\text{-}Cl_2C_2H_4$	$[Au_2(\mu\text{-dppe})_2](PF_6)_2 \bullet CHCl_3$	$[Au_2(\mu\text{-dppe})_2](PF_6)_2$	$[Au_2(\mu\text{-dppe})_2](SbF_6)_2$	$[Au_2(\mu\text{-dppe})_2](OTf)_2 \bullet 2CHCl_3$
Distances (Å)						
Au-Au	2.8954(4)	2.8787(9)	2.9414(5)	2.9329(5)	2.9460(4)	2.9593(5)
Au1-P1	2.302(2)	2.301(1)	2.3087(9)	2.319(2)	2.305(1)	2.3146(9)
Au1-P4	2.302(2)	2.299(1)	2.3060(7)	2.313(2)	2.307(1)	2.312(1)
Au2-P2	2.325(1)	2.3133(9)	2.3056(9)	2.299(2)	2.307(1)	2.308(1)
Au2-P3	2.316(2)	2.3254(9)	2.3157(7)	2.313(2)	2.304(1)	2.312(1)
Angles (deg)						
P1-Au1-P4	164.82(6)	164.82	166.09(3)	170.88(7)	171.32(5)	171.37(3)
P2-Au2-P3	174.61(6)	174.14	177.86(3)	179.21(7)	176.92(5)	176.17(3)
Torsional angles (deg)						
P2-Au2···Au1-P1	54.79(6)	38.56(3)	41.81(3)	42.73(7)	47.76(5)	47.06(3)
P3-Au2···Au1-P4	39.16(6)	54.65(3)	45.32(3)	45.40(7)	46.64(5)	47.23(3)

Spectroscopic Properties the dication, $[Au_2(\mu\text{-dppe})_2]^{2+}$. Each of the six salts reported here exhibit green luminescence in the solid state at room temperature. The excitation and emission spectra of crystals of $[Au_2(\mu\text{-dppe})_2](BF_4)_2 \bullet CHCl_3$ are shown in Figure 4. The excitation and emission spectra of the other crystals are similar and are shown in the Supporting Information. The excitation and emission wavelengths and lifetimes for these salts are given in Table 2. Based on the large Stokes' shifts in these spectra and the microsecond lifetimes, it appears that the emissions of these salts are due to phosphorescence.

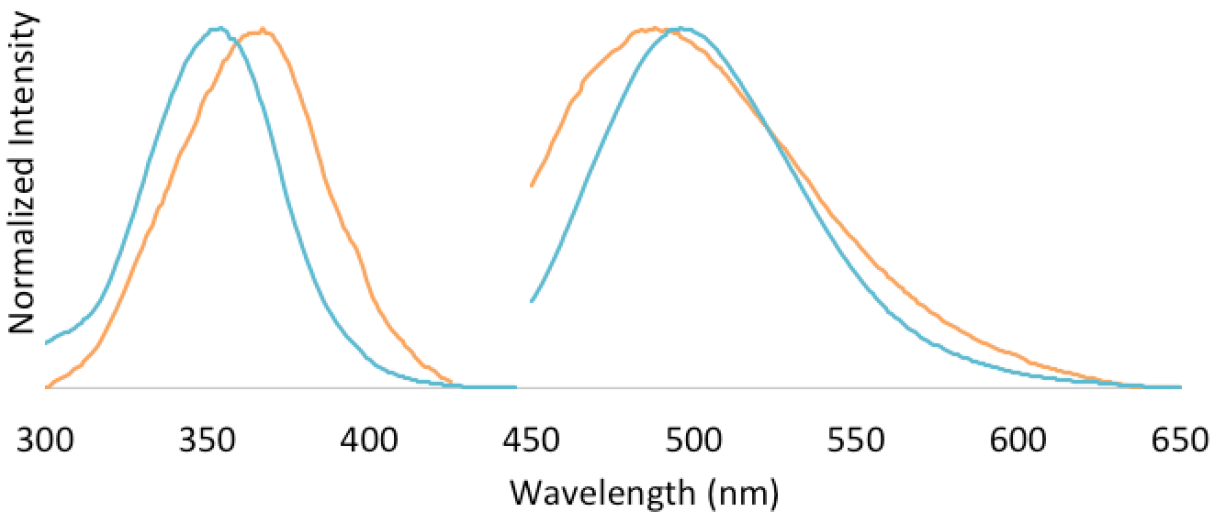

Figure 4. The excitation and emission spectra of crystals of $[Au_2(\mu\text{-dppe})_2](BF_4)_2 \bullet CHCl_3$ at room temperature in blue (emission obtained with excitation at 367 nm, excitation obtained for emission at 493 nm) and at 77 K in orange (emission obtained with excitation at 354 nm, excitation obtained for emission at 488 nm).

Table 2. Data for Excitation and Emission of Salts Containing $[Au_2(\mu\text{-dppe})_2]^{2+}$

			298K			77K		
Crystal Composition	Au--Au bond distance (Å)	Visual Color	Emission (nm)	Lifetime (ms)	Excitation (nm)	Emission (nm)	Lifetime (ms)	Excitation (nm)
$[Au_2(\mu\text{-dppe})_2](BF_4)_2 \bullet CHCl_3$	2.878(6)	green	484	32	367	486	33	354
$[Au_2(\mu\text{-dppe})_2](BF_4)_2 \bullet 1,2\text{-}Cl_2C_2H_4$	2.878(6)	green	484	32	355	486	33	348
$[Au_2(\mu\text{-dppe})_2](PF_6)_2 \bullet CHCl_3$	2.941(5)	green	474	32	378	485	34	364
$[Au_2(\mu\text{-dppe})_2](PF_6)_2$	2.9329(5)	green	494		374	495		350
$[Au_2(\mu\text{-dppe})_2](SbF_6)_2$	2.95(2)	green	494	11	361	501	34	357
$[Au_2(\mu\text{-dppe})_2]OTf_2 \bullet CHCl_3$	2.959(4)	green	491	32	364	491	32	358

The UV spectrum of an acetonitrile solution of $[Au_2(\mu\text{-dppe})_2](PF_6)_2$ is shown in Figure 5. Notice that there is no significant absorption at 365 nm, where the crystalline forms of this cation display their excitation maxima. This observation suggests that the structure of $[Au_2(\mu\text{-dppe})_2]^{2+}$ in solution differs from the structure found in the solid state. It is possible that this dication in solution has a structure like that calculated by Awuah and coworkers with a long separation between the gold(I) ions and no significant aurophilic interaction, which is why there is no luminescence.[26]

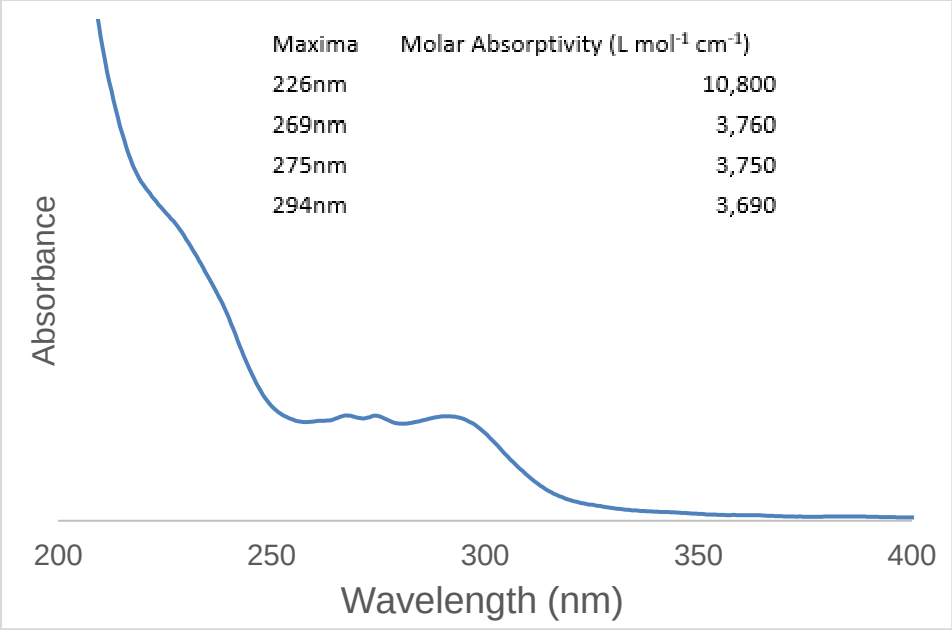

Figure 5. UV spectrum of $[Au_2(\mu\text{-dppe})_2](PF_6)_2$ in acetonitrile solution at room temperature.

At room temperature, colorless solutions of salts containing the dication, $[Au_2(\mu\text{-dppe})_2]^{2+}$, are not emissive. However, upon freezing in liquid nitrogen, these solutions become luminescent. Relevant spectra for solid $Au_2(\mu\text{-dppe})_2](PF_6)_2$ and frozen solutions of this salt in a variety of solvents are shown in Figure 6. As the spectra show, there is a dependence of the excitation and emission wavelengths on the nature of the frozen solvent involved. Solvation effects, particularly in the vicinity of the gold ions are the likely cause of the minor differences in these spectra in Figure 6. There is a precedent for such behaviour, the dimeric dication, $[Au_2(\mu\text{-dpae})_2]^{2+}$ (dpae is 1,2-bis(diphenylarsino)ethane) has a helical structure analogous to that of $[Au_2(\mu\text{-dppe})_2]^{2+}$.[35] Over time crystals of the di-solvate $[Au_2(\mu\text{-dpae})_2](AsF_6)_2\bullet 2(CHCl_3)$ loose chloroform and are converted into the mono-solvate, $[Au_2(\mu\text{-dpae})_2](AsF_6)_2\bullet(CHCl_3)$. This process is accompanied by a change in luminescence and a change in the surroundings of one of the gold ions in the dication.

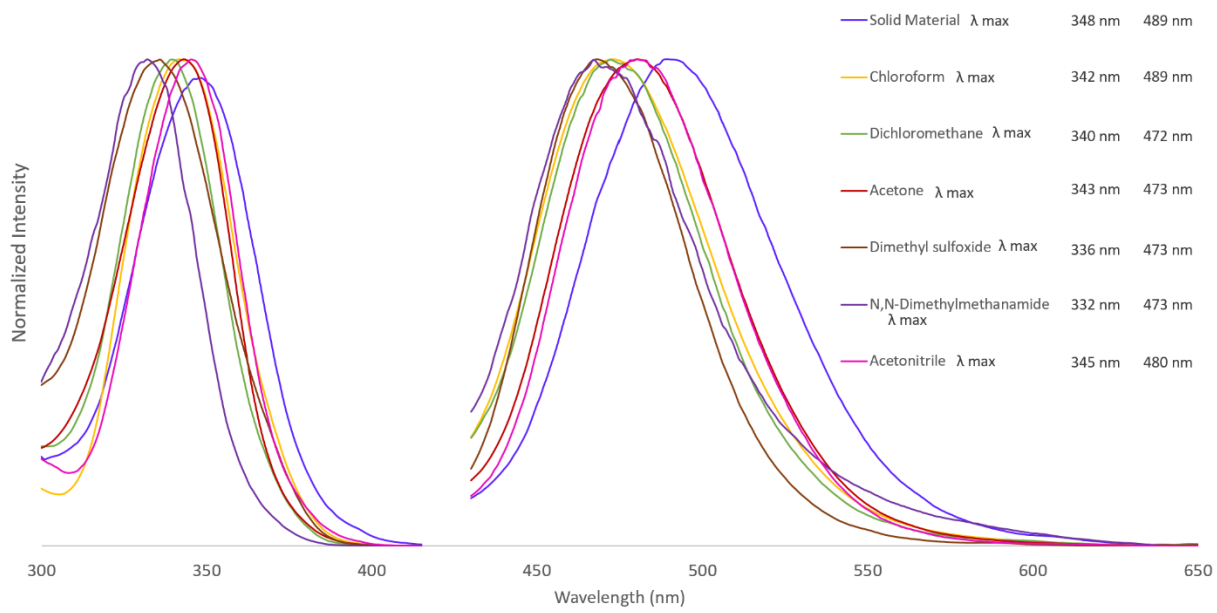

Figure 6. The excitation (left) and emission (right) spectra of $[Au_2(\mu\text{-dppe})_2](PF_6)_2$ as a solid and in various frozen solutions at 77 K.

The $^{31}P\{^1H\}$ NMR spectrum of $[Au_2(\mu\text{-dppe})_2](BF_4)_2$ in chloroform-*d* solution shows a single resonance at 38.4 ppm at 290 K. Cooling the solution results only in a slight downfield shift to 38.2 ppm at 273 K, 38.2 ppm at 263 K, and 38.1 ppm at 253 K. These results are consistent with the data reported by Peringer and coworkers, who observed only a single $^{31}P\{^1H\}$ NMR resonance at all temperatures for a solution of $[Au_2(\mu\text{-dppe})_2](OTf)_2 \bullet 2CH_3OH$.[25] The observation of only a single $^{31}P\{^1H\}$ resonance could be explained by either rapid exchange of the phosphorus atoms between the two different environment seen in the crystal or by the existence of a more symmetrical, non-helical structure like that computed by Awuah and coworkers in solution.[26]

Infrared spectra are reported for these salts in the experimental section. These spectra are dominated by vibrations of the diphosphine ligand, but there are also characteristic vibrational bands due to the individual anions that distinguish each spectrum.

$[Au_2(\mu\text{-dppp})_2]^{2+}$. Salts containing $[Au_2(\mu\text{-dppp})_2]^{2+}$ were obtained by mixing dichloromethane solutions of equimolar amounts of thtAuCl and dppe followed by the addition of ammonium hexafluorophosphate or potassium triflate in a mixture of dichloromethane and methanol as described for salts of $[Au_2(\mu\text{-dppe})_2]^{2+}$. Three crystalline forms of $[Au_2(\mu\text{-dppp})_2](PF_6)_2$ and $[Au_2(\mu\text{-dppp})_2](OTf)_2$ were grown concomitantly by diffusion of diethyl ether into a chloroform solution of the salt.

Structural Characterization of $[Au_2(\mu\text{-dppp})_2](PF_6)_2$ and $[Au_2(\mu\text{-dppp})_2](OTf)_2$. Three colorless crystalline salts containing the dication $[Au_2(\mu\text{-dppp})_2]^{2+}$ with hexafluorophosphate as the counter ion have been obtained: the solvate $[Au_2(\mu\text{-dppp})_2](PF_6)_2\bullet(CHCl_3)$, and two polymorphs (designated as the α and β forms) of the unsolvated salt.

The structure of the dication, $[Au_2(\mu\text{-dppp})_2]^{2+}$, in the solvate, $[Au_2(\mu\text{-dppp})_2](PF_6)_2\bullet(CHCl_3)$ is shown in part **A** of Figure 7, where its structure is compared with that of the α–polymorph $Au_2(\mu\text{-dppp})_2](PF_6)_2$ in part **B**. The dication in the solvate, $[Au_2(\mu\text{-dppp})_2](PF_6)_2\bullet(CHCl_3)$ has no crystallographic symmetry, while the dication in the α –polymorph $Au_2(\mu\text{-dppp})_2](PF_6)_2$ is centrosymmetric. Figure 8 offers another comparison of the structure of the dication in $[Au_2(\mu\text{-dppp})_2](PF_6)_2\bullet(CHCl_3)$ with the structure of the dication in the entrosymmetric α –polymorph of $Au_2(\mu\text{-dppp})_2](PF_6)_2$. In Figure 8 these dications are viewed down the P-Au-P axes of each dication. The structure of the dication in the β polymorph of $Au_2(\mu\text{-dppp})_2](PF_6)_2$ is also centrosymmetric with a structure similar to that of the α polymorph. Likewise, the dication in $[Au_2(\mu\text{-dppp})_2](OTf)_2$ is also centrosymmetric and has a similar structure

to the centrosymmetric dimer shown in Figures 7 and 8. In all these structures the P-Au-P units are nearly linear and parallel to one another with a rather long separation of the two gold ions, which ranges from 5.6613(6) to 5.3409(4) Å. Comparative structural data are contained in Table 3.

Figure 7 also shows the structure of the related three-coordinate dimer, $Au_2I_2(\mu\text{-dppp})_2$, whose structure was reported earlier.[32] $Au_2I_2(\mu\text{-dppp})_2$ also has a centrosymmetric structure with the two gold ions widely separated by 5.067(2) Å. Each gold ion is coordinated to two phosphorus atoms and an iodide ion. Since the complex contains three-coordinate gold(I), the P-Au-P angle (152.88(5)°) is far from linear.

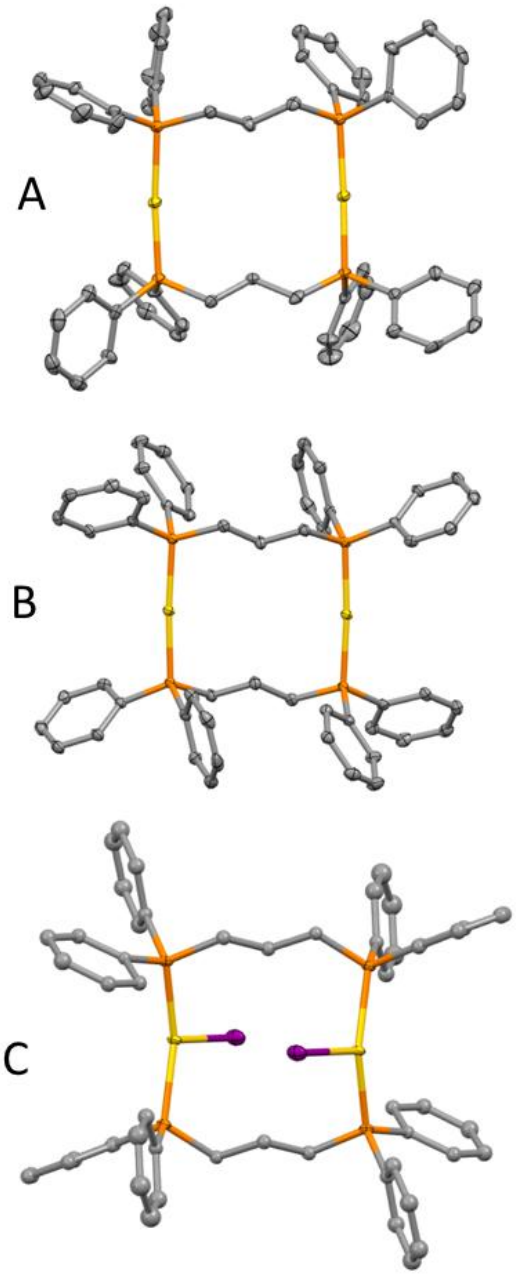

Figure 7. A, the structure of the dication, $[Au_2(\mu\text{-dppp})_2]^{2+}$, in crystalline $Au_2(\mu\text{-dppp})_2](PF_6)_2 \bullet CHCl_3$; **B**, the structure of the centrosymmetric dication, $[Au_2(\mu\text{-dppp})_2]^{2+}$, in the a polymorph of $Au_2(\mu\text{-dppp})_2](PF_6)_2$; and **C**, the structure of centrosymmetric $Au_2I_2(\mu\text{-dppp})_2$ drawn from coordinates from reference 32 with all thermal contours at the 50%

probability level. Color scheme: gold, yellow; phosphorus, orange; iodine, violet; carbon, grey.

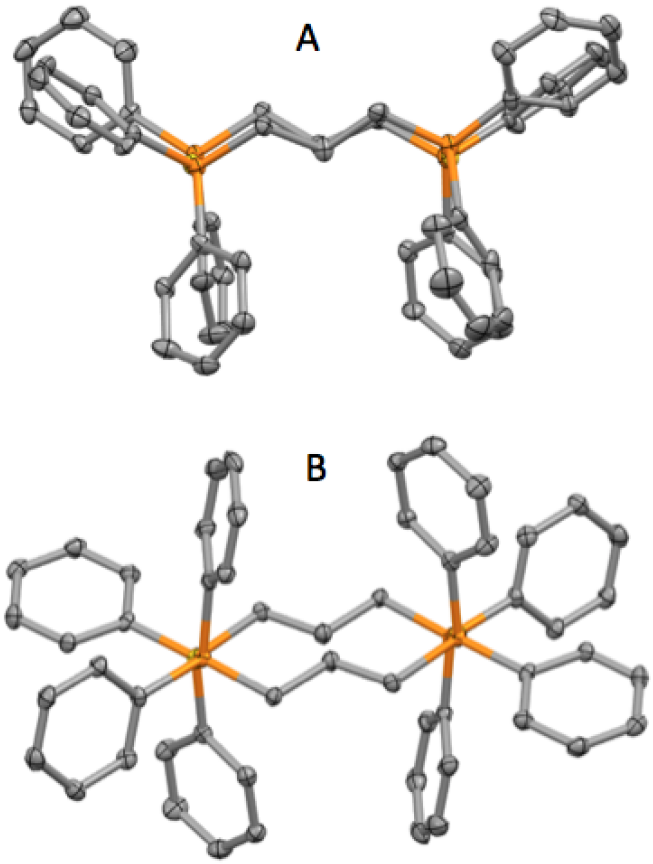

Figure 8. Views down the P-Au-P bonds of: **A**, the dication, $[Au_2(\mu\text{-dppp})_2]^{2+}$, in crystalline $Au_2(\mu\text{-dppp})_2](PF_6)_2 \bullet CHCl_3$; **B**, the centrosymmetric dication, $[Au_2(\mu\text{-dppp})_2]^{2+}$, in the a polymorph of $Au_2(\mu\text{-dppp})_2](PF_6)_2$. Color scheme: gold, yellow; phosphorus, orange; carbon, grey.

Table 3. Selected Bond Distances and Angles for $[Au_2(\mu\text{-dppp})_2]^{2+}$.

Complex	$[Au_2(\mu\text{-dppp})_2](PF_6)_2 \bullet (CHCl_3)$	α-$[Au_2(\mu\text{-dppp})_2](PF_6)_2$	β-$[Au_2(\mu\text{-dppp})_2](PF_6)_2$	$[Au_2(\mu\text{-dppp})_2](OTf)_2$
Distances (Å)				
Au-Au	5.6613(6)	5.6414(3)	5.3409(4)	5.602(1)
Intraligand P···P	5.558(3)	5.483	5.5478(8)	
	5.505(3)			
Au1-P1	2.309(2)	2.3176(7)	2.3045(9)	2.310(2)
Au1-P4	2.311(2)	2.3189(7)	2.3086(9)	2.310(2)
Au2-P2	2.308(2)	2.3189(7)	2.3086(9)	2.310(2)
Au2-P3	2.307(2)	2.3176(7)	2.3045(9)	2.310(2)
Angles (deg)				
P1-Au1-P4	174.60(7)	175.95(3)	169.44(3)	178.4(5)
P2-Au2-P3	175.31(8)	175.95(3)	169.44(3)	178.4(5)
Torsional angles (deg)				
P2-Au2-Au1-P1	6.81(7)	1.04(3)	9.40(3)	0.00
P3-Au2-Au1-P4	6.17(7)	1.04(3)	9.40(3)	0.00

Spectroscopic Properties the dication, $[Au_2(\mu\text{-dppp})_2]^{2+}$. The $^{31}P\{^1H\}$ NMR spectra of samples of $Au_2(\mu\text{-dppp})_2](PF_6)_2$ and $[Au_2(\mu\text{-dppp})_2](OTf)_2$ showed a single resonance at 41.5 ppm at room temperature. None of the salts containing the dication $[Au_2(\mu\text{-dppp})_2]^{2+}$ show any luminescence at 77 K or at room temperature. Solutions of these salts were not luminescent. The lack of luminescence is consistent with the large separation between the gold ions in these dimers, which prevents aurophilic interactions. In contrast, the neutral binuclear complex, $Au_2I_2(\mu\text{-dppp})_2$, whose structure is shown in Figure 7, is luminescent at room temperature with λ_{exc} = 350 nm and λ_{em} =

420 nm as reported previously.[32] The luminescence is of the dimer of $[Au_2(\mu\text{-dppp})_2]^{2+}$ is expected as it is seen in the three-coordinate gold complexes.

Conclusions

While the three-coordinate dppe-bridged dimers, $Au_2X_2(\mu\text{-dppe})_2$ (X = Br, I), show considerable variation in the distance between the gold(I) ions over the range 3.8479(3) to 3.0995(10) Å in various crystalline solvates, the structure of the dication, $[Au_2(\mu\text{-dppe})_2]^{2+}$, in the new salts reported here is remarkably consistent with a helical structure that brings the Au···Au separation into the narrow range 2.9593(5) Å to 2.8787(9). In other words, the anion or the solvate molecules produce only very minor changes in the Au···Au separation. With the two-coordinate gold ions experiencing aurophilic interactions in these salts, each emits a green luminescence at room temperature and at 77 K. However, solutions of the dication are non-luminescent, possibly due to a change in structure with an increase in the separation between the gold(I) ions.

The gold(I) ions in the dication $[Au_2(\mu\text{-dppp})_2]^{2+}$ are widely separated in the various crystals examined here. The longer dppp bridging ligand does not participate in helical twisting that is characteristic for the dication, $[Au_2(\mu\text{-dppe})_2]$ and does not allow the gold(I) ions to engage in aurophilic interactions. Other cases are known where bridging diphosphines with three or more methylene groups between the phosphorus atoms keep metal centers apart and restrict metallophilic interactions.[31,32,36]

Experimental

Preparation of compounds. Methanol, toluene, and dichloromethane were purchased from Sigma-Aldrich Co, LLC. Chloroauric acid was purchased from Strem Chemicals,

Inc. Ammonium hexafluorophosphate was purchased from Alfa Aeser, Inc. Solids were used as received. Solvents were used as received and all reactions were conducted on the bench top open to the atmosphere.

Preparation of $[Au_2(\mu\text{-dppe})_2](BF_4)_2 \bullet CHCl_3$. A 82.5 mg (0.207 mmol) portion of dppe was dissolved in 7 mL of dichloromethane and an equivalent amount of thtAuCl (66.4 mg, 0.207 mmol) which had been dissolved in 4 mL dichloromethane was added to the dppe solution. This solution was stirred for about 10 min followed by the addition of $NaBF_4$ (228.5 mg, 2.07 mmol) that was dissolved in 6 mL of dichloromethane and 2 mL of methanol. The colorless solution was then stirred over a 24-hour period. To remove the excess salt, the crude product was vacuum-dried and the resulting solid was dissolved in a minimum amount of dichloromethane. The colorless solution was filtered using a filter pipet and the filtrate was evaporated to dryness. A crude yield of 119.5 mg (85%) was obtained. The dried crude product was dissolved in chloroform and filtered. This solution was placed at the bottom of an outer diameter of 5 mm diameter glass tube and anti-solvent of diethyl ether or toluene was layered above it. Colorless crystals with green luminescence grew over a two-week period.

Infrared Spectrum (cm^{-1}): 3051 (w), 3018 (w), 2965 (w), 1585 (w), 1486 (w), 1434 (m), 1404 (w), 1270 (m), 1248 (m), 1227(w), 1171 (w), 1132 (m), 1098 (s), 1025 (vs), 996 (m), 919 (w), 872 (w), 841 (w), 796 (w), 737 (s), 689 (vs), 630 (s), 570 (w), 514 (w), 477 (m), 422 (m). The peak at 1025 (vs) cm^{-1} correlates to the B-F stretch of the BF_4^- anion.

$^{31}P\{^1H\}$ Nuclear Magnetic Resonance (ppm): 38.4 ppm in chloroform-*d* at 290 K.

Preparation of $[Au_2(\mu\text{-dppe})_2](PF_6)_2$. This salt was obtained in 70% yield following the procedure used to prepare $[Au_2(\mu\text{-dppe})_2](BF_4)_2 \bullet CHCl_3$ with the substitution of ammonium hexafluorophosphate for sodium tetrafluoroborate.

Infrared Spectrum (cm^{-1}): 3050 (w), 3018 (w), 2965 (w), 1479 (w), 1435 (m), 1399 (w), 1337 (w), 1303 (w), 1269 (w), 1184 (w), 1101(m), 1074 (w), 1030 (w), 994 (w), 828 (vs), 736 (m), 685 (s), 556 (m), 515 (s), 471 (m). The peaks at 828 (vs) and 556 (m) cm^{-1} correlate to the P-F stretch and bend of the PF_6^- anion.

$^{31}P\{^1H\}$ Nuclear Magnetic Resonance : 38.4 ppm in chloroform-*d* at 290 K.

^1H Nuclear Magnetic Resonance: complex multiplets for the aromatic resonances at 7.67, 7.65, 7.62, 7.60, 7.48, 7.46, and 7.43 ppm (40 protons); methylene resonance, quintet, 3.30 ppm (8 protons) chloroform-*d* at 290 K.

Preparation of $[Au_2(\mu\text{-dppe})_2](SbF_6)_2$. This salt was obtained in 6.8% yield following the procedure used to prepare $[Au_2(\mu\text{-dppe})_2](BF_4)_2 \bullet CHCl_3$ with the substitution of sodium hexafluoroantimonate for sodium tetrafluoroborate.

Infrared Spectrum (cm^{-1}): 3058 (w), 2973 (w), 1585 (w), 1483 (w), 1436 (s), 1407 (w), 1333 (w), 1307 (w), 1270 (w), 1189 (w), 1132 (w), 1099 (m), 1070 (w), 1023 (w), 999 (w), 874 (w), 840 (w), 798 (w), 739 (m), 718 (w), 690 (s), 650 (vs), 565 (w), 524 (s), 512 (s), 467 (m), 439 (w), 418 (w) 396(w). The peak at 690 (s) cm^{-1} correlates to the Sb-F stretch of a SbF_6^- anion.

Preparation of $[Au_2(\mu\text{-dppe})_2](OTf)_2 \bullet 2(CHCl_3)$. This salt was obtained in 93% yield following the procedure used to prepare $[Au_2(\mu\text{-dppe})_2](BF_4)_2 \bullet CHCl_3$ with the substitution of potassium triflate for sodium tetrafluoroborate.

Infrared Spectrum (cm^{-1}): 3052 (w), 2971(w), 1579 (w), 1479 (w), 1433 (m), 1408 (w), 1337 (w), 1297 (w), 1265 (m), 1249 (m), 1222 (m), 1148 (m), 1101 (m), 1025 (m), 993 (w), 915 (w), 881 (w), 846 (w), 799 (w), 725 (m), 686 (s), 630 (w), 570 (w), 514 (s), 472 (m). The peaks at 1297 (w), 1265 (m), 1249 (m), 1222 (m), 1025 (m), 630(w) cm^{-1} correlate to the C-F and S-O stretch and bend of the OTf^- anion.

Preparation of $[Au_2(\mu\text{-dppp})_2](PF_6)_2$. A 68.5 mg (0.166 mmol) portion of dppp was dissolved in 7 mL of dichloromethane and an equivalent quantity of thtAuCl (51.9 mg, 0.162 mmol) dissolved in 4 mL dichloromethane was added to the dppp solution. This colorless solution was stirred for 10 min followed by the addition of potassium hexafluorophosphate (350 mg, 1.90 mmol) that was dissolved in a 6 mL portion of dichloromethane and 2 mL of methanol. This mixture was then stirred over a 24-hour period. To remove the excess salt, the crude product was evaporated to dryness. The resulting solid was dissolved in dichloromethane and filtered with a filter pipet. The dried, green luminescent crude product (yield: 184 mg, 75%) was dissolved in chloroform. Slow diffusion of diethyl ether into the colorless chloroform solution produced colorless crystals that did not luminesce under UV light at 77 K or at room temperature.

$^{31}P\{^1H\}$ Nuclear Magnetic Resonance (ppm): 41.5 ppm (cation) and -144.12(J_{PF}, 3.54) ppm (anion) in chloroform-*d*.

Infrared Spectrum (cm^{-1}): 3066 (w), 2913 (w), 2850 (w), 1573 (w), 1483 (w), 1436 (m), 1314 (w), 1191 (w), 1185 (w), 1105 (m), 1000 (w), 996 (w), 960 (m), 827 (s), 744 (m), 691 (m), 688 (m), 555 (m), 486 (m), 481 (m), 463 (m), 422 (w), 392 (w). The peaks at 827 (s) and 555 (m) cm^{-1} correlate to the P-F stretch and bend of the PF_6^- anion.

Preparation of $[Au_2(\mu\text{-dppp})_2]](OTf)_2$. This salt was obtained in 52% yield following the procedure used to prepare $[Au_2(\mu\text{-dppp})_2](PF_6)_2$ with the substitution of potassium hexafluorophosphate for potassium triflate.

$^{31}P\{^1H\}$ Nuclear Magnetic Resonance (ppm): 41.5 ppm.

Infrared Spectrum (cm^{-1}): 3050 (w), 2950 (w), 2920 (w), 2899 (w), 2853 (w), 1481 (m), 1436 (s), 1405 (w), 1381 (w), 1259 (s), 1221 (m), 1160 (m), 1102 (s), 1067 (w), 1026 (s), 997 (m), 967 (m), 939 (m), 835 (m), 798 (w), 742 (s), 690 (s), 635 (s). The peaks at 1259 (s), 1221 (m), 1160 (m), 1026 (m), 635(s) cm^{-1} correlate to the C-F and S-O stretch and bend of the OTf^- anion.

$^{31}P\{^1H\}$ Nuclear Magnetic Resonance: 41.4 ppm in chloroform-*d* at 290 K.

^1H Nuclear Magnetic Resonance: complex multiplets for the aromatic resonances at 7.64, 7.54, 7.53, 7.52 ppm (40 protons); methylene resonance, broad multiplet, 3.04 ppm (8 protons) and 2.16 broad multiplet, ppm (4 protons) in chloroform-*d* at 290 K.

Table 4. Crystal Data

	$[Au_2(\mu\text{-dppe})_2](BF_4)_2 \cdot CHCl_3$	$[Au_2(\mu\text{-dppe})_2](BF_4)_2 \cdot 1,2\text{-}Cl_2C_2H_4$	$[Au_2(\mu\text{-dppe})_2](PF_6)_2 \cdot 2CHCl_3$	$[Au_2(\mu\text{-dppe})_2](PF_6)$
Color/Habit	Colorless Block	Colorless Block	Colorless Block	Colorless block
Chemical formula	$C_{53}H_{49}Au_2B_2Cl_3F_8P_4$	$C_{54}H_{52}Au_2B_2Cl_2F_8P_4$	$C_{54}H_{50}Au_2Cl_6F_{12}P_6$	$C_{52}H_{48}Au_2F_{12}P_6$
formula weight	1483.72	1463.29	1719.39	1480.65
crystal system	monoclinic	monoclinic	triclinic	monoclinic
space group	$P2_1/c$	$P2_1/c$	$P\text{-}1$	$P2_1/c$
a/Å	21.0445(9)	21.075(6)	12.3528(17)	11.2050(2)
b/Å	13.0917(6)	13.134(4)	12.4980(17)	25.1101(5)
c/Å	20.1991(9)	19.698(5)	22.069(3)	18.5313(4)
α/deg	90	90	101.917(3)	90
β/deg	107.382(3)	104.334(7)	91.887(3)	96.3980(10)
γ/deg	90	90	114.272(3)	90
$V/Å^3$	5310.9(4)	5282(2)	3012.4(7)	5181.47(18)
Z	4	4	2	4
T(K)	90(2)	100(2)	100(2)	90(2)
λ(Å)	0.71073	0.71073	0.71073	0.71073
$\rho(g/cm^3)$	1.856	1.840	1.896	1.898
$\mu(mm^{-1})$	5.855	5.836	5.364	5.922
R_1(obsd data)[a]	0.0439	0.0499	0.021	0.0425
wR_2(all data, F_2 refinement)[b]	0.1408	0.0631	0.0371	0.1461

Table 4. Crystal Data (continued)

	$[Au_2(\mu\text{-dppe})_2](OTf)_2 \bullet 2(CHCl_3)$	$[Au_2(\mu\text{-dppe})_2](SbF_6)_2$	$[Au_2(\mu\text{-dppp})_2](PF_6)_2 \bullet (CHCl_3)$
Color/Habit	Colorless Needle	Colorless Parallelepiped	Colorless block
Chemical formula	$C_{56}H_{50}Au_2Cl_6F_6O_6P_4S_4$	$C_{52}H_{48}Au_2F_{12}P_4Sb_2$	$C_{55}H_{54}Au_2Cl_3F_{12}P_6$
formula weight	3335.81	1662.25	1629.08
crystal system	monoclinic	monoclinic	orthorhombic
space group	$P2_1/c$	$P2_1/c$	$P2_12_12_1$
a/Å	11.5718(10)	11.3952(9)	12.2983(2)
b/Å	36.444(3)	36.836(3)	18.3220(4)
c/Å	14.6822(13)	14.4435(12)	26.5245(5)
α/deg	90	90	90
β/deg	106.807(2)	106.711(3)	90
γ/deg	90	90	90
V/Å^3	5927.3(9)	5806.7(8)	5976.8(2)
Z	2	4	4
T(K)	100(2)	100(2)	90
λ(Å)	0.71073	0.71073	0.71073
ρ(g/cm^3)	1.869	1.901	1.806
μ(mm^{-1})	5.394	6.14	5.272
R_1(obsd data)[a]	0.0267	0.0394	0.0329
wR_2(all data, F_2 refinement)[b]	0.0505	0.0984	0.1026

Table 4. Crystal Data (continued)

	$[Au_2(\mu\text{-dppp})_2](PF_6)_2$ (α polymorph)	$[Au_2(\mu\text{-dppp})_2](PF_6)_2$ (β- polymorph)	$[Au_2(\mu\text{-dppp})_2](OTf)_2$
Color/Habit	Colorless Parallelapiped	Colorless plate	Colorless block
Chemical formula	$C_{54}H_{52}Au_2F_{12}P_6$	$C_{54}H_{52}Au_2F_{12}P_6$	$C_{56}H_{52}Au_2P_4F_6O_6S_2$
formula weight	1508.16	1508.72	1516.91
crystal system	triclinic	triclinic	orthorhombic
space group	*P*-1	*P*-1	*Ibam*
a/Å	9.0514(2)	10.5733(5)	15.2016(11)
b/Å	11.8984(2)	11.8113(5)	17.0643(12)
c/Å	14.0805(2)	13.4238(8)	21.6296(16)
α/deg	69.2180(10)	64.005(2)	90
β/deg	74.1960(10)	71.710(3)	90
γ/deg	79.3420(10)	64.425(2)	90
V/Å^3	1357.58(4)	1343.04(12)	5610.8(7)
Z	1	1	4
T(K)	90(2)	90(2)	190(2)
λ(Å)	0.71073	0.71073	0.71073
ρ(g/cm^3)	1.882	1.865	1.796
μ(mm^{-1})	5.654	5.713	5.481
R_1(obsd data)[a]	0.0177	0.0179	0.0242
wR_2(all data, F_2 refinement)[b]	0.0635	0.0678	0.0631

X-ray Crystallography and Data Collection. Crystals were coated with a hydrocarbon oil after being transferred with a covering of mother liquor to a microscope slide. Colorless crystals of $[Au_2(\mu\text{-dppe})_2](BF_4)_2 \bullet CHCl_3$, $[Au_2(\mu\text{-dppe})_2](PF_6)_2 \bullet 2CHCl_3$ $[Au_2(\mu\text{-dppe})_2](PF_6)_2$, $[Au_2(\mu\text{-dppe})_2](BF_4)_2 \bullet 1,2\text{-}Cl_2C_2H_4$, $[Au_2(\mu\text{-dppe})_2(OTf)_2] \bullet 2(CHCl_3)$, $[Au_2(\mu\text{-dppp})_2]$ $(PF_6)_2$ $\bullet(CHCl_3)$, $[Au_2(\mu\text{-dppp})_2](PF_6)_2$, $[Au_2(\mu\text{-dppp})_2](OTf)_2$, and were mounted under a nitrogen cold stream produced by an Oxford Cryostream low temperature apparatus on the goniometer head of a Bruker D8 Venture Kappa DUO diffractometer equipped with Bruker Photon II CMOS detector and a MoKα microsource. A colorless

paralleapiped of $Au_2(dppe)_2(SbF_6)_2$ was mounted in the 100 K nitrogen cold stream provided by a Cryo Industries low-temperature apparatus on the goniometer head of a Bruker APEX II sealed-tube diffractometer and CCD detector with the use of MoKα (λ = 0.71073 Å) radiation. A multi-scan absorption correction was applied with the program SADABS.[37] The structures was solved by a dual space method, (SHELXT)[38] and refined by full-matrix least-squares on F^2 (SHELXL-2017).[38] CCDC contain the supplementary crystallographic data for this paper.

Physical measurements

IR spectra were recorded on a Bruker Alpha FT-IR spectrometer using attenuated total reflectance (ATR). Fluorescence excitation and emission spectra were recorded on a Jobin Yvon Horiba Floromax-P luminescence spectrophotometer. UV-Vis spectra were recorded on a Shimadzu UV-3600 spectrophotometer.

Supporting Information

The data that support the crystallographic findings of this study are openly available in Cambridge Crystallographic Data Centre at https://ccdc.cam.ac.uk, reference number CCDC xx-xx .

Author Contributions

Synthetic studies and crystal growth (SC, DTW, LM) crystal data collection and analysis (SC, DTW, MMO); writing (SC, ALB).

Conflicts of Interest

There are no conflicts to declare.

Acknowledgements

We thank the National Science Foundation (Grant CHE-1807637) for partial support of this project, and Grant CHE-1531193 for the Dual source X-ray diffractometer.

References

1 Balch, A. L. Remarkable Luminescence Behaviors and Structural Variations of Two-Coordinate Gold(I) Complexes. *Struct. Bond.* **2007**, *123*, 1-.

2 He, X.; Yam, V. W.-W. Luminescent gold(I) complexes for chemosensing. *Coord. Chem. Rev.* **2011**, *255*, 2111-2123.

3 Yam, V. W. W.; Cheng, E. C. C. Highlights on the recent advances in gold chemistry—a photophysical perspective. *Chem. Soc. Rev.* **2008**, *37*, 1806 -1813.

4 Tiekink, E. R.T.; Kang, J.-G. Luminescence properties of phosphinegold(I) halides and thiolates. *Coord. Chem. Rev.* **2009**, *253*, 1627-1648. .

5 Yam, V.W.-W.; Au, V. K.-M.; Leung, S. Y.-L. Light-Emitting Self-Assembled Materials Based on d^8 and d^{10} Transition Metal Complexes. *Chem. Rev*. **2015**, *115*, 7589−7728

6 Jin, M.; Hajime Ito, H. Solid-state luminescence of Au(I) complexes with external stimuli-responsive properties. *J. Photochem. Photobiol. C* **2022**, *51*, 100478.

7 Ziolo, R.; Lipton, S.; Z. Dori, Z. The Photoluminescence of Phosphine Complexes of d^{10} Metals. *Chem. Comm*. **1970**, 1124-1125.

8 McCleskey, T. M.; Gray, H. B. Emission Spectroscopic Properties of l,2-Bis(dicyclohexylphosphino)ethane Complexes of Gold(I). *Inorg. Chem.* **1992**, *31*, 1773-1774.

9 King, C.; Khan, M. N. I.; Staples, R. J.; Fackler, Jr., J. P. Luminescent mononuclear gold(I) phosphines. *Inorg. Chem.* **1992**, *31,* 3236.

10 Barakat, K. A.; Cundari, T. R.; Omary, M. A. Jahn−Teller Distortion in the Phosphorescent Excited State of Three-Coordinate Au(I) Phosphine Complexes. *J. Am. Chem. Soc*. **2003**, *125*, 14228-14229.

11 Sinha, P.; Wilson, A. K.; Omary, M. A. Beyond a T-Shape. *J. Am. Chem. Soc*. **2005**, *127*, 12488-12489.

12 Pyykkö. P.; Li, J.; Runeberg, N. Predicted ligand dependence of the Au (I) ···Au (I) attraction in ($XAuPH_3$). *Chem. Phys. Lett*. **1994**, *218*, 133-137.

13 Pyykkö. P. Strong Closed-Shell Interactions in Inorganic Chemistry. *Chem. Rev*. **1997**, *97*, 597-636.

14 Schmidbaur, H.; Schier, A. Aurophilic Interactions In and Between Molecules as a Subject of Current Interest. *Chem. Soc. Rev*. **2012**, *41*, 370−412.

15 Mirzadeh, N.; Privér, S. H.; Blake, A. J.; Schmidbaur, H.; Bhargava, S. K. Innovative Molecular Design Strategies in Materials Science Following the Aurophilicity Concept. *Chem. Rev*. **2020**, *120*, 7551−7591.

16 White-Morris, R. L.; Olmstead, M. M.; Balch, A. L. Aurophilic Interactions in Cationic Gold Complexes with Two Isocyanide Ligands. Polymorphic Yellow and Colorless Forms of [(Cyclohexyl Isocyanide)$_2$Au^{I}](PF_6) with Distinct Luminescence *J. Am. Chem. Soc.* **2003**, *125*, 103-1040.

17 Malwitz, M. A.; Lim, S. H.; White-Morris, R. L.; Pham, D. M.; Olmstead, M. M.; Balch, A. L. Crystallization and Interconversions of Vapor-Sensitive, Luminescent Polymorphs of [($C_6H_{11}NC$)$_2$Au^{I}](AsF_6) and [($C_6H_{11}NC$)$_2$Au^{I}](PF_6). *J. Am. Chem. Soc.* **2012**, *134*, 10885-10893.

18 Luong, L. M. C.; Malwitz, M. A.; Moshayedi, V.; Olmstead, M. M.; Balch, A. L. Role of Anions and Mixtures of Anions on the Thermochromism, Vapochromism, and Polymorph Formation of Luminescent Crystals of a Single Cation, [($C_6H_{11}NC$)$_2$Au]$^{+}$. *J. Am. Chem. Soc*. **2020**, *142*, 5689−5701.

19 Luong, L. M. C.; Lowe, C. D.; Adams, A. V.; Moshayedi, V.; Olmstead, M. M.; Balch, A. L. Seeing luminescence appear as crystals crumble. Isolation and subsequent self-association of individual $[(C_6H_{11}NC)_2Au]^+$ ions in crystals. *Chem. Sci*. **2020**, *11*, 11705–11713.

20 Luong, L. M. C.; Olmstead, M. M.; Balch, A. L. A Non-Luminescent Polymorph of [(Cyclohexyl Isocyanide)$_2$Au]PF_6 that Becomes Luminescent Upon Grinding or Exposure to Dichloromethane Vapor. *Chem. Commun*. **2021**, *57*, 793-796.

21 Lim, S. H.; Olmstead, M. M.; Balch, A. L. Molecular Accordion: Vapoluminescence and Molecular Flexibility in the Orange and Green Luminescent Crystals of the Dimer, Au_2(μ-bis-(diphenylphosphino)ethane)$_2Br_2$. *J. Am. Chem. Soc*. **2011**, *133*, 10229-10238.

22 Lim, S. H.; Olmstead, M. M.; Balch, A. L. Inorganic topochemistry. Vapor-induced solid state transformations of luminescent, three-coordinate gold(I) complexes. *Chem. Sci*. **2013**, *4, 311–318.*

23 Al-Baker, S.; Hill, W. E.; McAuliffe, C. A. Novel Ring Compounds of Bidentate Phosphines with Gold(I). Two-, Three-, and Four-co-ordination. *J. Chem. Soc., Dalton Trans.* **1985**, 2655-2659.

24 Yau, J.; Mingos, D. M. P. Synthesis and applications of $[Au(NCPh)_2]^+$, a versatile labile gold(I). *J. Chem. Soc., Dalton Trans.* **1997**, 1103-1111.

25 Schuh, W.; Kopacka, H.; Wurst, K.; Peringer, P. Observation of a P/M interconversion of a gold–phosphine helicate via ^{31}P NMR. *Chem. Commun*. **2001**, 2186–2187.

26 Kim, J. H.; Reeder, E.; Parkin, S.; Awuah, S. G. Gold(I/III)-phosphine complexes as potent Antiproliferative Agents. *Sci. Rep*. **2019**, *9, 12335.*

27 Ecken, H.; Olmstead, M. M.; Noll, B. C.; Attar, S.; Schlyer, B.; Balch, A. L.Effects of anions on the solid state structures of linear gold(I) complexes of the type (*o*-xylyl isocyanide)gold(I) (monoanion). *J. Chem. Soc., Dalton Trans*. **1998**, 3715-3720.

28 White-Morris, R. L.; Olmstead, M. M.; Jiang, F.; Tinti, D. S.; Balch, A. L. Remarkable Variations in the Luminescence of Frozen Solutions of [Au{C(NHMe)2}2]-(PF6)·0.5(Acetone). Structural and Spectroscopic Studies of the Effects of Anions and Solvents on Gold(I) Carbene Complexes. *J. Am. Chem. Soc*. **2002**, *124*, 2327-2336.

29 Rios, D.; Pham, D. M.; Fettinger, J. C.; Olmstead, M. M.; Balch, A. L. Blue or Green Glowing Crystals of the Cation $[Au\{C(NHMe)_2\}_2]^+$. Structural Effects of Anions, Hydrogen Bonding, and Solvate Molecules on the Luminescence of a Two-Coordinate Gold (I) Carbene Complex. *Inorg. Chem*. **2008**, *47*, 3442-3451.

30 Saitoh, M.; Balch, A. L.; Yuasa, J.; Kawai, T. Effects of Counter Anions on Intense Photoluminescence of 1-D Chain Gold (I) Complexes. *Inorg. Chem*. **2010**, *49*, 7129-7134.

31 Streitberger, M.; Schmied, A.; Hey-Hawkins, E. Selective Formation of Gold(I) Bis-Phospholane Macrocycles, Polymeric Chains, and Nanotubes. *Inorg. Chem*. **2014**, *53*, 6794−6804.

32 Lim, S. H.; Schmitt, J. C.; Shearer, J.; Jia, J.; Olmstead, M. M.; Fettinger, J. C.; Balch, A. L. Crystallographic and Computational Studies of Luminescent, Binuclear Gold(I) Complexes, $Au^I_2(Ph_2P(CH_2)_nPPh_2)_2I_2$ (n = 3−6). *Inorg. Chem*. **2013**, *52*, 823−831.

33 Bates, P. A.;Waters, J. M. The Crystal and Molecular Structure of Dichloro-1,2-bis(diphenylphosphino)-ethanedigold(I). *Inorg. Chim. Acta*. **1985**, *98*, 125-129.

34 Walters, D. T.; England, K. R.; Ghiassi, K. B.; Semma, F. Z.; Olmstead, M. M.; Balch, A. L. Steric effects and aurophilic interactions in crystals of Au_2(□-1,2-bis(diphenylphosphino)ethane)X_2 and Au_2(□-1,2-bis(dicyclohexylphosphino)ethane)X_2 (X = Cl, Br, I). *Polyhedron* **2016**, *117*, 535–541.

35 England, K. R.; Lim, S. H.; Luong, L. M. C.; Olmstead, M. M.; Balch, A. L. Vapoluminescent Behavior and the Single-Crystal-to Single-Crystal Transformations of Chloroform Solvates of [Au_2(μ-1,2-bis(diphenylarsino)ethane)$_2$](AsF_6)$_2$. *Chem. Eur. J.* **2019**, *25*, 874 – 878.

36 Balch, A. L.; Tulyathan, B. Interactions between Rhodium(I) Centers in Dimeric Complexes. *Inorg. Chem*. **1997**, *16*, 2840-2845.

37 Krause, L.; Herbst-Irmer, R.; Sheldrick, G. M.; Stalke, D. Comparison of silver and molybdenum microfocus X-ray sources for single-crystal structure determination.*J. Appl. Cryst*., **2015**, *48*, 3-10.

38 Sheldrick, G. M. SHELXT - Integrated space-group and crystal-structure determination. *Acta Crystallogr., Sect. A **2015**, 71*, 3-8.

39 Sheldrick, G. M. *SHELXL,* Crystal structure refinement with SHELXL. *Acta Crystallogr., Sect. C* **2015,** *71*, 3-8.

Chapter 3

Bridging 1,2-Bis-(diphenylphosphino)methane Ligands Facilitate the Formation of Binuclear Complexes with Both Two-Coordinate and Three-Coordinate Gold(I) Ions †

† Reprinted in part with permission from **Costa, S.**; Chui, S. M.; Espinoza, K. A.; Olmstead, M. M.; Fettinger, J. C.; Balch, A. L. "Bridging 1,2-Bis-(diphenylphosphino)methane Ligands Facilitate the Formation of Binuclear Complexes with Both Two-Coordinate and Three-Coordinate Gold(I) Ions" *Inorg. Chem.* **2024**, *63* (52), 24563–24572.

https://doi.org/10.1021/acs.inorgchem.4c03657.

Abstract

Five new crystalline gold(I) complexes (β-$Au_2(\mu\text{-dppm})_2Br_2 \bullet 2CH_2Cl_2$ (**1**), $[Au_2(\mu\text{-dppm})_2Br]Br \bullet 2CH_2Cl_2$ (**2**), $[Au_2(\mu\text{-dppm})_2Br](PF_6)$ (**3**), $[Au_2(\mu\text{-dppm})_2Cl](BPh_4) \bullet 3CH_2Cl_2$ (**4**) and $[(Au_2(\mu\text{-dppm})_2]Cl(AsF_6) \bullet 2CH_2Cl_2$ (**5**) (where dppm is bis-(diphenylphosphino)methane) have been prepared and structurally characterized by single crystal X-ray diffraction. Colorless β-$Au_2(\mu\text{-dppm})_2Br_2 \bullet 2CH_2Cl_2$ (**1**) has centrosymmetric structure with two three-coordinate gold(I) ions held in close proximity by the dppm ligands. Crystals of $[Au_2(\mu\text{- dppm})_2Br]Br \bullet 2CH_2Cl_2$ (**2**), $[Au_2(\mu\text{-dppm})_2Br](PF_6)$ (**3**), and $[Au_2(\mu\text{-dppm})_2Cl](BPh_4) \bullet 3CH_2Cl_2$ (**4**) have a cation with an unusual arrangement that binds a two-coordinate gold(I) ion to a three-coordinate gold(I) ion through an aurophilic interaction. Whereas $Au_2(\mu\text{-dppm})_2Cl](BPh_4) \bullet 3CH_2Cl_2$ (**4**) has a chloride ion bound to only one of the gold ions in the complex, $[(Au_2(\mu\text{-dppm})_2]Cl(AsF_6) \bullet 2CH_2Cl_2$ (**5**) has an ion paired chloride ion that is symmetrically disposed between the two gold ions at a rather long distance. Each complex displays luminescence under UV irradiation.

Introduction

Frequently gold(I) complexes form colorless crystals, but many crystalline gold(I) compounds become luminescent under UV irradiation and can produce colors ranging from blue

to red.[1-5] This luminescent behavior makes gold(I) complexes promising candidates for the development of various electro-optical devices and sensors.[6-10]

Individual two-coordinate, linear gold(I) complexes are generally not luminescent unless one of the ligands involved is emissive itself.[3] However, two-coordinate gold(I) complexes can become luminescent upon aggregation due to aurophilic interactions. Thus, the two-coordinate cation, $[(cyclohexylNC)_2Au]^+$, is not luminescent when it is surrounded by two large tetrakis[3,5-bis(trifluoromethyl)phenyl]borate anions.[11] However, this cation becomes luminescent due to assembly into extended chains with close Au···Au contacts when smaller anions like hexafluorophosphate are the counterions.[10,12-15] In contrast, monomeric, three-coordinate gold(I) complexes are usually luminescent.[16,18] Consequently, luminescence cannot be utilized to identify cases where three-coordinate gold(I) complexes associate through aurophilic interactions.

The aurophilic interactions responsible for the aggregation of two-coordinate gold(I) complexes result from a combination of London dispersion forces and relativistic effects,[19,20] and have been used to assist in the construction of various supramolecular arrays.[8,21,22] The aurophilic interaction between two closed-shell, d^{10} gold(I) ions has a bond strength comparable to a hydrogen bond.[23]

While the aggregation of cationic, anionic, and neutral two-coordinate gold(I) complexes is well established, much less is known about the ability of three-coordinate gold(I) complexes to participate in aurophilic interactions. There is only one example of self-association of a three-coordinate gold(I) complex that we have found. The planar cations in crystals of [(bipyridine)Au(2,6.dimethylphenylisocyanide)](N{SO_2CF_3}$_2$) pack around centers of symmetry to form dimers connected by a Au···Au bond at a distance of 3.2201(6) Å.[24] Computational analysis indicates that the strength of this bond is 6.3 kcal/mol. Nothing has been reported about the absorption and possible emisssion spectra of this compound.

As shown in structure A of Scheme 1, diphosphine ligands of the type $R_2P(CH_2)_nPR_2$ can be used to form binuclear metal complexes with varying spacings between metal centers.[25-29] When *n* is 3 or greater, the metal centers are generally far apart. For example, in Au_2(μ-$Ph_2P(CH_2)_3PPh_2)_2I_2$ the gold ions are separated by 5.0671(6) Å, well beyond the point where aurophilic interactions occur, and the distance between the gold(I) ions is even larger as *n* increases. However, for crystals of the accordion-like dimers, Au_2(μ-dppe)$_2X_2$ (where dppe is bis-

(diphenylphosphino)ethane and X is I or Br), the separations between the two gold ions varied depending upon the solvate molecules incorporated into the crystals. For X = I the separation between the gold(I) ions varied from 3.192(1) Å to 3.7866(3) Å,[14,15] while for X = Br the separation ranged from to 3.0943(2) Å to 3.8479(3) Å.[16] While the short end of these ranges suggest that aurophilic interactions are present, computational studies indicate that aurophilic interactions are not a significant contributor to the bonding within $Au_2(\mu\text{-dppe})_2I_2$ unless the Au···Au distance shrunk down to 2.987 Å.[31] Such a short Au···Au distance was not found in any of the solvated forms of three-coordinate $Au_2(\mu\text{-dppe})_2X_2$, but can be found in the dimeric dication $[Au_2(\mu\text{-dppe})_2]^{2+}$ with two-coordinate gold(I) ions.[31]

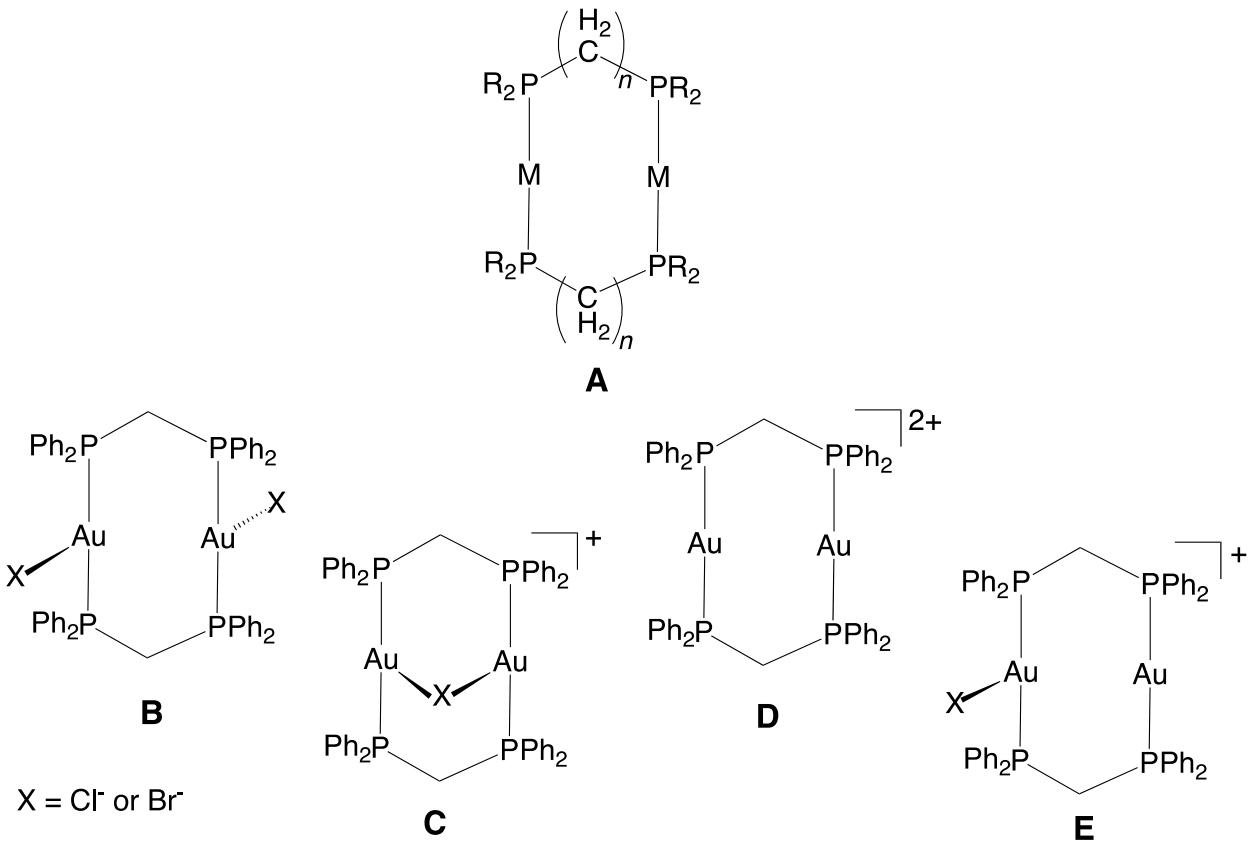

Scheme 1. (**A**), Binuclear complexes bridged by two diphosphine ligands. (**B**)-(**E**), Ligand dispositions in gold(I) dimers bridged by dppm.

To examine the flexibility of interactions of three-coordinate gold(I) ions in close proximity, we turned to compounds bridged by bis-(diphenylphosphino)methane (dppm).[33] $Au_2(\mu\text{-dppm})_2Br_2$ and $Au_2(\mu\text{-dppm})_2Cl_2$ were known to possess a face-to-face structure shown as (**B**) in Scheme 1 and $[Au_2(\mu\text{-dppm})_2(\mu\text{-I})]^+$ was shown to have an A-frame structure[34-36] shown as (**C**) in Scheme 1, but the possible luminescence of these compounds had not been examined.[37-39]

Results and Discussion.

Formation and Structure of the β-polymorph of $Au_2(\mu\text{-dppm})_2Br_2 \cdot 2CH_2Cl_2$ (1) and $[Au_2(\mu\text{-dppm})_2Br]Br \cdot 2CH_2Cl_2$ (2). Treatment of a solution of dppm with a suspension of gold(I) bromide in dichloromethane and a solution of potassium bromide in dichloromethane/methanol produced a yellow solid. Colorless crystals were obtained by diffusion of diethyl ether into a dichloromethane solution of the product. Examination of the crystals under a microscope using UV light revealed the presence of two types of crystals that had grown concomitantly as shown in Figure 1. The blue luminescent plates were crystallographically identified as a new polymorph of molecular β-$Au_2(\mu\text{-dppm})_2Br_2 \cdot 2CH_2Cl_2$ (**1**), while the teal luminescent blocks were found to be ionic $[Au_2(\mu\text{-dppm})_2Br]Br \cdot 2CH_2Cl_2$ (**2**). The proportion of the molecular compound, β-$Au_2(\mu\text{-dppm})_2Br_2 \cdot 2CH_2Cl_2$ (**1**), could be enhanced when carefully dried dichloromethane was used as solvent, while the fraction of the ionic compound, $[Au_2(\mu\text{-dppm})_2Br]Br \cdot 2CH_2Cl_2$ (**2**), could be increased by using dichloromethane that had been saturated with water to provide a more polar environment. Occasionally crystals of the α–polymorph of $Au_2(\mu\text{-dppm})_2Br_2 \cdot 2CH_2Cl_2$ were found along with crystals of molecular β-$Au_2(\mu\text{-dppm})_2Br_2 \cdot 2CH_2Cl_2$ (**1**) and ionic $[Au_2(\mu\text{-dppm})_2Br]Br \cdot 2CH_2Cl_2$ (**2**). However, we were unable to reliably produce enough of the α–polymorph of $Au_2(\mu\text{-dppm})_2Br_2 \cdot 2CH_2Cl_2$ to collect spectroscopic data on these crystals. The original report on the α–polymorph of $Au_2(\mu\text{-dppm})_2Br_2 \cdot 2CH_2Cl_2$ did not indicate how the crystal were grown.[36] Consequently, we limit further discussion to the β-polymorph of $Au_2(\mu\text{-dppm})_2Br_2 \cdot 2CH_2Cl_2$ (**1**).

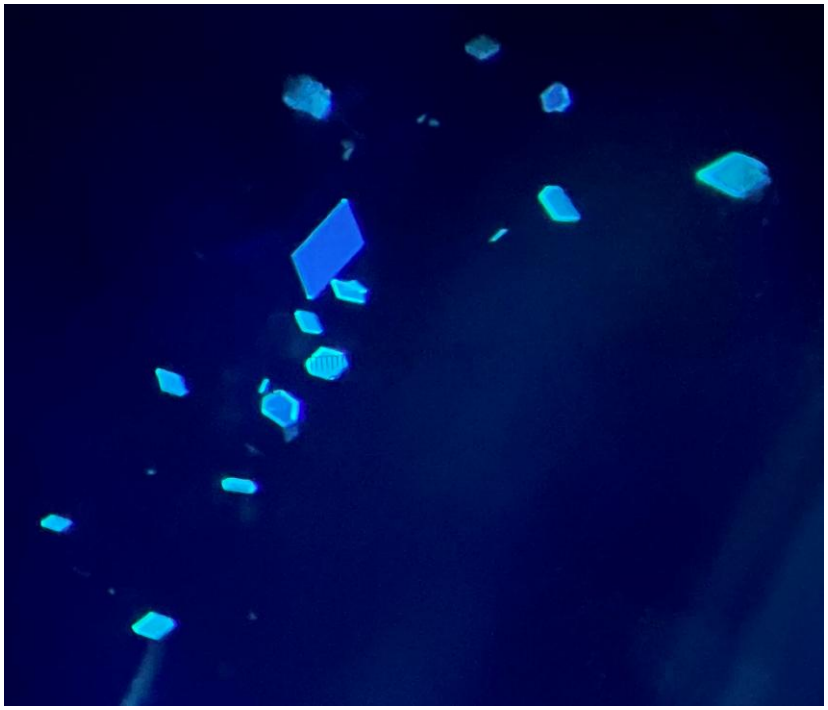

Figure 1. Photograph of crystalline plates of blue luminescent β-$Au_2(\mu\text{-dppm})_2Br_2 \bullet 2CH_2Cl_2$ (**1**) and teal luminescent blocks of ionic $[Au_2(\mu\text{-dppm})_2Br]Br \bullet 2CH_2Cl_2$ (**2**) taken under UV irradiation.

The structure of the β-polymorph of $Au_2(\mu\text{-dppm})_2Br_2 \bullet 2CH_2Cl_2$ has been determined by single crystal X-ray diffraction. Crystal data are given in Table 1 and selected bond distances and angles are presented in Table 2. A view of the β-$Au_2(\mu\text{-dppm})_2Br_2$ molecule is shown in Figure 2. The dimer is located on a crystallographic center of symmetry, which lies at the midpoint of the bond between the two gold ions. The Au···Au distance is 3.0771(4) Å, which is suggestive of an aurophillic interaction between the two gold ions. Each gold ion is in a nearly planar, three-

coordinate geometry, which is quite similar to the coordination environment found in the various solvates of $Au_2(\mu\text{-dppe})_2Br_2$.[32] The Au-Br distance is 2.8978(5) Å, which is a bit longer than the range of Au-Br distances (2.7115(11) - 2.8848(3) Å) in the solvates of $Au_2(\mu\text{-dppe})_2Br_2$ and quite a bit longer than the Au-Br distance (2.625(2) Å) in $Au(PPh_3)_2Br$.[40] The Au-P distances, 2.3060(7) Å and 2.3390(7) Å, fall near the range of Au-P distances (2.2995(6) - 2.3205(6) Å) observed in the solvates of $Au_2(\mu\text{-dppe})_2Br_2$. As usual with complexes of this sort, the P-Au-P angle (159.06(3) °) is much larger than the P-Au-Br angle (96.46(1) °). The Au···Au-Br angle is 96.46(1) °, and the bromide ion is quite far (4.4580(5) Å) from the adjacent, non-bonded gold(I) ion. As can be seen from the data in Table 2, the bond distances and angles in $\beta\text{-}Au_2(\mu\text{-dppm})_2Br_2\bullet 2CH_2Cl_2$ (**1**) are similar to those in $\alpha\text{-}Au_2(\mu\text{-dppm})_2Br_2\bullet 2CH_2Cl_2$.[36] Drawings comparing these two polymorphs can be found in the Supporting Information, Figures SI-1and 2.

Table 1. Crystal Data for Gold(I) Complexes

	$\beta\text{-}Au_2(\mu\text{-dppm})_2Br_2\bullet 2CH_2Cl_2$ (**1**)	$\alpha\text{-}Au_2(\mu\text{-dppm})_2Br_2\bullet 2CH_2Cl_2$ [c]	$[Au_2(\mu\text{-dppm})_2Br]Br\bullet 2CH_2Cl_2$ (**2**)
color/habit	colorless plate	pale yellow	colorless block
chemical formula	$C_{52}H_{48}Au_2Br_2Cl_4P_4$	$C_{52}H_{48}Au_2Br_2Cl_4P_4$	$C_{52}H_{48}Au_2Br_2Cl_4P_4$
formula weight	1492.32	1492.33	1492.33
crystal system	triclinic	triclinic	orthorhombic
space group	*P*-1	*P*-1	*P 21 21 21*
a (Å)	10.1292(12)	10.970(2)	13.6747(5)
b (Å)	11.0548(14)	11.332(1)	14.5276(6)
c (Å)	12.9356(16)	12.343(1)	25.8882(10)
α (deg)	71.338(2)	109.54(1)	90
β (deg)	86.797(2)	107.81(1)	90
γ (deg)	67.197(2)	97.88(1)	90
V ($Å^3$)	1261.2(3)	1326.81	5143.0(3)
Z	1	1	4
T (K)	90(2)	298	90(2)
λ (Å)	0.71073		0.71073
ρ (g/cm^3)	1.965	1.868	1.927

μ (mm^{-1})	7.769		7.620
R_1 (obsd data)[a]	0.0183	0.0535	0.0160
wR_2 (all data, F^2 refinement)[b]	0.0389		0.0359

[a] $R_1 = (\Sigma||F_o| - |F_c||)/\Sigma|F_o|$
[b] $wR_2 = ((\Sigma[w(F_o^2 - F_c^2)^2])/\Sigma[w(F_o^2)^2])^{1/2}$
[c] From data in Shain, J.; Fackler, Jr., J. P. *Inorg. Chim. Acta*, **1987**, *131*, 157-158.

Table 1. (Continued) Crystal Data for Gold(I) Complexes

	$[Au_2(\mu\text{-dppm})_2Br](PF_6)$ (**3**)	$[Au_2(\mu\text{-dppm})_2Cl](BPh_4)\bullet 3CH_2Cl_2$ (**4**)	$[Au_2(\mu\text{-dppm})_2]Cl(AsF_6)\bullet 2CH_2Cl_2$ (**5**)
color/habit	colorless block	yellow block	colorless block
chemical formula	$C_{50}H_{44}Au_2BrF_6P_5$	$C_{77}H_{70}Au_2BCl_7P_4$	$C_{52}H_{48}AsAu_2Cl_5F_6P_4$
formula weight	1387.54	1772.11	1556.89
crystal system	monoclinic	Triclinic	monoclinic
space group	P 21/n	P -1	*C 1 2/c 1*
a (Å)	18.6625(10)	12.0702(4)	27.274(7)
b (Å)	13.3339(7)	16.8803(6)	20.4594(18)
c (Å)	20.1402(10)	20.5697(7)	15.035(4)
α (deg)	90	69.1994(18)	90
β (deg)	105.504(3)	71.2565(18)	92.187(4)
γ (deg)	90	90	90
V ($Å^3$)	94829.4(4)	3636.9(2)	5357(2)
Z	4	2	4
T (K)	90(2)	90(2)	90(2)
λ (Å)	0.71073	0.71073	0.71073
ρ (g/cm^3)	1.908	1.618	1.930
μ (mm^{-1})	7.120	4.417	6.510

R_1 (obsd data)[a]	0.0433	0.0288	0.0177
wR_2 (all data, F^2 refinement)[b]	0.1185	0.0720	0.0783

[a] $R_1 = (\Sigma||F_o| - |F_c||)/\Sigma|F_o|$
[b] $wR_2 = ((\Sigma[w(F_o^2 - F_c^2)^2])/\Sigma[w(F_o^2)^2])^{1/2}$

Table 2. Selected Bond Distances and Angles for Gold(I) Complexes

Complex	β-(Au_2(μ-dppm)$_2Br_2$)•$2CH_2Cl_2$ **(1)**	α-(Au_2(μ-dppm)$_2Br_2$)•$2CH_2Cl_2$ [a]	[(Au_2(μ-dppm)$_2$Br)Br]•$2CH_2Cl_2$ **(2)**
Distances (Å)			
Au···Au	3.0771(4)	3.015(2)	2.9475(5)
Intra-ligand P···P	3.0580(8)	3.049(5)	3.057(1)(P1-P2) 3.053(2)(P3-P4)
Au1-P1	2.3060(7)	2.312(4)	2.318(1)
Au1-P4	2.3390(7)	2.354(4)	2.313(1)
Au2-P2	2.3060(7)	2.354(4)	2.304(1)
Au2-P3	2.3390(7)	2.312(4)	2.305(1)
Au1-X1	2.8978(5)	2.869(2)	2.9148(7)
Au2-X1			3.2223(6)
Au2-X2	2.8978(5)	2.869(2)	

Angles (deg)			
P1-Au1-P4	159.06(3)	156.50(1)	169.65(4)
P2-Au2-P3	159.06(3)	156.50(1)	166.40(4)
Au1···Au2-X1	96.46(1)	102.68(6)	66.68(1)
Au1···Au2-X2	96.46(1)	102.68(6)	
Torsional angles (deg)			
P2-Au2···Au1-P1	20.73(2)	23.4(1)	0.61(4)
P3-Au2···Au1-P4	-20.73(2)	-23.4(1)	4.15(4)

Table 2. Continued Selected Bond Distances and Angles for Gold(I) Complexes

Complex	[(Au_2(μ-dppm)$_2$Br)(PF_6) **(3)**	[(Au_2(μ-dppm)$_2$Cl)](BPh_4)•3CH_2Cl_2 (**4**)	[(Au_2(μ-dppm)$_2$Cl)](AsF_6)•2CH_2Cl_2 (**5**)
Distances (Å)			
Au···Au	2.9435(3)	2.9522(4)	2.9968(8)
Intra-ligand P···P	3.081(2)(P3-P4) 3.059(2)(P1-P2)	3.068(1)(P1-P2) 3.053(1)(P3-P4)	3.068(1)
Au1-P1	2.328(2)	2.3042(9)	2.311(1)
Au1-P4	2.301(2)	2.307(1)	2.311(1)
Au2-P2	2.321(2)	2.3042(9)	2.134(1)
Au2-P3	2.317(2)	2.3040(9)	2.134(1)
Au1-X1	2.9687(7)	3.0220(7)	3.1035
Au2-X1	3.4461(7)	2.8956(9)	3.1035
Au2-X2			
Angles (deg)			

P1-Au1-P4	159.12(5)	177.59(3)	175.87(3)
P2-Au2-P3	169.80(5)	175.75(3)	175.87(3)
Au1···Au2-X1	71.31(2)	62.22(2)	61.13
Au1···Au2-X2			
Torsional angles (deg)			
P2-Au2···Au1-P1	-8.03(5)	-1.18(3)	7.61(3)
P3-Au2···Au1-P4	2.84(5)	-4.26(3)	7.61(3)

[a] From data in Shain, J.; Fackler, Jr., J. P. *Inorg. Chim. Acta*, **1987**, *131*, 157-158.

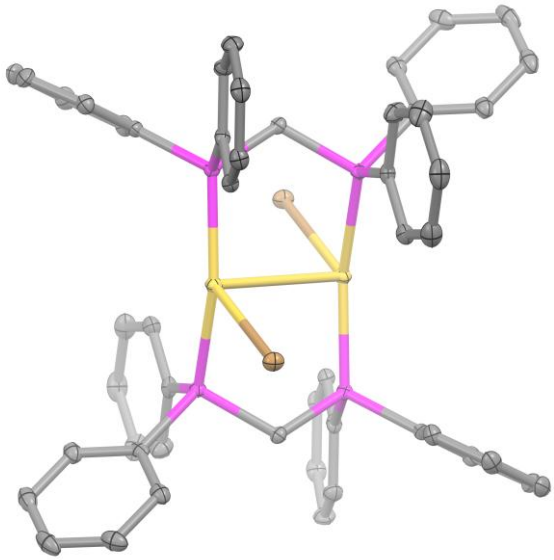

Figure 2. The structure of $Au_2(\mu\text{-dppm})_2Br_2$ in the β-polymorph of $Au_2(\mu\text{-dppm})_2Br_2 \bullet 2CH_2Cl_2$ (**1**). Hydrogen atoms and solvate molecules are not shown for clarity. Drawn with thermal contours at the 30% probability level. Color code: gold, yellow; phosphorus, pink; bromine, brown; carbon, grey.

The structure of the cation in the other product from this reaction, $[Au_2(\mu\text{-}dppm)_2Br]Br\bullet 2CH_2Cl_2$ (**2**), is shown in part **A** of Figure 3. This cation contains an unusual combination of a three-coordinate gold(I) ion and two-coordinate gold(I) ion. The distance between the two gold(I) ions is 2.9475(5) Å, which is indicative of an aurophilic bond between the two ions. The coordinated bromide ion is displaced toward the adjacent gold(I) ion so that the Au···Au-Br angle is 66.68(1) ° and the distance to the other gold(I) ion is 3.2223(6) Å. The remaining bromide ion is quite far (8.9378(6), 10.3285(6) Å) from either gold(I) ion.

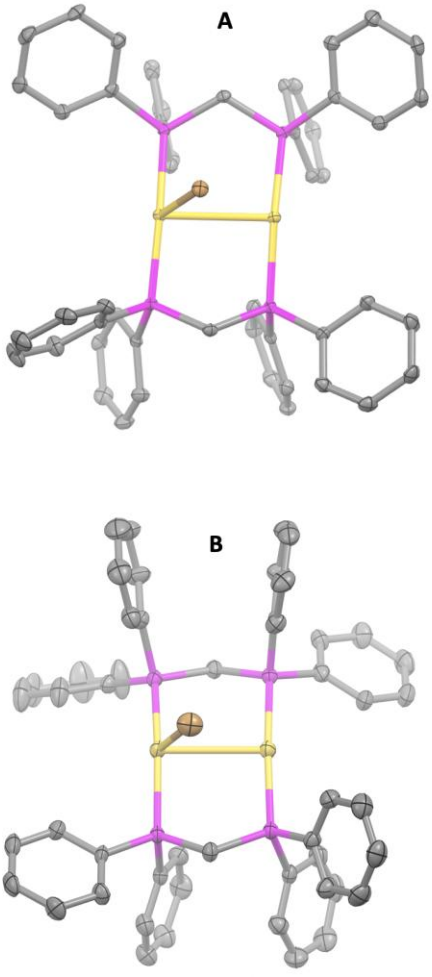

Figure 3. The structures of the cations in: **A**, $[Au_2(\mu\text{-dppm})_2Br]Br\bullet 2CH_2Cl_2$ (**2**); and **B**, $[Au_2(\mu\text{-dppm})_2Br](PF_6)$ (**3**). Hydrogen atoms are not shown for clarity. Drawn with thermal contours at the 30% probability level. Color code: gold, yellow; phosphorus, pink; bromine, brown; carbon, grey.

The Preparation and Structure of $[Au_2(\mu\text{-dppm})_2Br](PF_6)$ (3). Colorless crystals of $Au_2(\mu\text{-dppm})_2Br](PF_6)$ (**3**) were obtained by mixing dppm, gold(I) bromide, and ammonium hexafluorophosphate in dichloromethane/methanol as outlined in the experimental section. The structure of the cation in $[Au_2(\mu\text{-dppm})_2Br](PF_6)$ (**3**) is shown in part **B** of Figure 3. While the structures of the two cations shown in Figure 3 are similar (as are the Au···Au distances (2.9475(5) Å in (**2**), 2.9435(3) Å in (**3**)), there also some significant differences. For example, in $[Au_2(\mu\text{-dppm})_2Br](PF_6)$ (**3**) the P-Au-P angle (159.12(5) °) at the three-coordinate gold center is more acute than the corresponding angle (169.65(4) °) in $[Au_2(\mu\text{-dppm})_2Br]Br\bullet 2CH_2Cl_2$ (**2**). In $[Au_2(\mu\text{-dppm})_2Br]Br\bullet 2CH_2Cl_2$ (**2**), the two methylene groups reside on the same side of the Au_2P_4 group as the bromide ligand. However, in $[Au_2(\mu\text{-dppm})_2Br](PF_6)$ (**3**) one methylene group is on the same side as the bromide ligand while the other one is on the opposite side. Otherwise, $[Au_2(\mu\text{-dppm})_2Br]Br\bullet 2CH_2Cl_2$ (**2**) and $[Au_2(\mu\text{-dppm})_2Br](PF_6)$ (**3**) have similar structures and similar bonding.

The Preparations and Structures of $[Au_2(\mu\text{-dppm})_2Cl](BPh_4)\bullet 3CH_2Cl_2$ (4) and $[(Au_2(\mu\text{-dppm})_2]Cl(AsF_6)\bullet 2CH_2Cl_2$ (5). These salts were produced by mixing (tetrahydrothiophene)gold(I) chloride with dppm in dichloromethane followed by the addition of either sodium tetraphenyl borate or sodium hexafluoroarsenate as outlined in the experimental

section. The structure of the cation in $[Au_2(\mu\text{-dppm})_2Cl](BPh_4)\bullet 3CH_2Cl_2$ (**4**), as determined by single crystal X-ray diffraction, is shown in Figure 4 **A.** This cation has a structure that is similar to those of the bromo analogs found in $[Au_2(\mu\text{-dppm})_2Br]Br\bullet 2CH_2Cl_2$ (**2**); and $[Au_2(\mu\text{-dppm})_2Br](PF_6)$ (**3**) shown in Figure 3. $[Au_2(\mu\text{-dppm})_2Cl](BPh_4)\bullet 3CH_2Cl_2$ (**4**), has a three-coordinate gold(I) ion as well as a two-coordinate gold(I) ion connected by two bridging dppm ligands**.** The distance between the two gold(I) ions is 2.9522(4) Å, which is suggests that there is an aurophilic interaction between the two ions. The Au-Cl bond distance is 2.8956(9) Å, which is significantly longer than the known Au-Cl distance (2.533(4) Å) in $Au(PPh_3)_2Cl$ or the Au-Cl distance (2.500(4) Å) in $Au(PPh_3)_2Cl\bullet 0.5(C_6H_6)$.[37] The coordinated chloride ion is displaced toward the adjacent gold(I) ion so that the Au···Au-Cl angle is 62.22(2) °. The distance from the chloride ion to the adjacent two-coordinate gold(I) ion is 3.0220(7) Å.

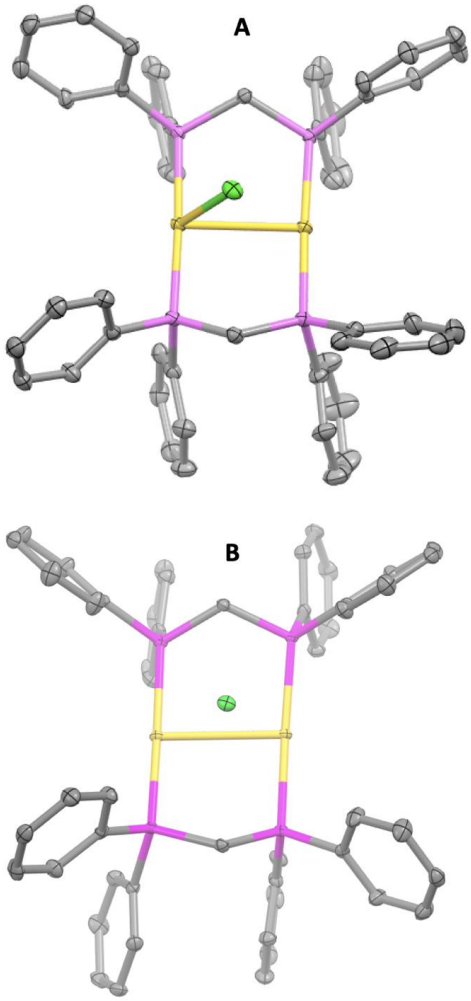

Figure 4. The structures of the cations in: **A**, $[Au_2(\mu\text{-dppm})_2Cl](BPh_4)\bullet 3CH_2Cl_2$ (**4**), and **B**, $[(Au_2(\mu\text{-dppm})_2]Cl(AsF_6)\bullet 2CH_2Cl_2$ (**5**). Hydrogen atoms are not shown. Thermal contours are at the 30% probability level. Color code: gold, yellow; phosphorus, pink; chlorine, green; carbon, grey.

The structure of the cation and the loosely associated chloride ion in $[(Au_2(\mu\text{-dppm})_2]Cl(AsF_6)\bullet 2CH_2Cl_2$ (**5**) is shown in Figure 4**B**. The asymmetric unit consists of one half of the cation, which resides on a mirror plane that bisects the two methylene carbon atoms and the midpoint of the Au···Au bond. In addition, the asymmetric unit contains half of an ordered

hexafluoroarsenate ion that resides on a mirror plane, half of a hexafluoroarsenate ion that resides on a mirror plain and is disordered over two orientations, and a disordered dichloromethane molecule in a general position. In the cation, the Au···Au distance, 2.9968(8) Å, is similar to the Au···Au distance (2.9522(4) Å) in $[Au_2(\mu\text{-dppm})_2Cl](BPh_4)\bullet 3CH_2Cl_2$ (**4**). The loosely associated chloride ion is symmetrically positioned 3.1035 Å from either gold(I) ion in the dication. A similar situation occurs in $[Au_2(\mu\text{-dppm})_2]Cl_2\bullet (CH_3)_2CO\bullet H_2O$, where there is a chloride ion in a similar position but closer to the gold(I) ions with Au···Cl distances of 2.9492(13) and 2.9776(12) Å.

We have identified three salts ($[Au_2(\mu\text{-dppm})_2Br]Br\bullet 2CH_2Cl_2$ (**2**), $[Au_2(\mu\text{-dppm})_2Br](PF_6)$ (**3**), $[(Au_2(\mu\text{-dppm})_2Cl)](BPh_4)\bullet 3CH_2Cl_2$ (**4**) that contain the unusual arrangement of a two-coordinate gold(I) ion connected to a three-coordinate gold(I) through an aurophilic interaction. In looking for other such arrangements, we found that $[Au_2(\mu\text{-dcmp})_2Cl]Cl\bullet 0.25CH_3OH$ (where dcmp is bis(dicyclohexylphosphino)methane) also has a two-coordinate gold(I) ion connected to a three-coordinate gold(I) but in a somewhat different orientation with a nearly linear Cl-Au···Au unit and an Au···Au distance of 2.9925(2) Å as shown in (**A**) in Figure 5.[19] That crystal also contained a second isomeric cation shown in (**B**) in Figure 5 that was not mentioned in the original article. The cation shown in (**B**) is quite similar to the cation in $[Au_2(\mu\text{-dppm})_2Cl](BPh_4)\bullet 3CH_2Cl_2$ (**4**). Both cations have acute Cl-Au···Au angles (62.22(2) ° for (**4**), 68.64(2) ° for $[Au_2(\mu\text{-dcmp})_2Cl]Cl\bullet 0.25CH_3OH$), nearly equivalent Au-Cl distances (2.8956(9) Å for (**4**), 2.8731(9) Å for $[Au_2(\mu\text{-dcmp})_2Cl]Cl\bullet 0.25CH_3OH$), and similar Au···Au distances (2.9522(4) Å for (**4**), 2.9445(2) Å) for $[Au_2(\mu\text{-dcmp})_2Cl]Cl\bullet 0.25CH_3OH$.

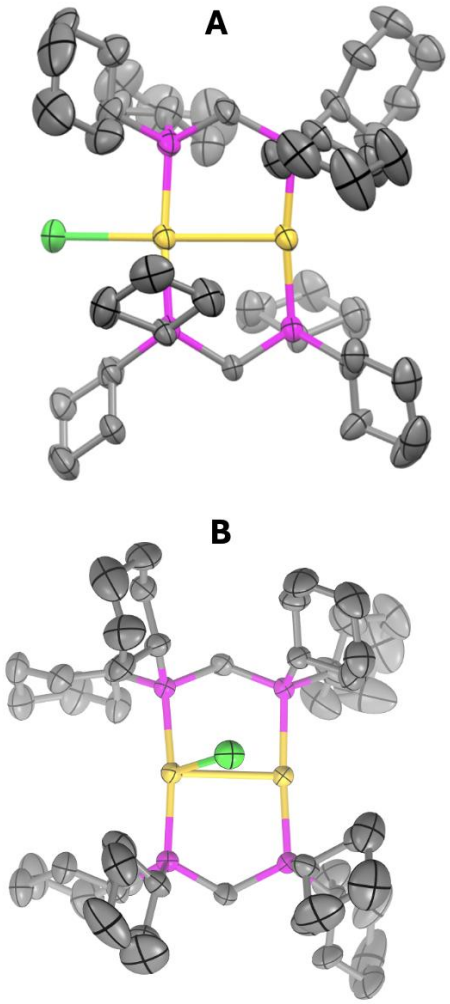

Figure 5. The structures of the cations in $[Au_2(\mu\text{-dcmp})_2Cl]Cl\bullet 0.25CH_3OH$ drawn from data in Fu, W.-F.; Chan, K.-C.; Cheung, K.-K.; Che, C.-M. *Chem. Eur. J.* **2001**, *7*, 4656-4664. Selected dimensions. (**A**), bond lengths; Au···Au, 2.9925(2); Au-Cl, 2.7756(9) Å; bond angle, Cl-Au···Au, 171.89(2) °. (**B**), bond lengths; Au···Au, 2.9445(2); Au-Cl, 2.8731(9) Å; bond angle, Cl-Au···Au, 68.64(2) °. Hydrogen atoms are not shown. Thermal contours are at the 30% probability level. Color code: gold, yellow; phosphorus, pink; chlorine, green; carbon, grey.

Within the gold(I) dimers bridged by two dppm ligands, the Au···Au distances are confined to a rather narrow range (2.9475(5) to 3.0771(4) Å) for the five compounds reported here. In comparison, the variability of Au/Cl interactions is remarkable for compounds with a $Au_2(\mu$-

dppm)$_2^{2+}$ core. Molecular $Au_2(\mu\text{-dppm})_2Cl_2$ with the structure shown in (**B**) in Scheme 1 exists in two forms: an acetone solvate with an Au-Cl distance of 2.771(4) Å,[34] and an acetonitrile solvate with a longer Au-Cl distance of 2.951(4) Å.[35] In contrast, crystalline $[Au_2(\mu\text{-dppm})_2]Cl_2\bullet(CH_3)_2CO\bullet H_2O$, has an A-frame structure (**C** in Scheme 1) with a bridging chloride ions somewhat asymmetrically placed between the gold(I) ions with Au-Cl distances of 2.9492 (13) and 2.9776(12) Å while $[Au_2(\mu\text{-dppm})_2]Cl(AsF_6)\bullet 2CH_2Cl_2$ (**5**) contains a symmetrically positioned chloride ion that is 3.1035 Å away from either gold(I) ion.[36] Finally, $[(Au_2(\mu\text{-dppm})_2Cl)](BPh_4)\bullet 3CH_2Cl_2$ (**4**) has a structure with a chloride ion connected to only one gold(I) ion with an Au-Cl distance of 2.8956(9) Å. All of these binuclear compounds have Au-Cl distances that are much longer than the Au-Cl distance (2.533(4) Å) in monomeric $Au(PPh_3)_2Cl$.[38] It appears that this lengthening of the Au-Cl bonds in these dimeric complexes may be a consequence of the aurophilic interactions.

Excitation and Emission Data.

Each of the five crystalline complexes reported here is luminescent in the solid state. For solvated crystals, the loss of solvate molecules can affect the excitation and emission spectra. [11,20] Consequently, we were particularly careful to obtain spectra on homogeneous samples that were protected to avoid solvate evaporation.

Table 3 contains the excitation and emission maxima for each compound. Figure 1 shows how we were visually able to differentiate $\beta\text{-}Au_2(\mu\text{-dppm})_2Br_2\bullet 2CH_2Cl_2$ (**1**) from $[Au_2(\mu\text{-dppm})_2Br]Br\bullet 2CH_2Cl_2$ (**2**) based on differences in luminescence and crystal morphology. Figure

6 shows the excitation and emission spectra for these two compounds and for [Au_2(μ-dppm)$_2$Br](PF$_6$) (**3**). Crystalline β-Au_2(μ-dppm)$_2Br_2$•2CH_2Cl_2 (**1**) has its emission at 458 nm at room temperature, while [Au_2(μ-dppm)$_2$Br]Br•2CH_2Cl_2 (**2**) shows emission at 472 nm under the same conditions. Notice that while the spectra are similar, there is enough difference to allow the two compounds to be identified.

Table 3. Excitation and Emission Data for Crystalline Solids

Complexes	Room Temperature (298 K)		Low Temperature (77 K)	
	Excitation (nm)	Emission (nm)	Excitation (nm)	Emission (nm)
(β-Au_2(μ-dppm)$_2Br_2$•2CH_2Cl_2 (**1**)	398	458	395 & 420	470
[Au_2(μ- dppm)$_2$Br]Br•2CH_2Cl_2 (**2**)	380	472	375	472
[Au_2(μ-dppm)$_2$Br](PF$_6$) (**3**)	363	468	365	482
[Au_2(μ-dppm)$_2$Cl](BPh$_4$)•3CH_2Cl_2 (**4**)	371	467	355	474
[(Au_2(μ-dppm)$_2$]Cl(AsF_6)•2CH_2Cl_2 (**5**)	358	464	363	454

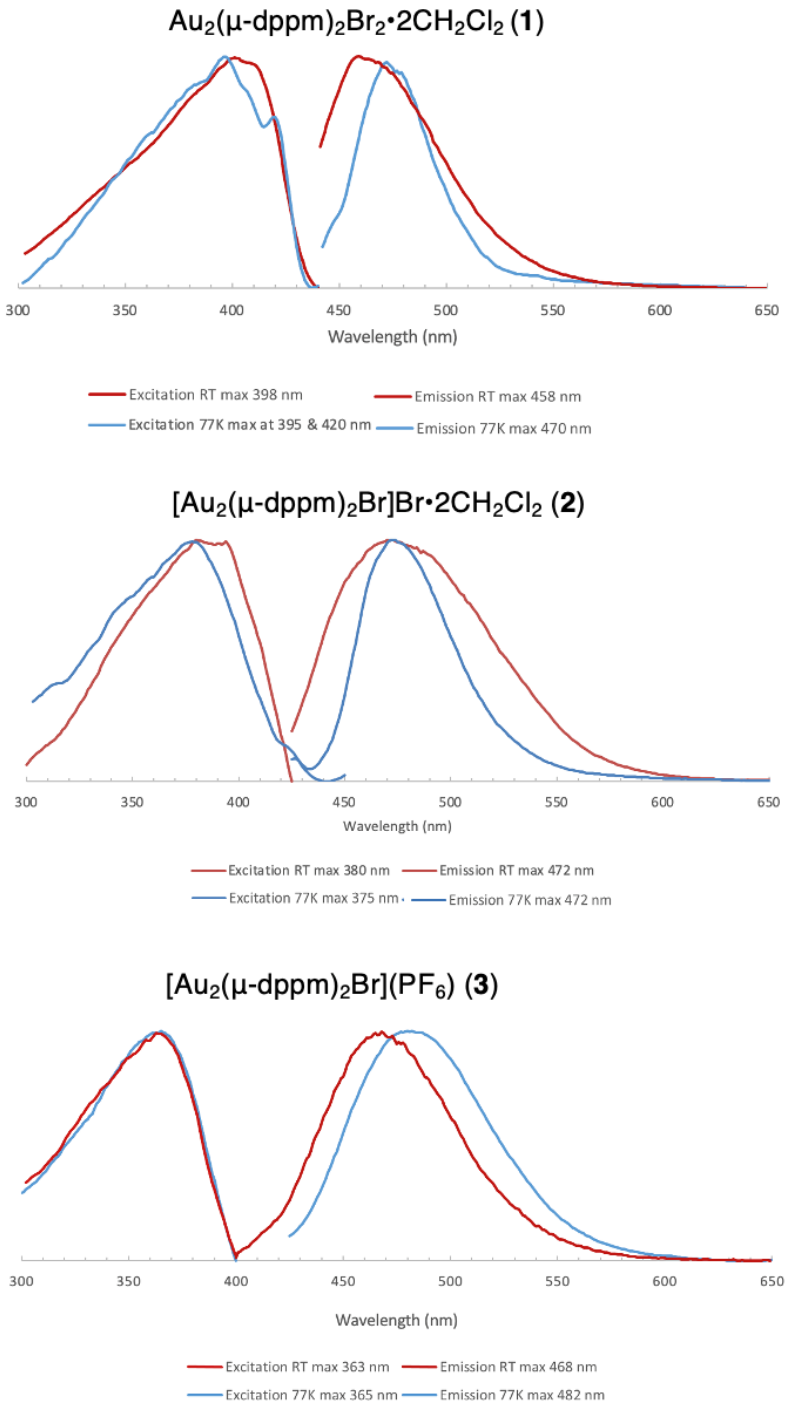

Figure 6. The excitation and emission spectra of crystalline samples of β-$Au_2(\mu\text{-dppm})_2Br_2\bullet 2CH_2Cl_2$ (**1**), $[Au_2(\mu\text{-dppm})_2Br]Br\bullet 2CH_2Cl_2$ (**2**) and $[Au_2(\mu\text{-dppm})_2Br](PF_6)$ (**3**) at room temperature and at 77 K.

For these compounds, the emission varies over a rather short range, which is perhaps not surprising given the structural similarities within this group of complex ions. Cooling the crystals results in a narrowing of the emission bands as expected for the reduction in vibrational motion. While $[Au_2(\mu\text{-dppm})_2Br]Br\bullet 2CH_2Cl_2$ (**2**) and $[Au_2(\mu\text{-dppm})_2Br](PF_6)$ (**3**) nominally contain a common cation, the structures of these cations differ as shown in Figure 3 and the emission spectra differ as well.

As seen in Table 3, the excitation and emission maxima for $[Au_2(\mu\text{-dppm})_2Cl](BPh_4)\bullet 3CH_2Cl_2$ (**4**), and $[(Au_2(\mu\text{-dppm})_2]Cl(AsF_6)\bullet 2CH_2Cl_2$ (**5**) differ slightly but fall near the range seen for the bromo salts.. Again, the effect of cooling the crystals results in only small changes with a narrowing of the emission bands be the most common feature. The spectra for these two salts can be found in the Supporting Information, Figure SI-3.

Solution Behavior. To better understand the solution behavior of these new gold(I) complexes, we examined their $^{31}P\{^1H\}$ NMR spectra. Due to poor solubility, we were unable to obtain $^{31}P\{^1H\}$ NMR spectra for $\beta\text{-}Au_2(\mu\text{-dppm})_2Br_2\bullet 2CH_2Cl_2$ (**1**) or $[Au_2(\mu\text{- dppm})_2Br]Br\bullet 2CH_2Cl_2$ (**2**). In acetonitrile solution, $[Au_2(\mu\text{-dppm})_2Br](PF_6)$ (**3**) displayed a singlet at 31.5 ppm for the cation and a heptet at for the $(PF_6)^-$ ion. The spectrum for $[Au_2(\mu\text{-dppm})_2Cl](BPh_4)\bullet 3CH_2Cl_2$ (**4**) in chloroform solution consisted of a singlet at 32.1 ppm, while the spectrum for $[(Au_2(\mu\text{-dppm})_2]Cl(AsF_6)\bullet 2CH_2Cl_2$ (**5**) displayed a singlet at 32.2 ppm in chloroform solution. Cooling the samples of each of these three compounds to 255 K produced some line broadening and shifting. These data suggest that the halide ions move about the cations in solution, but the actual identity of the species present in solution has not been ascertained. Additional evidence for the mobility of the halide ions in solution comes from the observation that $\beta\text{-}Au_2(\mu\text{-}$

dppm)$_2$Br$_2$•2CH$_2$Cl$_2$ (**1**) and [Au$_2$(μ-dppm)$_2$Br]Br•2CH$_2$Cl$_2$ (2) crystallize from a single solution concomitantly. Consequently, we did not continue to investigate the solution properties of these complexes further and limited our studies to the crystalline state, where the structures of the complexes are well-established.

Conclusions

Unlike the situation in the flexible dppe-bridged dimers, Au$_2$(μ-dppe)$_2$X$_2$ and [Au$_2$(μ-dppe)$_2$]$^{2+}$, where the separation between the two gold(I) ions can vary from 2.8787(9) Å to 3.8479(3) Å,[29-32] the dppm-bridged dimers reported here have short, intra-ionic Au···Au distances that fall in a narrow range from 2.9435(3) to 3.0771(4) Å. No inter-ionic aurophilic interactions occur in these salts. The variability in the structures of these dppm-bridged dimers involves the bonding to the bromide or chloride ions, while all maintain aurophilic bonding. In the three cations ([Au$_2$(μ-dppm)$_2$Br]Br•2CH$_2$Cl$_2$ (**2**), [Au$_2$(μ-dppm)$_2$Br](PF$_6$) (**3**) and [Au$_2$(μ-dppm)$_2$Cl](BPh$_4$)•3CH$_2$Cl$_2$ (**4**), the halide ion is clearly bonded only to only one gold(I) producing unusual complexes with a two-coordinate gold(I) ion connected to a three-coordinate gold(I) ion. In contrast, in β-Au$_2$(μ-dppm)$_2$Br$_2$•2CH$_2$Cl$_2$ (**1**) both bromine ions are coordinated to produce a face-to-face arrangement of two three-coordinate gold(I) ions, while in [(Au$_2$(μ-dppm)$_2$]Cl(AsF$_6$)•2CH$_2$Cl$_2$ (**5**), the chloride ions is ion paired between the two gold(I) ions.

Each of the new compounds is luminescent in the crystalline state. This result is not surprising since dimers of two-coordinate gold are luminescent as are many three-coordinate gold(I) complexes, and these new compounds contain both structural elements. The excitation and emission maxima for these complexes show only small variations, which may reflect the fact that bromide or chloride coordination is rather weak. Thus, the luminescence may be attributed to

transitions involving the interactions between the two gold ions, which has been discussed elsewhere.[38]

Finally, this article reports three compounds in which the unusual combination of a three-coordinate gold(I) ion with a two-coordinate gold(I) ion are held together by bridging dppm ligands and aurophilic interactions. As shown in Figure 5, there are two possible positions for the X-Au bond in these complexes: nearly perpendicular to the Au-Au bond as found in the new compounds reported here or parallel to the Au-Au bond.

Experimental Section.

Materials. Gold(I) bromide was purchased from Alfa Chemistry and dppm was purchased from Sigma-Aldrich. All solvents were reagent grade and used as received.

Preparation of Molecular β-$Au_2(\mu\text{-dppm})_2Br_2 \cdot 2CH_2Cl_2$ (1) and Ionic $[Au_2(\mu\text{-dppm})_2Br]Br \cdot 2CH_2Cl_2$ (2).

A 79.8 mg (0.208 mmol) portion of dppm was dissolved in 5 ml of dichloromethane, and an equivalent amount of AuBr (50.0 mg, 0.180 mmol) suspended in 4mL of dichloromethane was added to the dppm solution under agitation. The solution was stirred for 5 minutes followed by the addition of KBr (34.1 mg, 0.287 mmol) dissolved in 4 mL of dichloromethane and 1 mL of methanol. The light yellow solution was stirred for 3 hours and the crude mixture was evaporated to dryness. The resulting yellow solid was dissolved in a minimum amount of dichloromethane. The yellow solution was filtered using a filter pipet, and the filtrate was evaporated to dryness. A

purified yield of 70.1 mg (29.5%) was obtained. The dried crude product was dissolved in dichloromethane. This solution was filtered into the bottom of an outer diameter of 5 mm glass tube and a few drops of dichloromethane were layered over this solution. Subsequently, diethyl ether was layered over the dichloromethane. As the solutions diffused together, colorless block crystals with blue luminescence and colorless parallelepiped crystals with teal luminescence formed. For spectroscopic measurements, the two types of crystals were manually separated.

Infrared spectrum, molecular β-$Au_2(\mu\text{-dppm})_2Br_2 \bullet 2CH_2Cl_2$ (**1**): 3051(w), 3013(w), 2968(w), 2928(w), 2854(w), 1965(w), 1884(w), 1818(w), 1773(w), 1586(w), 1573(w), 1484(m), 1435(s), 1369(w), 1360(w), 1321(w), 1310(w), 1266(w), 1186(m), 1158(w), 1090(w), 1097(m), 1070(w), 1028(m), 998(m), 918(w), 843(w), 750(m), 736(s), 688(vs), 615(w) cm^{-1}.

Infrared spectrum, ionic $[Au_2(\mu\text{-dppm})_2Br]Br \bullet 2CH_2Cl_2$ (**2**): 3055(w), 3022(w), 2949(w), 2875(w), 1483(w), 1435(m), 1359(w), 1265(w), 1149(w), 1099(m), 1070(w), 1026(w), 999(w), 783(s), 740(s), 721 (s), 688(vs), 617(w) cm^{-1}.

Preparation of $[Au_2(\mu\text{-dppm})_2Br](PF_6)$ (3)

A 78.7 mg (0.205 mmol) portion of dppm was dissolved in 5 ml of dichloromethane, and an equivalent amount of AuBr (56.7 mg, 0.205 mmol) suspended in 4mL of dichloromethane was added to the dppm solution under agitation. The solution was stirred for 5 minutes followed by the addition of NH_4PF_6 (31.9 mg, 0.205 mmol) dissolved in 4 mL of dichloromethane and 1 mL of methanol. The light yellow solution was stirred for 3 hours and the crude mixture was evaporated to dryness. The resulting yellow solid was dissolved in a minimum amount of dichloromethane. The yellow solution was filtered using a filter pipet, and the filtrate was evaporated to dryness. A purified yield of 82.3 mg (28.9%) was obtained. The dried crude product was dissolved in

dichloromethane. This solution was filtered into the bottom of an outer diameter of 5 mm glass tube, a few drops of dichloromethane was layered over that solution and then diethyl ether was layered over the mixture. Colorless blocks with blue luminescence grew as diffusion mixed the solutions.

Infrared spectrum: 3049(w), 3016(w), 2966(w), 2918(w), 2362(w), 2337(w), 1485(m), 1436(s), 1317(w), 1311(w), 1186(w), 1163(m), 1101(s), 1024(w), 999(m), 918(w), 837(vs), 742(s), 740(s), 721(s), 688(vs), 619(w) cm^{-1}.

Preparation of $[Au_2(\mu\text{-dppm})_2Cl](BPh_4)\bullet 3CH_2Cl_2$ (4).

A 65.7 mg (0.169 mmol) portion of dppm was dissolved in 5 ml of dichloromethane, and an equivalent amount of thtAuCl (54.7mg, 0.171 mmol) dissolved in 4 mL of dichloromethane was added to the dppm solution under agitation. The solution was stirred for 10 minutes followed by the addition of $Na(BPh_4)$ (55.6 mg, 0.161 mmol) dissolved in 4 mL of dichloromethane and 1 mL of methanol. The light yellow solution was stirred for 3 hours and the crude mixture was evaporated to dryness. The resulting light yellow solid was dissolved in a minimum amount of dichloromethane. The solution was filtered using a filter pipet, and the filtrate was evaporated to dryness. A purified yield of 202.1 mg (78.9%) was obtained. The dried product was dissolved in dichloromethane. This solution was filtered into the bottom of an outer diameter of 5 mm glass tube and a small amount of dichloromethane was layered of the solution. Diethyl ether was then layered over this mixture. Yellow block crystals with blue luminescence were formed and were isolated.

Infrared spectrum: 3052(w), 2850(w), 1434(m), 1418(m), 1344(w), 1265 (w), 1238(m), 1112(w), 1102(m), 1026(w), 996(w), 944(w), 869(w), 776(m), 705(s), 685(s), 571(w), 515(m), 471(w) cm^{-1}.

Preparation of $[(Au_2(\mu\text{-dppm})_2]Cl(AsF_6)\bullet 2CH_2Cl_2$ (5)

A 69.9 mg (0.1818 mmol) portion of dppm was dissolved in 1 ml of dichloromethane and 1 ml of acetonitrile, and an equivalent amount of thtAuCl (58.9 mg, 0.1837 mmol) dissolved in 2 mL of dichloromethane was added under agitation. The solution was stirred for 5 minutes and then a solution of $NaAsF_6$ (194.63 mg, 0.9185 mmol) in 1 mL of dichloromethane and 1 mL of methanol was added. The colorless solution was stirred for 3 hr and the crude mixture was evaporated to dryness. The resulting yellow solid was dissolved in a minimum amount of dichloromethane. The solution was filtered using a filter pipet, and the filtrate was evaporated to dryness. A yield of 29.6 mg (2.13%) was obtained. The dried product was dissolved in dichloromethane. This solution was filtered into the bottom of a 5 mm diameter glass tube and a small amount of dichloromethane was layered over it. Diethyl ether was subsequently layered over these solutions. This mixture was cooled to -20 °C and allowed to stand. Colorless block-like crystals with green luminescence formed and were isolated.

Infrared spectrum: 2929(w), 2922(w), 2854(w), 2355(w), 2331(w), 1481(w), 1437(m), 1352(w), 1311(w), 1263(w), 1184(w), 1159(w), 1107(m), 1068(w), 1029(w), 999(w), 850(w), 783(m), 744(s), 684(vs) cm^{-1}.

X-ray Crystallography and Data Collection. The crystals were removed from the glass tubes in which they were grown together with a small amount of mother liquor and immediately coated

with a hydrocarbon oil on a microscope slide. A suitable crystal of each compound was mounted on a glass fiber with silicone grease and placed in the liquid nitrogen cold stream of a Bruker SMART CCD with graphite monochromated Mo Kα radiation at 90(2) K. Check reflections were stable throughout the data collection.

The structures were solved by direct methods and refined using all data (based on F^2) using the software SHELXTL 5.1. A semiempirical method utilizing equivalents was employed to correct for absorptions. Hydrogen atoms were added geometrically and refined with a riding model. [21]

Physical Measurements. Infrared spectra were recorded on a Bruker ALPHA FT-IR spectrometer. Excitation and emission spectra were recorded on a Perkin-Elmer LS50B luminescence spectrophotometer.

Associated Content

Supporting Information Available: CCDC 2379676-2379680 contain the supplementary crystallographic data for this paper. These data can be obtained free of charge via www.ccdc.cam.ac.uk/data_request/cif, by emailing data_request@ccdc.cam.ac.uk, or by contacting The Cambridge Crystallographic Data Centre, 12 Union Road, Cambridge CB2 1EZ, U.K.; fax: +44 1223 336033.

Author Information

Corresponding Author

Alan. L. Balch − *Department of Chemistry, University of California-Davis, Davis, California 95616, United States;* orcid.org/0000-0002-8813-6281; Email: albalch@ ucdavis.edu

Authors

Sarah Costa − *Department of Chemistry, University of California-Davis, Davis, California 95616, United States:* orcid.org/0000-0002-1498-0762

Sarah M. Chui, *Department of Chemistry, University of California-Davis, Davis, California 95616, United States*

Katelyn A. Espinoza *Department of Chemistry, University of California-Davis, Davis, California 95616, United States*

James C. Fettinger − *Department of Chemistry, University of California-Davis, Davis, California 95616, United States*

Notes

The authors declare no competing financial interest.

Acknowledgments. We thank the U. S. National Science Foundation [Grant CHE-1807637] for support.

References

(1) Ziolo, R.; Lipton, S.; Z. Dori, Z. The Photoluminescence of Phosphine Complexes of d^{10} Metals. *Chem. Comm*. **1970**, 1124-1125. .

(2) King, C.; Wang, J. chun; Khan, M. N. I.; Fackler, J. P. Luminescence and Metal-Metal Interactions in Binuclear Gold Compounds. *Inorg. Chem.* **1989**, *28* (11), 2145–2149.

(3) Balch, A. L. Remarkable Luminescence Behaviors and Structural Variations of Two-Coordinate Gold(I) Complexes. *Struct. Bond.* **2007**, *123*, 1-.

(4) Yam, V. W.-W.; Wong, K. M.-C. Luminescent metal complexes of d^6, d^8 and d^{10} transition metal centres. *Chem. Commun*. **2011**, *47*, 11579–11592.

(5) Yam, V. W. W.; Cheng, E. C. C. Highlights on the recent advances in gold chemistry—a photophysical perspective. *Chem. Soc. Rev.* **2008**, *37*, 1806 -1813.

(6) He, X.; Yam, V. W. W. Luminescent Gold(I) Complexes for Chemosensing. *Coord. Chem. Rev.* **2011**, *255*, 2111–2123.

(7) Yam, V.W.-W.; Au, V. K.-M.; Leung, S. Y.-L. Light-Emitting Self-Assembled Materials Based on d^8 and d^{10} Transition Metal Complexes. *Chem. Rev*. **2015**, *115*, 7589−7728.

(8) Mirzadeh, N.; Privér, S. H.; Blake, A. J.; Schmidbaur, H.; Bhargava, S. K. Innovative Molecular Design Strategies in Materials Science Following the Aurophilicity Concept. *Chem. Rev*. **2020**, *120*, 7551−7591.

(9) Jin, M.; Hajime Ito, H. Solid-state luminescence of Au(I) complexes with external stimuli-responsive properties. *J. Photochem. Photobiol. C* **2022**, *51*, 100478.

(10) Lee, L. C.-C.; Lo, K. K.-W. Shining New Light on Biological Systems: Luminescent Transition Metal Complexes for Bioimaging and Biosensing Applications. *Chem. Rev.* **2024**, *124*, 8825−9014.

(11) Luong, L. M. C.; Lowe, C. D.; Adams, A. V.; Moshayedi, V.; Olmstead, M. M.; Balch, A. L. Seeing luminescence appear as crystals crumble. Isolation and subsequent self-association of individual $[(C_6H_{11}NC)_2Au]^+$ ions in crystals. *Chem. Sci*. **2020**, *11*, 11705–11713.

(12) White-Morris, R. L.; Olmstead, M. M.; Balch, A. L. Aurophilic Interactions in Cationic Gold Complexes with Two Isocyanide Ligands. Polymorphic Yellow and Colorless Forms of $[(\text{Cyclohexyl Isocyanide})_2Au^I](PF_6)$ with Distinct Luminescence *J. Am. Chem. Soc.* **2003**, *125*, 103-1040.

(13) Malwitz, M. A.; Lim, S. H.; White-Morris, R. L.; Pham, D. M.; Olmstead, M. M.; Balch, A. L. Crystallization and Interconversions of Vapor-Sensitive, Luminescent Polymorphs of $[(C_6H_{11}NC)_2Au^I](AsF_6)$ and $[(C_6H_{11}NC)_2Au^I](PF_6)$. *J. Am. Chem. Soc.* **2012**, *134*, 10885-10893.

(14) Luong, L. M. C.; Malwitz, M. A.; Moshayedi, V.; Olmstead, M. M.; Balch, A. L. Role of Anions and Mixtures of Anions on the Thermochromism, Vapochromism, and Polymorph Formation of Luminescent Crystals of a Single Cation, $[(C_6H_{11}NC)_2Au]^+$. *J. Am. Chem. Soc*. **2020**, *142*, 5689−5701.

(15) Luong, L. M. C.; Olmstead, M. M.; Balch, A. L. A Non-Luminescent Polymorph of $[(\text{Cyclohexyl Isocyanide})_2Au]PF_6$ that Becomes Luminescent Upon Grinding or Exposure to Dichloromethane Vapor. *Chem. Commun*. **2021**, *57*, 793-796.

(16) Alconchel, A.; Crespo, O.; Gimeno, M. C. Versatile Emissive Three-Coordinated Gold(I) Systems- Properties and Perspectives. *Eur. J. Inorg. Chem.* **2021**, 3913 – 3925.

(17) Barakat, K. A.; Cundari, T. R.; Omary, M. A. Jahn−Teller Distortion in the Phosphorescent Excited State of Three-Coordinate Au(I) Phosphine Complexes. *J. Am. Chem. Soc*. **2003**, *125*, 14228-14229.

(18) Sinha, P.; Wilson, A. K.; Omary, M. A. Beyond a T-Shape. *J. Am. Chem. Soc*. **2005**, *127*, 12488-12489.

(19) Pyykkö. P.; Li, J.; Runeberg, N. Predicted ligand dependence of the Au (I) ··· Au (I) attraction in ($XAuPH_3$). *Chem. Phys. Lett*. **1994**, *218*, 133-137.

(20) Pyykkö. P. Strong Closed-Shell Interactions in Inorganic Chemistry. *Chem. Rev*. **1997**, *97*, 597-636.

(21) Katz, M. J.; Sakai, K.; Leznoff, D. B. The use of aurophilic and other metal-metal interactions as crystal engineering design elements to increase structural dimensionality, *Chem. Soc. Rev.,* **2008,** 1884-1895.

(22) Schmidbaur, H.; Schier, A. Aurophilic Interactions In and Between Molecules as a Subject of Current Interest. *Chem. Soc. Rev*. **2012**, *41*, 370−412.

(23) Harwell, D. E.; Mortimer, M. D.; Knobler, C. B.; Anet, F. A. L.; Hawthorne, M. F. Auracarboranes with and without Au-Au interactions: An unusually strong aurophilic interaction (1996). *J. Am. Chem. Soc.* **1996**, *118*, 2679–2685.

(24) Grudova, M. V.; Novikov, A. S.; Kubasov, A. S.; Khrustalev, V. N.; Kirichuk, A. A.; Nenajdenko, V. G.; Tskhovrebov, A. G. Aurophilic Interactions in Cationic Three-Coordinate Gold(I) Bipyridyl/Isocyanide Complex. *Crystals* **2022**, *12*, 613.

(25) Streitberger, M.; Schmied, A.; Hey-Hawkins, E. Selective Formation of Gold(I) Bis-Phospholane Macrocycles, Polymeric Chains, and Nanotubes. *Inorg. Chem*. **201**4, *53*, 6794−6804.

(26) Lim, S. H.; Schmitt, J. C.; Shearer, J.; Jia, J.; Olmstead, M. M.; Fettinger, J. C.; Balch, A. L. Crystallographic and Computational Studies of Luminescent, Binuclear Gold(I) Complexes, $Au^{I}_2(Ph_2P(CH_2)_nPPh_2)_2I_2$ (n = 3−6). *Inorg. Chem*. **2013**, *52*, 823−831.

(27) Boar, P.; Streitberger, M.; Lönnecke, P.; Hey-Hawkins, E. Copper(I) Complexes of a Flexible Bis-phospholane Ligand: Route to Paddle-Wheel- and Box-Type Macrocycles. *Inorg. Chem*. **2017**, *56*, 7285−7291.

(28) Balch, A. L.; Tulyathan, B. Interactions between Rhodium(I) Centers in Dimeric Complexes. *Inorg. Chem*. **1977**, *16*, 2840−2845.

(29) Costa, S.; Walters, D. T.; McNamara, L. E.; Olmstead, M. M.; Fettinger, J. C.; Balch, A. L. Structure and Luminescence Studies of Salts of the Helical Dication, $[Au_2(\mu$-bis(diphenylphosphine)ethane$)_2]^{2+}$ and Comparison with Salts of $[Au_2(\mu$-bis(diphenylphosphine)propane$)_2]^{2+}$. *Inorg. Chem.* **2023**, *62*, 15902−15911.

(30) Lim, S. H.; Olmstead, M. M.; Balch, A. L. Inorganic topochemistry. Vapor-induced solid state transformations of luminescent, three-coordinate gold(I) complexes. *Chem. Sci*. **2013**, *4*, 311–318.

(31) Costa, S.; Aristov, M. M.; Lim, S. H.; Chui, S. M.; Espinoza, K. A.; Olmstead, M. M.; Fettinger, J. C.; Berry, J. F.; Balch, A. L. Molecular Flexibility in Solvated Crystals of the Dimer, $Au_2(\mu$-1,2- bis(diphenylphosphino)ethane$)_2I_2$, with Three-Coordinate Gold(I). *Inorg. Chem.* 2024, 63, 12752−12763.

(32) Lim, S. H.; Olmstead, M. M.; Balch, A. L. Molecular Accordion: Vapoluminescence and Molecular Flexibility in the Orange and Green Luminescent Crystals of the Dimer, Au_2(μ-bis-(diphenylphosphino)ethane)$_2Br_2$. *J. Am. Chem. Soc*. **2011**, *133*, 10229-10238.

(33) Puddephatt, R. J. Chemistry of Bis(dipheny1phosphino)methane. *Chem. Soc. Rev.* **1983**, *12*, 99-127.

(34) Kubiak, C. P.; Eisenberg, R. Binuclear Rhodium(I) Complexes. Molecular A Frames, *J. Am. Chem. Soc*. **1977**, *99*, 6129-6131.

(35) Olmstead, M. M.; Hope, H.; Benner, L. S.; Balch, A. L. Insertion of Isocyanides and Carbon Monoxide into Metal-Metal Bonds. Preparation and Structure of $[Pd_2(CNCH_3)_3[(C_6H_5)_2PCH_2P(C_6H_5)_2]_2][PF_6]_2$. *J. Am. Chem. Soc.*, **1977**, *99*, 5502-5503. .

(36) Hoffman, D. M.; Hoffmann R. A-Frames *Inorg. Chem.* **1981**, *20*, 3543- 3555.

(37) Schmidbaur, H.; Wohlleben, A.; Schubert, U.; Frank, A.; Huttner, G. Synthese und Kristallstruktur achtgliedriger Ringverbindungen von Gold(1) mit Au - Au-Wechselwirkung. *Chem. Ber*. **1977**, *110***,** 2751-2757.

(38) Liou, L.-S.; Liu, C.-P.; Wang, J.-C. The Monoclinic Phase $[Au_2(C_{25}H_{22}P_2)_2]Cl_2.2CH_3CN$. Acta Cryst. **1994**, *C50*, 538-540.

(39) Shain, J.; Fackler, Jr., J. P. The first example of a gold bis(diphenylphosphino)methane cationic dimer with a bridging iodide. The X-ray crystal structures of (μ-I)$[Au(dppm)]_2[I]$ and $[Au(dppm)Br]_2$ *Inorg. Chim. Acta*, **1987**, *131*, 157-158.

(40) Bowmaker, G. A.; Dyason, J. C.; Healy, P. C.; Engelhardt, L. M.; Pakawatchai, C.; White, A. H. Lewis-Base Adducts of Group 11 Metal(I) Compounds. Part 27. Solid-state Phosphorus-31 Cross-polarization Magic-angle Spinning Nucleat Magnetic Resonance, Far-infrared, and Structural Studies on the Mononuclear 2:1 Adducts of

Triphenylphosphine with Copper(I) and Gold(I) Halides. *J. Chem. Soc. Dalton Trans*. **1987**, 1089-1097.

(41) Fu, W.-F.; Chan, K.-C.; Cheung, K.-K.; Che, C.-M. Substrate-Binding Reactions of the ^{3}[dσ*pσ] Excited State of Binuclear Gold(I) Complexes with Bridging Bis(dicyclohexylphosphino)methane Ligands: Emission and Time-Resolved Absorption Spectroscopic Studies. *Chem. Eur. J.* **2001**, *7*, 4656-4664.

(42) England, K. R.; Lim, S. H.; Luong, L. M. C.; Olmstead, M. M.; Balch, A. L. Vapoluminescent Behavior and the Single-Crystal-to Single-Crystal Transformations of Chloroform Solvates of $[Au_2(\mu\text{-}1,2\text{-bis(diphenylarsino)ethane})_2](AsF_6)_2$. *Chem. Eur. J.* **2019**, *25*, 874 – 878.

(43) Sheldrick, G. M. A short history of *SHELX*. *Acta Crystallogr., Sect. A*, **2008**, *64*, 112-122.

TOC Image

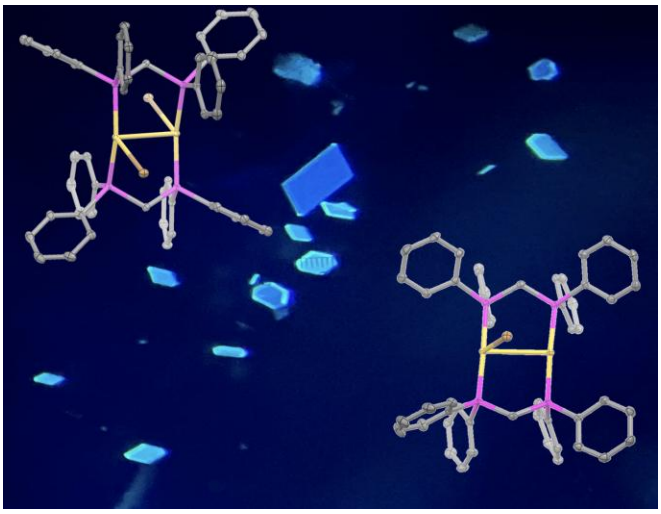

TOC Text

The structures and luminescence of five new dinuclear gold(I) complexes are reported, including three with the unusual arrangement of a two-coordinate gold(I) ion undergoing an aurophilic interaction with a three-coordinate gold(I) ion.

Chapter 4

A Molecular Planetarium: Evidence for an Iodide Ligand Orbiting two Gold (I) Ions in $[Au_2(\mu\text{-}1,2\ Bis\text{-}(diphenylphosphino)methane)_2I]^+$ †

Costa, S.; Chui, S. M.; Espinoza, K. A.; Olmstead, M. M.; Fettinger, J. C.; Balch, A. L. "A Molecular Planetarium: Evidence for an Iodide Ligand Orbiting two Gold (I) Ions in $[Au_2(\mu\text{-}1,2\ Bis\text{-}(diphenylphosphino)methane)_2I]^+$"

Manuscript in Submission

Abstract

Four new crystalline gold(I) complexes, $[Au_2(\mu\text{-dppm})_2I][Au_2(\mu\text{-dppm})_2(\mu\text{-I})](AsF_6)_4\bullet 4CH_2Cl_2$ (**1**), $[Au_2(\mu\text{-dppm})_2(\mu\text{-I})]I\bullet 2CH_2Cl_2$ (**2**), $[Au_2(\mu\text{-dppm})_2(\mu\text{-I})](PF_6)\bullet CH_2Cl_2$ (**3**), and $[Au_2(\mu\text{-dppm})_2](AsF_6)_2\bullet CH_2Cl_2$ (**4**) where dppm is bis-(diphenylphosphino)methane), have been prepared and structurally characterized by single crystal X-ray diffraction and nuclear magnetic resonance spectroscopy (NMR). Yellow crystals of $[Au_2(\mu\text{-dppm})_2(\mu\text{-I})]I\bullet 2CH_2Cl_2$ (**2**) and $[Au_2(\mu\text{-dppm})_2(\mu\text{-I})](PF_6)\bullet CH_2Cl_2$ (**3**) have a structure with two three-coordinate gold(I) ions held in close proximity by the dppm and bridging iodide ligands. Crystals of $[Au_2(\mu\text{-dppm})_2I][Au_2(\mu\text{-dppm})_2(\mu\text{-I})](AsF_6)_4\bullet 4CH_2Cl_2$ (**1**) have two different cations: one similar to complexes **2** and **3** and the other cation with a terminal iodide ligand in an unusual arrangement that binds a two-coordinate gold(I) ion to a three-coordinate gold(I) ion through an aurophilic interaction. In contrast, $[Au_2(\mu\text{-dppm})_2](AsF_6)_2\bullet CH_2Cl_2$ (**4**) has no anion bound and only has the gold ions as two-coordinate centers. Each complex displays luminescence under UV irradiation in solid and solution state. The NMR spectra of solutions of the iodide complexes (**1**), (**2**), and (**3**) suggest that the iodide ion is bound to the $[Au_2(\mu\text{-dppm})_2]^{2+}$ core but is able to circulate around this core.

Introduction

Gold(I) complexes have been investigated for their biological, biochemical, electronic, catalytic, and optical uses due to their tunable luminescent properties.[1-4] These emissive properties

are frequently correlated to aurophilic interactions between neighboring gold(I) ions particularly in two-coordinate gold complexes. Aurophilic interactions are a result of correlation and relativistic effects that promote weak bonding between closed-shell gold(I) ions.[5,6] The noncovalent interactions can lead to aggregation of gold(I) complexes into dimers, chains, and polymers.[7]

Crystalline gold(I) complexes display an interesting and varied array of properties and have the virtue of a well-defined structures that can be determined by single crystal X-ray diffraction. The luminescence of several gold(I) complexes show variation when polymorphic crystals form.[8,9] For example, $[Au(CNC_6H_{11})_2](PF_6)$ crystallizes as three polymorphs; a) yellow crystal with green-luminescent, b) colorless crystal with blue-luminescent, and c) colorless non-luminescent crystals.[10,11] The yellow, green-luminescent crystals contain kinked extended chains of gold(I) ions connected through aurophilic interactions, while the colorless, blue-luminescent crystals contained linear extended chairs of gold(I) ions. In the colorless non-luminescent crystals, the gold(I) ions are widely dispersed and there are no aurophilic interaction. Several crystalline gold(I) complexes are mechanochromic and display alteration in their luminescence upon grinding.[12,13,14] For example, mechanical pressure transforms the blue-luminescent polymorph of (PhNC)AuPh into a yellow-luminescent polymorph through rearrangement of the packing between the molecules.[15]

Diphosphine ligands, $R_2P(CH_2)_nPR_2$, allow the formation of dinuclear complexes in which the interactions between two gold(I) ions can be somewhat constrained. For dimers built around an $[M_2(\mu\text{-}R_2P(CH_2)_nPR_2)_2]^{+m}$ core, the distance and bonding between the metal centers can be dictated by the length of the methylene bridge in the diphosphine. When three or more methylene groups are present, the metal ions are widely separated and no metallophilic interactions occur.[16]

However, with one or two methylene groups, the metal centers are close enough that metallophilic interactions may occur.[23] In particular, for complexes with a $[Au_2(\mu\text{-dppm})_2]^{2+}$ core, the gold(I) ions are constrained to be rather close together, but an array of structural possibilities exist as shown in Scheme 1.

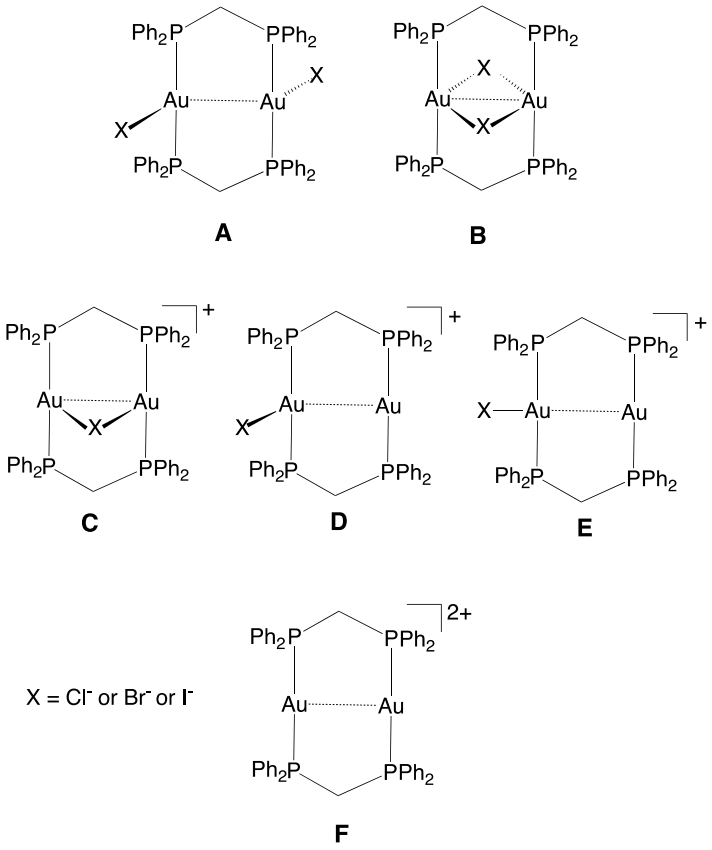

Scheme 1. Structural possibilities for complexes with an $[Au_2(\mu\text{-dppm})_2]^{2+}$ core.

Despite the constraints placed by the bridging phosphine ligands, in solution gold(I) complexes frequently form mixtures from which a variety of compounds can be isolated. For example, a 1:1 mixture of AuBr and 1,2-bis(diphenylphosphino)ethane (dppe) can produce colorless, orange luminescent crystals of the dimer $Au_2(\mu\text{-dppe})_2Br_2$ with Au···Au separations ranging from 3.8479(3) to 3.5142(3) Å, colorless, green luminescent crystals of the same dimer with shorter Au···Au separations ranging from 3.3249(2) to 3.0943(2) Å, or colorless, orange luminescent crystals of the polymer $\{Au(\mu\text{-dppe})Br\}_n$ with no close interactions between the gold(I) ions.[21] Similarly, a 1:1 mixture of AuI and dppe can produce colorless, orange luminescent or colorless, green luminescent crystals of the dimer, $Au_2(\mu\text{-dppe})_2I_2$, colorless, orange luminescent crystals of another dimer, $Au_2(\mu\text{-dppe})_2(\mu\text{-}I_2)$, or colorless crystals of the polymer $\{Au(\mu\text{-dppe})I\}_n \cdot n(CHCl_3)$, which is luminescent only at 77 K.[22,23] In another example, the same synthetic procedure and crystallization method leads to two completely different products: $[Au_6(Triphos)_4(CuCl_2)](PF_6)_5 \cdot (CH_2Cl_2)_4$, (where Triphos is tridentate ligand bis(2-diphenyl-phosphinoethyl)phenylphosphine) with a box-like structure and a copper ion suspended between two Au(I) ions,[24] or $[Au_6(Triphos)_4](PF_6)_6 \cdot 2CH_2Cl_2 \cdot 6C_6H_5CH_3 \cdot H_2O$, which contains two helical segments in which two different gold(I) ions are bridged by two $Ph_2PCH_2CH_2PPh$ segments and no copper ion.[25] In an example that is immediately relevant to the present paper, blue luminescent plates of the molecular compound, $Au_2(\mu\text{-dppm})_2Br_2 \bullet 2CH_2Cl_2$, and teal luminescent blocks of the ionic complex, $[Au_2(\mu\text{-dppm})_2Br]Br \bullet 2CH_2Cl_2$, formed from the same dichloromethane solution.[26] As a consequence of these observations, it has been difficult to thoroughly understand the solution dynamics involved. Finally, an examination of the solution behavior of [ClAu(μ-dppm)Au(μ-dppm)AuCl]Cl by $^{31}P\{^1H\}$ NMR spectroscopy showed that the compound is in equilibrium with $Au_2(\mu\text{-dppm})_2Cl_2$ and $(\mu\text{-dppm})Au_2Cl_2$.[27]

In this paper, we explore a series of luminescent dppm-bridged gold(I) complexes with an $[Au_2(\mu\text{-dppm})_2I]^+$ core and propose a mechanism to explain their behavior in solution.

Results and Discussion.

Formation and Structure of the $[Au_2(\mu\text{-dppm})_2I][Au_2(\mu\text{-dppm})_2(\mu\text{-I})](AsF_6)_4\bullet 4CH_2Cl_2$ (1).

Treatment of a solution of dppm with a suspension of gold(I) iodide in dichloromethane and a solution of sodium hexafluoroarsenate in dichloromethane/methanol produced a yellow solid. Yellow crystals were obtained by diffusion of diethyl ether into a dichloromethane solution of the product. Crystal data for these and other compounds are given in the experimental section, while structural data can be found on Table 1. The structures of the two different cations in $[Au_2(\mu\text{-dppm})_2I][Au_2(\mu\text{-dppm})_2(\mu\text{-I})](AsF_6)_4\bullet 4CH_2Cl_2$ (**1**), as determined by single crystal X-ray diffraction, are shown in Figure 1. The cation **A** has a rare arrangement with three-coordinate gold(I) ion as well as a two-coordinate gold(I) ion connected by two bridging dppm ligands**.** The distance between the two gold(I) ions is 2.9180(5) Å, which consistent with an aurophilic interaction between the two ions. The Au-I bond distance is 3.0051(9) Å, while the distance from the iodine ion to the adjacent two-coordinate gold(I) ion is 3.6458(9) Å. The coordinated iodide ion is displaced toward the adjacent gold(I) ion so that the Au···Au-I angle is 75.96(2)°. The methylene groups in cation **A** lie in the same direction as the iodide bridge.

Cation labeled **B** has a structure that is similar the structures of the cations in $[Au_2(\mu\text{-dppm})_2(\mu\text{-I})]I\bullet Et_2O$,[28] $[Au_2(\mu\text{-dppm})_2(\mu\text{-I})][Au(CN)_2]$,[29] and $[Au_2(\mu\text{-dppm})_2(\mu\text{-I})][(Au(C_7H_9Si)_2)]$.[30] The cation **B** contains a bridging iodide between two three-coordinate gold(I) ions, which are connected by two bridging dppm ligands. The distance between the two

gold(I) ions is 2.9791(5) Å, which is consistent with an aurophilic interaction between the two ions. The iodide ion is asymmetrically disposed between the two gold(I) ions: the Au1-I1 bond distance is 3.195(1) Å while the Au2-I1 bond distance is 3.2379(9) Å. Additionally, the Au-I bond distances in cation **B** are significantly longer than the Au-I distance in cation **A** (3.0051(9) Å) or in the classic example $Au(PPh_3)_2I$ (2.753(9) Å).[17]

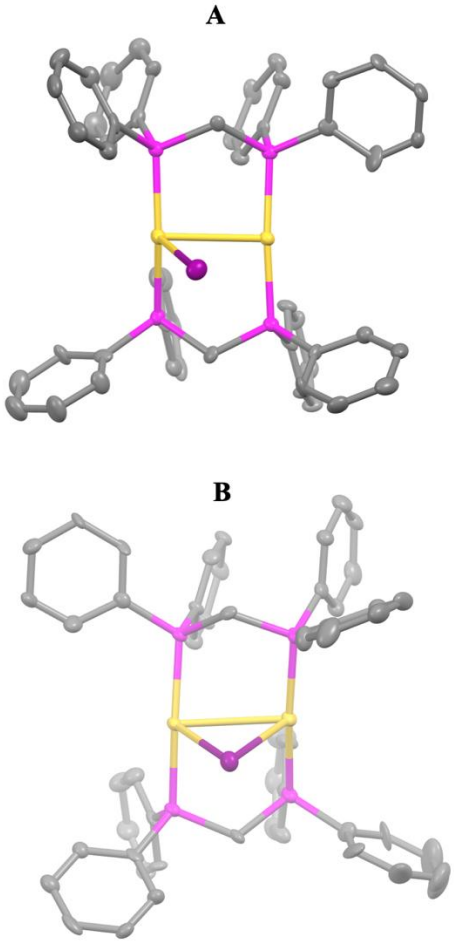

Figure 1. The structures of the cations in $[Au_2(\mu\text{-dppm})_2I][Au_2(\mu\text{-dppm})_2(\mu\text{-I})](AsF_6)_4 \bullet 4CH_2Cl_2$ (**1**): **A**, $[Au_2(\mu\text{-dppm})_2I]^+$, and **B**, $[Au_2(\mu\text{-dppm})_2(\mu\text{-I})]^+$. Hydrogen atoms are not shown for clarity. Drawn with thermal contours at the 30% probability level. Color code: gold, yellow; phosphorus, pink; iodide, purple; carbon, grey.

Table 1. Selected Bond Distances and Angles for Gold(I) Complexes

Complex	$[Au_2(\mu\text{-}dppm)_2I]^+$ in $[Au_2(\mu\text{-}dppm)_2I][Au_2(\mu\text{-}dppm)_2(\mu\text{-}I)](AsF_6)_4 \bullet 4CH_2Cl_2$ (**1**)	$[Au_2(\mu\text{-}dppm)_2(\mu\text{-}I)]^+$ in $[Au_2(\mu\text{-}dppm)_2I][Au_2(\mu\text{-}dppm)_2(\mu\text{-}I)](AsF_6)_4 \bullet 4CH_2Cl_2$ (**1**)	$[Au_2(\mu\text{-}dppm)_2(\mu\text{-}I)]I \bullet 2CH_2Cl_2$ (**2**)	$[Au_2(\mu\text{-}dppm)_2(\mu\text{-}I)](PF_6) \bullet CH_2Cl_2$ (**3**)
Distances (Å)				
Au···Au	Au51···Au52 2.9791(5)	Au1···Au2 2.9180(5)	2.9473(6)	2.949(1)
Intra-ligand P···P	P51-P52 3.082(4) P53-P54 3.054(4)	P1-P2 3.096(4) P3-P4 3.098(4)	P1-P2 3.072(4) P3-P4 3.070(4)	P1-P2 3.050(1) P3-P4 3.084(1)
Au1-P1	2.327(3)	2.327(3)	2.320(3)	2.3054(8)
Au1-P4	2.325(3)	2.334(3)	2.321(3)	2.3074(8)
Au2-P2	2.294(3)	2.315(3)	2.310(3)	2.3100(8)
Au2-P3	2.293(3)	2.313(3)	2.312(3)	2.3101(8)
Au1-I1	3.0051(9)	3.195(1)	3.098(1)	3.2953(8)
Au2-I1	3.6458(9)	3.2379(9)	3.169(1)	3.0694(6)
Δ |Au-I1-Au-I2|	0.6407	0.0429	0.071	0.159
Angles (deg)				
P1-Au1-P4	160.6(1)	164.6 (1)	165.2(1)	173.37(4)
P2-Au2-P3	171.7(1)	169.4(1)	169.04(9)	169.82(4)
Au1-Au2-X1	75.96(2)	61.69(2)	63.18(2)	66.36(2)
Torsional angles (deg)				
P2-Au2···Au1-P1	-4.6(1)	19.0(1)	0.84(9)	-3.08(3)
P3-Au2···Au1-P4	17.6(1)	13.6(1)	4.98(9)	1.42(3)

Table 1. Continued Selected Bond Distances and Angles for Gold(I) Complexes

Complex	$[Au_2(\mu\text{-}dppm)_2](AsF_6)_2 \bullet CH_2Cl_2$ (**4**)	$[Au_2(\mu\text{-}dppm)_2(\mu\text{-}I)]I \bullet C_4H_{10}O$[a]	$[Au_2(\mu\text{-}dppm)_2(\mu\text{-}I)][Au(C_4SiMe_3)_2]$[b]	$[Au_2(\mu\text{-}dppm)_2(\mu\text{-}I)][Au(CN)_2]$[c]
Distances (Å)				
Au···Au	2.9758(6)	2.948(2)	2.9577(4)	2.967(3)
Intra-ligand P···P	P1-P2 3.048(1) P3-P4 3.072(1)		P1-P2 3.114(3) P3-P4 3.094(2)	P1-P2 3.086(5) P3-P4 3.095(5)
Au1-P1	2.315(1)		2.311(3)	2.310(4)
Au1-P4	2.312(1)		2.317(3)	2.322(3)
Au2-P2	2.315(1)		2.310(3)	2.317(3)
Au2-P3	2.312(1)		2.320(3)	2.322(3)
Au1-I1		3.127(2)	3.1015(6)	3.162(3)
Au2-I1		3.196(2)	3.1069(6)	3.343(3)
Δ |Au-I1-Au-I2|		0.069	0.0054	0.181
Angles (deg)				
P1-Au1-P4	177.86(4)	167.7(2)	166.33(7)	170.1(1)
P2-Au2-P3	177.86(4)		61.46(1)	66.01(6)
Au1-Au2-I1				
Torsional angles (deg)				
P2-Au2···Au1-P1	0.00(4)		-6.58(7)	-2.4(1)
P3-Au2···Au1-P4	0.00(4)			

[a] From data in Shain, J.; Fackler, Jr., J. P. *Inorg.Chim. Acta*, **1987**, *131*, 57-158.

[b] From data in Bruce, M. I.; Jevric, M.; Skelton, B. W.; Smith, M. E.; White, A. H.; Zaitseva, N. N. *J. Organometal. Chem*. **2006**, *691*, 361–370.

[c] From data in Khan, M. N. I.; King, C.; Heinrich, D. D.; Fackler, J. P.; Porter, L. C. *Inorg. Chem.* **1989**, *28*, 2150–2154.

Formation and Structure of the $[Au_2(\mu\text{-dppm})_2(\mu\text{-I})]I\bullet 2CH_2Cl_2$ (2) and $[Au_2(\mu\text{-dppm})_2(\mu\text{-I})](PF_6)\bullet CH_2Cl_2$ (3). With the goals of preparing the hypothetical neutral molecule "$Au_2(\mu\text{-dppm})_2I_2$" and a salt containing solely the cation $[Au_2(\mu\text{-dppm})_2I]$, we undertook the following studies. Treatment of a solution of dppm with a suspension of gold(I) iodide in dichloromethane and a solution of potassium iodide or ammonium hexafluorophosphate in mixture of dichloromethane/methanol produced two yellow solids. Yellow crystals of each compound were obtained by diffusion of diethyl ether into a dichloromethane solution of the product. The asymmetric units in $[Au_2(\mu\text{-dppm})_2(\mu\text{-I})]I\bullet 2CH_2Cl_2$ (**2**) and $[Au_2(\mu\text{-dppm})_2(\mu\text{-I})](PF_6)\bullet CH_2Cl_2$ (**3**) contain the entirety of the cation, anion, and solvate molecules. The cations in $[Au_2(\mu\text{-dppm})_2(\mu\text{-I})]I\bullet 2CH_2Cl_2$ (**2**) and $[Au_2(\mu\text{-dppm})_2(\mu\text{-I})](PF_6)\bullet CH_2Cl_2$ (**3**) have similar A-frame structures with a slightly asymmetry in the position of the bridging iodide ligand. Figure 2 shows two views of the cation and anion in $[Au_2(\mu\text{-dppm})_2(\mu\text{-I})]I\bullet 2CH_2Cl_2$ (**2**) with the iodide counter ion located over 8 Å away from the nearest gold(I) ion. While a compound of this composition could have had a face-to-face structure with both iodide ions bonded to gold, the compound crystallized with an A-frame structure for the cation and non-coordinated iodide counter ion. A similar situation exists in $[Au_2(\mu\text{-dppm})_2(\mu\text{-I})]I\bullet Et_2O$, whose structure was reported previously. Thus, we did not achieve the goal of preparing molecular "$Au_2(\mu\text{-dppm})_2I_2$". Both $[Au_2(\mu\text{-dppm})_2(\mu\text{-I})]I\bullet 2CH_2Cl_2$ (**2**) and $[Au_2(\mu\text{-dppm})_2(\mu\text{-I})](PF_6)\bullet CH_2Cl_2$ (**3**) as well as $[Au_2(\mu\text{-dppm})_2(\mu\text{-I})]I\bullet Et_2O$ have close contacts between the gold(I) ions (2.9473(6), 2.949(1) and 2.9180(5) Å, respectively) and the methylene groups of the bridging diphosphine pointed in the same direction over the bridging iodide anion.

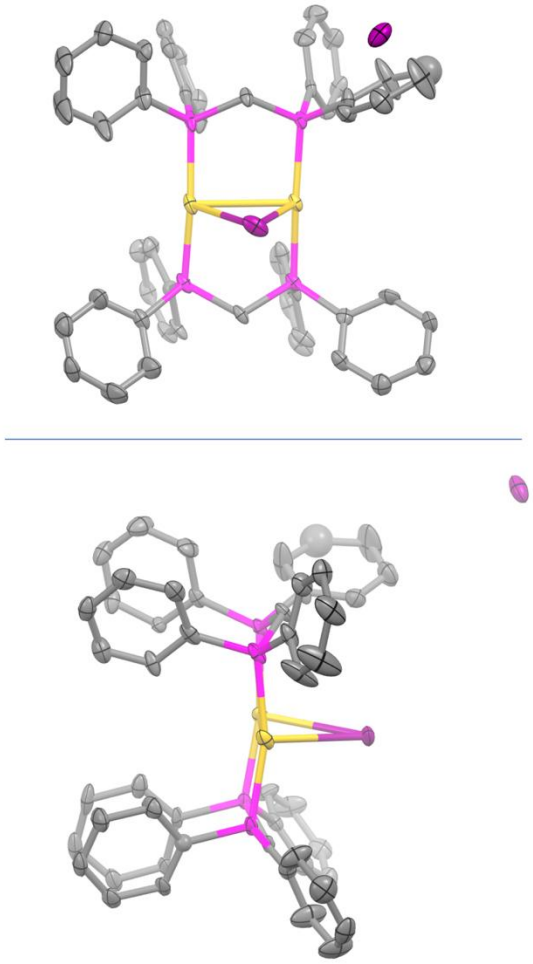

Figure 2. The two views of the structure of the cation and anion in $[Au_2(\mu\text{-dppm})_2(\mu\text{-I})]I\bullet 2CH_2Cl_2$ (**2**) showing the location of the nearest iodide ion to a gold(I) ion in the cation. Hydrogen atoms are not shown for clarity. Drawn with thermal contours at the 30% probability level. Color code: gold, yellow; phosphorus, pink; iodide, purple; carbon, grey.

Formation and Structure of the $[Au_2(\mu\text{-dppm})_2](AsF_6)_2\bullet CH_2Cl_2$ (4).

For comparison with these iodide-containing cations, we prepared $[Au_2(\mu\text{-dppm})_2](AsF_6)_2\bullet CH_2Cl_2$ (**4**) as an example of the simple cation, $[Au_2(\mu\text{-dppm})_2]^{2+}$ without a iodide ligand. Treatment of a solution of dppm with a solution of chloro(tetrahydrothiophene)gold(I) in

dichloromethane and a solution of silver hexafluoroarsenate (to provide a non-coordinating anion and to remove halide ions) in mixture dichloromethane/methanol produced a colorless solid. Colorless crystals were obtained by diffusion of diethyl ether into a dichloromethane solution of the product. The structure of the dication in $[Au_2(\mu\text{-dppm})_2](AsF_6)_2 \bullet CH_2Cl_2$ (**4**) is shown in Figure 3. The asymmetric unit consists of one half of the cation, which resides on a mirror plane that bisects the two methylene carbon atoms and the midpoint of the Au···Au bond along with half of an ordered hexafluoroarsenate ion that resides on a mirror plane, half of a disordered hexafluoroarsenate ion that resides on a mirror plane and is disordered over two orientations, and a disordered dichloromethane molecule in a general position. The distance between the two gold(I) ions is 2.9758(6) Å, which is indicative of an aurophilic interaction. The methylene groups of $[Au_2(\mu\text{-dppm})_2](AsF_6)_2 \bullet CH_2Cl_2$ (**4**) are pointed in opposing directions; unlike the complexes **1**, **2**, and **3** where both methylene groups are pointed towards the same side and over the bridging iodide. In comparison to the other complexes reported here, the P-Au-P angles are more nearly linear in $[Au_2(\mu\text{-dppm})_2](AsF_6)_2 \bullet CH_2Cl_2$ (**4**). The structure of the cation, $[Au_2(\mu\text{-dppm})_2]^{2+}$, is similar to that found in the salts, $[Au_2(\mu\text{-dppm})_2]Cl_2$,[31] $[Au_2(\mu\text{-dppm})_2](NO_3)_2$,[32] $[Au_2(\mu\text{-dppm})_2](ClO_4)_2$,[33] $[Au_2(\mu\text{-dppm})_2](BF_4)_2$,[34] $[Au_2(\mu\text{-dppm})_2](PF_6)_2$.[35]

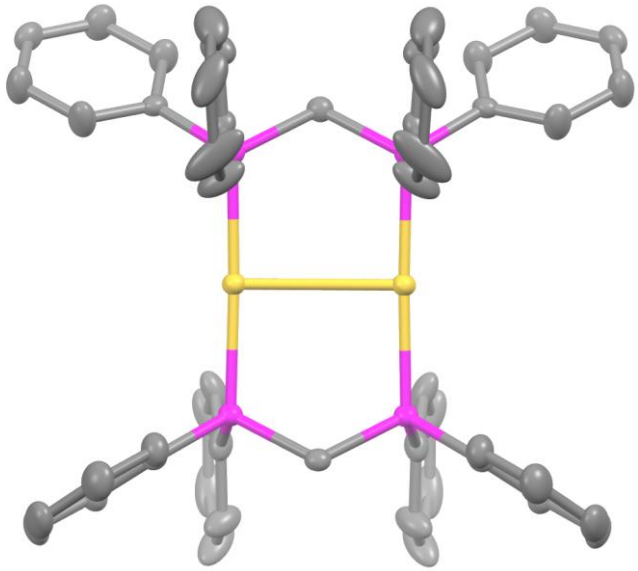

Figure 3. The structures of the cation $[Au_2(\mu\text{-dppm})_2](AsF_6)_2 \bullet CH_2Cl_2$ (**4**). Hydrogen atoms are not shown for clarity. Drawn with thermal contours at the 30% probability level. Color code: gold, yellow; phosphorus, pink; carbon, grey.

^{1}H and ^{31}P{^{1}H} NMR Studies of the Structure of the Binuclear Dications in Solution.

^{1}H and ^{31}P{^{1}H} NMR spectral data for acetonitrile-d_3 solutions of $[Au_2(\mu\text{-dppm})_2I][Au_2(\mu\text{-dppm})_2(\mu\text{-I})](AsF_6)_4 \bullet 4CH_2Cl_2$ (**1**), $[Au_2(\mu\text{-dppm})_2(\mu\text{-I})]I \bullet 2CH_2Cl_2$ (**2**), $[Au_2(\mu\text{-dppm})_2(\mu\text{-I})](PF_6) \bullet CH_2Cl_2$ (**3**) and $[Au_2(\mu\text{-dppm})_2](AsF_6)_2 \bullet CH_2Cl_2$ (**4**) at 290K are compiled in Table 2. As expected, $[Au_2(\mu\text{-dppm})_2](AsF_6)_2 \bullet CH_2Cl_2$ (**4**) shows a single resonance in its ^{31}P{^{1}H} spectrum and a quintet for the methylene protons with J(HP) of 5.10 Hz. Solutions of $[Au_2(\mu\text{-dppm})_2I][Au_2(\mu\text{-dppm})_2(\mu\text{-I})](AsF_6)_4 \bullet 4CH_2Cl_2$ (**1**), $[Au_2(\mu\text{-dppm})_2(\mu\text{-I})]I \bullet 2CH_2Cl_2$ (**2**) and $[Au_2(\mu\text{-dppm})_2(\mu\text{-I})](PF_6) \bullet CH_2Cl_2$ (**3**) also show only one ^{31}P{^{1}H} resonance, whereas three resonances would have been expected for $[Au_2(\mu\text{-dppm})_2I][Au_2(\mu\text{-dppm})_2(\mu\text{-I})](AsF_6)_4 \bullet 4CH_2Cl_2$ (**1**), if it maintained its structure in solution. The similarity of the ^{1}H and ^{31}P{^{1}H} NMR spectral data for $[Au_2(\mu\text{-dppm})_2I][Au_2(\mu\text{-dppm})_2(\mu\text{-I})](AsF_6)_4 \bullet 4CH_2Cl_2$ (**1**), $[Au_2(\mu\text{-dppm})_2(\mu\text{-}$

I)]I•2CH_2Cl_2 (**2**) and [Au_2(μ-dppm)$_2$(μ-I)](PF_6)•CH_2Cl_2 (**3**) indicate that all produce a common species in solution. Moreover, that species is distinct from [Au_2(μ-dppm)$_2$](AsF_6)$_2$•CH_2Cl_2 (**4**), which displays different ^{1}H and ^{31}P{^{1}H} NMR spectral data. Thus, we conclude that the iodide ligand remains attached to the [Au_2(μ-dppm)$_2$]$^{2+}$ core in solutions of [Au_2(μ-dppm)$_2$I][Au_2(μ-dppm)$_2$(μ-I)](AsF_6)$_4$•4CH_2Cl_2 (**1**), [Au_2(μ-dppm)$_2$(μ-I)]I•2CH_2Cl_2 (**2**) and [Au_2(μ-dppm)$_2$(μ-I)](PF_6)•CH_2Cl_2 (**3**).

Table 2. ^{1}H and ^{31}P NMR results at 290K in acetonitrile-d_3

	^{31}P δ (ppm)	^{1}H methylene δ (ppm)	^{1}H methylene J(HP)
[Au_2(μ-dppm)$_2$I][Au_2(μ-dppm)$_2$(μ-I)](AsF_6)$_4$•4CH_2Cl_2 (**1**)	27.8	4.68 (quintet)	4.72
[Au_2(μ-dppm)$_2$(μ-I)]I•2CH_2Cl_2 (**2**)	27.9	4.66 (quintet)	4.76
[Au_2(μ-dppm)$_2$(μ-I)](PF_6)•CH_2Cl_2 (**3**)	27.9	4.63 (quintet)	4.76
[Au_2(μ-dppm)$_2$](AsF_6)$_2$•CH_2Cl_2 (**4**)	35.6	4.43 (quintet)	5.10

The ^{1}H NMR resonances for the methylene protons in acetonitrile-d_3 solutions of [Au_2(μ-dppm)$_2$(μ-I)]I•2CH_2Cl_2 (**2**) and [Au_2(μ-dppm)$_2$](AsF_6)$_2$•CH_2Cl_2 (**4**) at room temperature and at 235 K are shown in Figures 4 and 5, respectively. At room temperature, each complex displays a single 1:4:6:4:1 quintet due to the virtual coupling of the methylene protons to the four phosphorus nuclei. The virtual coupling is caused by the very large coupling (ca 300 Hz) between the trans phosphorus

atoms on the gold ions. Similar quintets for the methylene protons have been observed for other binuclear complexes bridged by two dppm ligands.[36,37] The observation of a single resonance for the dppm methylene protons in these complexes indicate that both methylene protons are situated in equivalent orientations. Note that in the crystallographic structures of $[Au_2(\mu\text{-dppm})_2(\mu\text{-I})]I\bullet 2CH_2Cl_2$ (**2**) and $[Au_2(\mu\text{-dppm})_2(\mu\text{-I})](PF_6)\bullet CH_2Cl_2$ (**3**) one methylene proton lies close to the bridging iodide, while the other methylene proton is further from that bridging iodide. Hence, two different resonances would be expected for these A-frame cations. Similarly, if $[Au_2(\mu\text{-dppm})_2I][Au_2(\mu\text{-dppm})_2(\mu\text{-I})](AsF_6)_4\bullet 4CH_2Cl_2$ (**1**) retained its structure in solution, four methylene resonances would be expected, two for each cation. To account for the observation of a single $^{31}P\{^1H\}$ NMR resonance and a single methylene resonance for compounds (**1**), (**2**), and (**3**), we suggest that the dynamic process shown in Scheme 2 occurs in solution. In this process, the iodide ligand orbits the $[Au_2(\mu\text{-dppm})_2]^{2+}$ core while remaining attached to it. There are crystallographic precedents for each of the three different structures shown in the scheme. For, example, $[Au_2(\mu\text{-dppm})_2I][Au_2(\mu\text{-dppm})_2(\mu\text{-I})](AsF_6)_4\bullet 4CH_2Cl_2$ (**1**) contains both the A-frame structure and the structure with two and three-coordinate gold ions with an iodide ligand nearly perpendicular to the Au···Au bond. A structure with a two and a three-coordinate gold(I) ion but with the iodide ligand positioned parallel with the Au···Au bond has also been observed.[30,38]

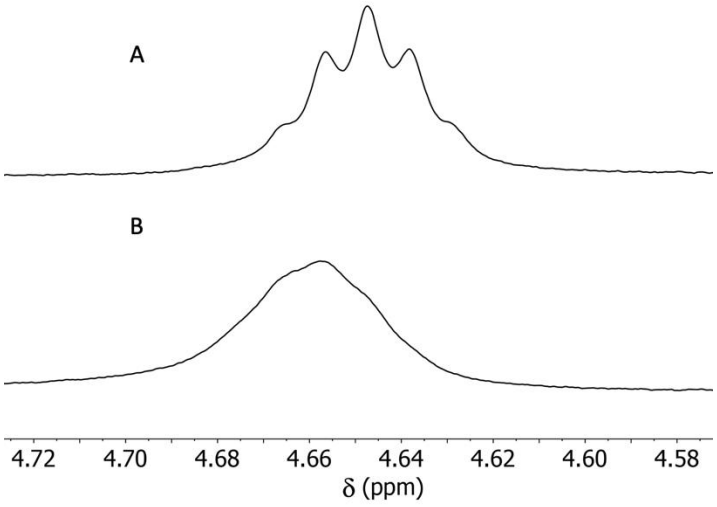

Figure 4. The ^{1}H NMR spectrum of the methylene region of $[Au_2(\mu\text{-dppm})_2(\mu\text{-I})]I\bullet 2CH_2Cl_2$ (**2**): **A** at 290 K and **B** at 235 K

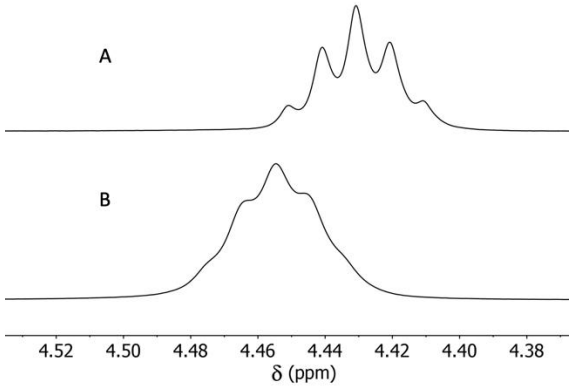

Figure 5. The ^{1}H NMR spectrum of the methylene region of $[Au_2(\mu\text{-dppm})_2](AsF_6)_2\bullet CH_2Cl_2$ (**4**): **A** at 296 K, and **B** at 235 K.

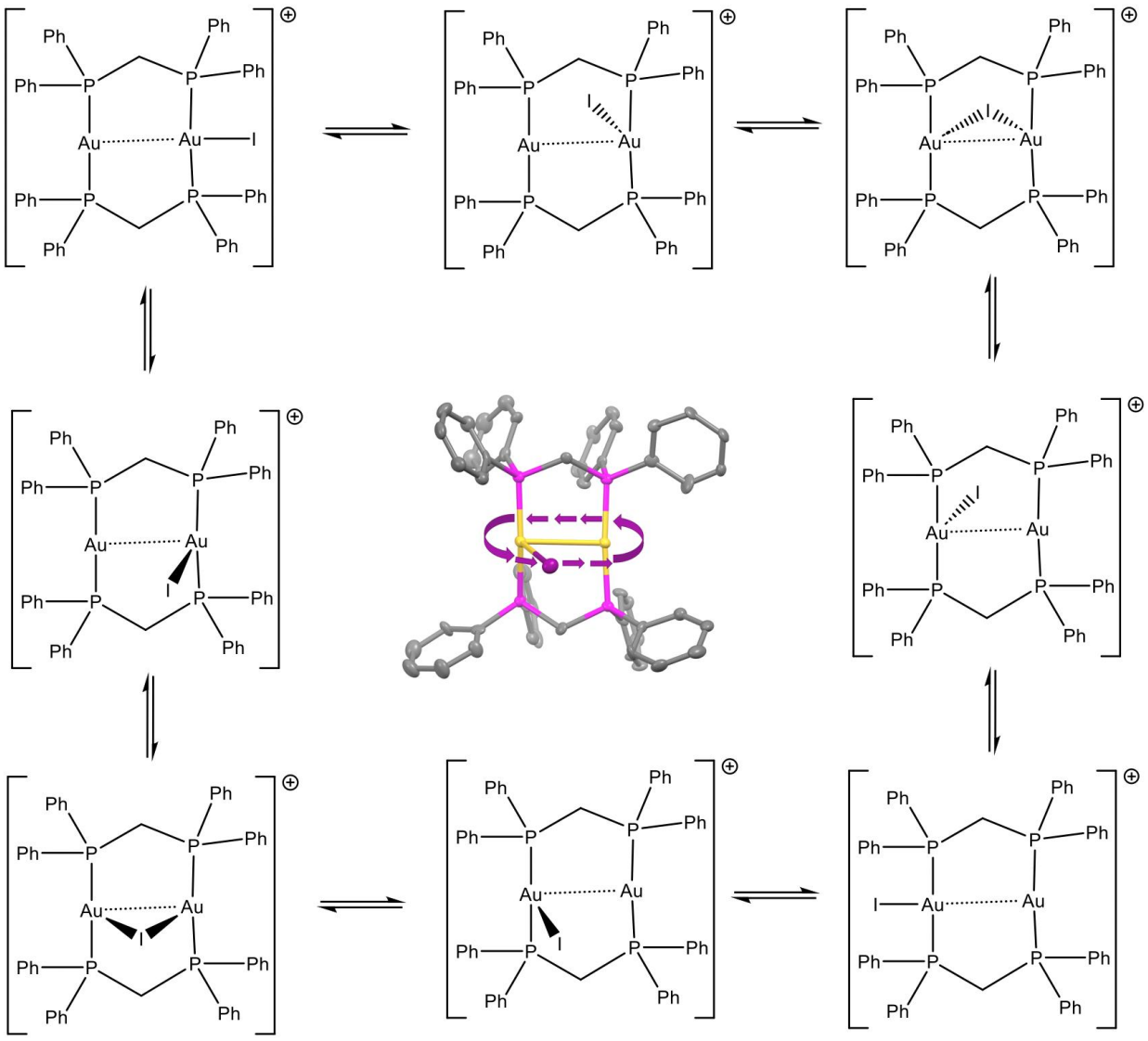

Scheme 2. Suggested dynamic behavior in solutions of $[Au_2(\mu\text{-dppm})_2I][Au_2(\mu\text{-dppm})_2(\mu\text{-I})](AsF_6)_4 \bullet 4CH_2Cl_2$ (**1**), $[Au_2(\mu\text{-dppm})_2(\mu\text{-I})]I \bullet 2CH_2Cl_2$ (**2**) and $[Au_2(\mu\text{-dppm})_2(\mu\text{-I})](PF_6) \bullet CH_2Cl_2$ (**3**) showing the movement of the iodide anion.

Cooling solutions of $[Au_2(\mu\text{-dppm})_2I][Au_2(\mu\text{-dppm})_2(\mu\text{-I})](AsF_6)_4 \bullet 4CH_2Cl_2$ (**1**), $[Au_2(\mu\text{-dppm})_2(\mu\text{-I})]I \bullet 2CH_2Cl_2$ (**2**) or $[Au_2(\mu\text{-dppm})_2(\mu\text{-I})](PF_6) \bullet CH_2Cl_2$ (**3**) resulted only in slight broadening of the $^{31}P\{^1H\}$NMR resonance of the cation in each solution. Similarly, cooling to

235 K produced broadening of the methylene quintet for these complexes as seen in4 for the methylene protons of $[Au_2(\mu\text{-dppm})_2(\mu\text{-I})]I\bullet 2CH_2Cl_2$ (**2**). This we were unable to freeze out the dynamic process in the range of temperatures were these salts had sufficient solubility for measurements.

Excitation and Emission Data.

Each of the four crystalline complexes reported here is luminescent in the solid state and solution state. Figure 6 shows the solid-state excitation and emission spectra for the three iodide containing crystals. Table 3 contains excitation and emission maxima for all four compounds. Since the loss of solvate molecules can affect the excitation and emission from crystalline samples,[5,9] we were particularly careful to be sure we obtained spectra on homogeneous samples that were protected to avoid solvate evaporation. For these compounds, the emission varies over a rather short range, which is perhaps not surprising given the structural similarities within this group of complex ions. Crystalline $[Au_2(\mu\text{-dppm})_2(\mu\text{-I})]I\bullet 2CH_2Cl_2$ (**2**) has its emission at 503 nm at room temperature; $[Au_2(\mu\text{-dppm})_2(\mu\text{-I})](PF_6)\bullet CH_2Cl_2$ (**3**) shows emission at 510 nm; and $[Au_2(\mu\text{-dppm})_2I][Au_2(\mu\text{-dppm})_2(\mu\text{-I})](AsF_6)_4\bullet 4CH_2Cl_2$ (**1**) emission is at 500 nm under the same conditions. Cooling the crystals results in a narrowing of the emission bands as expected for the reduction in vibrational motion. While $[Au_2(\mu\text{-dppm})_2(\mu\text{-I})]I\bullet 2CH_2Cl_2$ (**2**) and $[Au_2(\mu\text{-dppm})_2(\mu\text{-I})](PF_6)\bullet CH_2Cl_2$ (**3**) nominally contain a common cation, the structures of these cations differ slightly as seen by the Au···Au distances in Table 1; thus the emission spectra differ slightly.

Table 3. Excitation and Emission Data for Crystalline Solids

Complexes	Room Temperature (298 K)		Low Temperature (77 K)	
	Excitation (nm)	Emission (nm)	Excitation (nm)	Emission (nm)
$[Au_2(\mu\text{-dppm})_2I][Au_2(\mu\text{-dppm})_2(\mu\text{-I})](AsF_6)_4 \bullet 4CH_2Cl_2$ (**1**)	396	500	396	540
$[Au_2(\mu\text{-dppm})_2(\mu\text{-I})]I \bullet 2CH_2Cl_2$ (**2**)	414	503	395	502
$[Au_2(\mu\text{-dppm})_2(\mu\text{-I})](PF_6) \bullet CH_2Cl_2$ (**3**)	416	510	419	521
$[Au_2(\mu\text{-dppm})_2](AsF_6)_2 \bullet CH_2Cl_2$ (**4**)	376	515	370	508

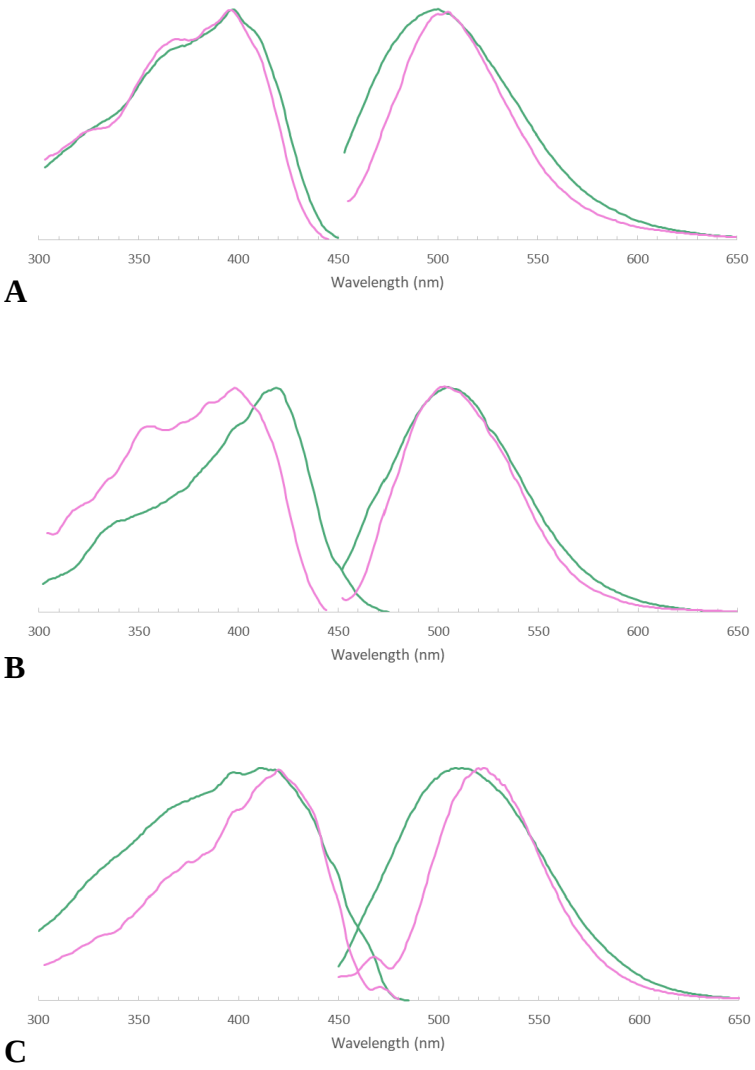

Figure 6. The luminescence of crystalline complexes **A** $[Au_2(\mu\text{-dppm})_2I][Au_2(\mu\text{-dppm})_2(\mu\text{-I})]$ $(AsF_6)_4 \bullet 4CH_2Cl_2$ (**1**), **B** $[Au_2(\mu\text{-dppm})_2(\mu\text{-I})]I \bullet 2CH_2Cl_2$ (**2**), and $[Au_2(\mu\text{-dppm})_2(\mu\text{-I})](PF_6) \bullet CH_2Cl_2$ (**3**) at room temperature green and 77 K in pink.

These compounds are also luminescent in solution. Figure 7 compares the excitation and emission spectra of solutions of $[Au_2(\mu\text{-dppm})_2(\mu\text{-I})]I \bullet 2CH_2Cl_2$ (**2**) and $[Au_2(\mu\text{-dppm})_2](AsF_6)_2 \bullet CH_2Cl_2$ (**4**) in acetonitrile. Clearly, the two spectra are different as expected from

the NMR studies that showed these two complexes contained different cations in solution. Previous studies reported that acetonitrile solutions of $[Au_2(\mu\text{-dppm})_2](BF_4)_2$ were luminescent with emission occurring at 593 nm in agreement with our results.[39] However, acetonitrile solutions of $[Au_2(\mu\text{-dppm})_2](ClO_4)_2$ are reported to produce luminescence at 565 nm.[40] We have no explanation for the discrepancy. For $[Au_2(\mu\text{-dppm})_2]$, the excitation involves promotion of an electron from the antibonding orbital arising from the combination of the two gold d_{z^2} orbitals (where the z axis lies along the gold-gold bond) to the bonding orbital.[41]

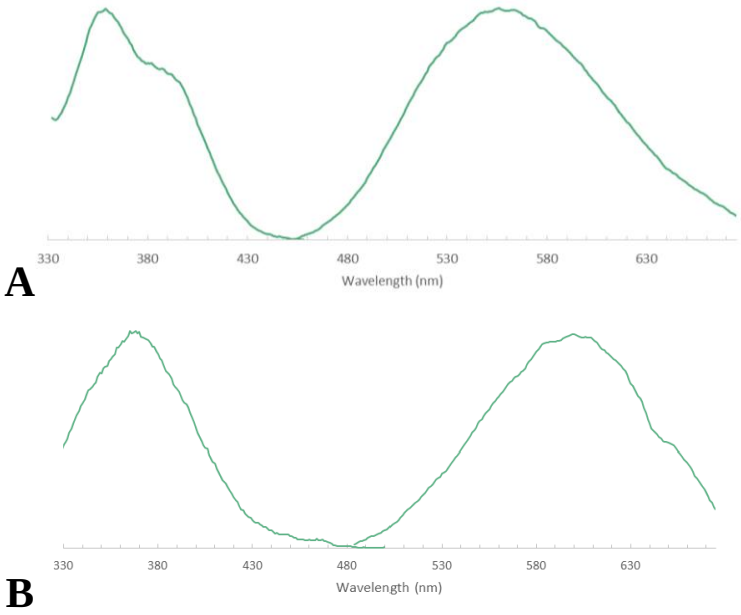

Figure 7. The excitation and emission spectra of acetonitrile solutions of: **A**, $[Au_2(\mu\text{-dppm})_2(\mu\text{-I})]I\bullet 2CH_2Cl_2$ (**2**) and **B**, $[Au_2(\mu\text{-dppm})_2](AsF_6)_2\bullet CH_2Cl_2$ (**4**) at room temperature.

Conclusions

In the luminescent complex $[Au_2(\mu\text{-dppm})_2I][Au_2(\mu\text{-dppm})_2(\mu\text{-I})](AsF_6)_4\bullet 4CH_2Cl_2$ (**1**) the iodide can be seen in two different positions. In one cation the iodide is nearly centered between the two gold(I) ions to give an A-frame structure, while the other cation contains a two-coordinate gold(I) interacting with a three-coordinate gold(I) center that is bonded to a terminal iodide ligand. This cation exhibits the shortest Au-I bond reported in this paper at 3.0051(9) Å, but it is significantly longer than the Au-I distance (2.753(9) Å) in $Au(PPh_3)_2I$.[17] The cations in the luminescent salts, $[Au_2(\mu\text{-dppm})_2(\mu\text{-I})]I\bullet 2CH_2Cl_2$ (**2**) or $[Au_2(\mu\text{-dppm})_2(\mu\text{-I})](PF_6)\bullet CH_2Cl_2$ (**3**), have an A-frame structure with a bridging iodide ligand. We have been unable to form a neutral complex with composition $Au_2(\mu\text{-dppm})_2I_2$ although the analogous complexes, $Au_2(\mu\text{-dppm})_2Br_2$ and $Au_2(\mu\text{-dppm})_2Cl_2$, have been prepared and characterized as containing the face-to-face structure shown as **A** in Scheme 1.

$^{31}P\{^1H\}$ and ^1H NMR studies reveal that each complex, $[Au_2(\mu\text{-dppm})_2I][Au_2(\mu\text{-dppm})_2(\mu\text{-I})](AsF_6)_4\bullet 4CH_2Cl_2$ (**1**), $[Au_2(\mu\text{-dppm})_2(\mu\text{-I})]I\bullet 2CH_2Cl_2$ (**2**) or $[Au_2(\mu\text{-dppm})_2(\mu\text{-I})](PF_6)\bullet CH_2Cl_2$ (**3**), forms a single species in solution. In that species the iodide ion remains attached to the $[Au_2(\mu\text{-dppm})_2I]$ core but is free to orbit around that core as shown in Scheme 2. Additionally, that species is distinct from the dication, $[Au_2(\mu\text{-dppm})_2]^{2+}$, which produces different $^{31}P\{^1H\}$ and ^1H NMR spectra. It is interesting to note that the orbiting movement of the iodide ligand in solutions of (**1**), (**2**), and (**3**) does not quench their luminescence in solution.

Experimental Section

Preparation of $[Au_2(\mu\text{-dppm})_2I][Au_2(\mu\text{-dppm})_2(\mu\text{-I})](AsF_6)_4 \bullet 4CH_2Cl_2$ (1)

A 68.7 mg (0.179 mmol) portion of dppm was dissolved in 5 ml of dichloromethane, and an equivalent amount of AuI (57.1 mg, 0.176 mmol) suspended in 4mL of dichloromethane was added to the dppm solution under agitation. The yellow solution was stirred for 10 minutes followed by the addition of $NaAsF_6$ (37.5 mg, 0.177 mmol) dissolved in 4 mL of dichloromethane and 1 mL of methanol. The light yellow solution was stirred for 3 hours and the crude mixture was air dried. The resulting yellow solid was dissolved in a minimum amount of dichloromethane. The yellow solution was filtered using a filter pipet, and the filtrate was evaporated to dryness. A purified yield of 112.7 mg (21.7%) was obtained. The dried product was dissolved in dichloromethane. This solution was filtered into the bottom of an outer diameter of 5 mm glass tube, a few drops of dichloromethane was layered over that solution and then diethyl ether was layered over the mixture. As the solutions diffused together, yellow block crystals with green luminescence were isolated.

Infrared spectrum: 3033(w), 3019(w), 2955(w) 2925(w), 2879(w), 2877(w), 2854(w), 1484(m), 1435(s), 1360(w), 1310(w), 1308(w), 1149(w), 1147(w), 1100(s), 1067(w), 1002(w), 1000(m), 969(w), 916(w), 796(w), 746(s), 704(s), 708(s), 686(vs), 615(w) cm^{-1}

UV-Vis: 355 nm, 2.098 abs, 27987.48 L/mol/cm; 385nm, 1.088 abs, 14514.0 L/mol/cm

$^{31}P\{^1H\}$ Nuclear Magnetic Resonance: 27.77 ppm in acetonitrile-d_3 at 295 K.

^1H Nuclear Magnetic Resonance: complex multiplets for the aromatic resonances at 7. 82, 7.81, 7.80, 7.79, 7.78, 7.77, 7.76, 7.70, 7.68, 7.67, 7.66, 7.64, 7.51, 7.50, 7.48, 7.47, 7.46,

7.43, 7.41, 7.38, and 7.36 ppm (40 protons); methylene resonance, broad quintet, 4.68 ppm (4 protons) in acetonitrile-d_3 at 295 K.

Preparation of $[Au_2(\mu\text{-dppm})_2(\mu\text{-I})]I \bullet 2CH_2Cl_2$ (2)

A 64.7 mg (0.168 mmol) portion of dppm was dissolved in 5 ml of dichloromethane, and an equivalent amount of AuI (54.3 mg, 0.168 mmol) suspended in 4mL of dichloromethane was added to the dppm solution under agitation. The solution was stirred for 10 minutes followed by the addition of KI (14.8 mg, 0.0892 mmol) dissolved in 4 mL of dichloromethane and 1 mL of methanol. The light yellow solution was stirred for 3 hours and the crude mixture was evaporated to dryness. The resulting yellow solid was dissolved in a minimum amount of dichloromethane. The yellow solution was filtered using a filter pipet, and the filtrate was evaporated to dryness. A purified yield of 128.9 mg (54.3%) was obtained. This product was redissolved in dichloromethane, filtered and placed in the bottom of an outer diameter of 5 mm glass tube and a few drops of dichloromethane were layered over this solution and diethyl ether was layered above. As the solutions diffused together, yellow blocks with green luminescence were isolated.

Infrared spectrum: 3049(w), 2903(w), 2635(m), 1587(w), 1570(w), 1646(s), 1606 (m), 1483(m), 1433(s), 1357(w), 1261(m), 1244(m), 1219(w), 1152(m), 1096(s), 1026(m), 999(m), 919(w), 849(w), 780(m), 738(s), 720(s), 687 (vs), 569(w), 512(vs), 468(s) cm^{-1}

UV-Vis: 355nm, 2.319 abs, 9124.75 L/mol/cm; 385nm, 1.301abs, 5119.146 L/mol/cm

$^{31}P\{^1H\}$ Nuclear Magnetic Resonance: 27.9 ppm in acetonitrile-d_3 at 290 K.

^1H Nuclear Magnetic Resonance: complex multiplets for the aromatic resonances at 7.82, 7.81, 7.80, 7.79, 7.78, 7.77, 7.76, 7.75, 7.53, 7.51, 7.48, 7.43, 7.41, and 7.38 ppm (40 protons); methylene resonance, quintet, 4.66 ppm (4 protons) in acetonitrile-d_3 at 290 K.

Preparation of $[Au_2(\mu\text{-dppm})_2(\mu\text{-I})](PF_6)\bullet CH_2Cl_2$ (3)

A 62.5 mg (0.166 mmol) portion of dppm was dissolved in 5 ml of dichloromethane, and an equivalent amount of AuI (52.4 mg, 0.162 mmol) suspended in 4mL of dichloromethane was added to the dppm solution under agitation. The yellow solution was stirred for 10 minutes followed by the addition of NH_4PF_6 (26.6 mg, 0.1632 mmol) dissolved in 4 mL of dichloromethane and 1 mL of methanol. The light yellow solution was stirred for 3 hours and the crude mixture was evaporated to dryness. The resulting yellow solid was dissolved in a minimum amount of dichloromethane. The yellow solution was filtered using a filter pipet, and the filtrate was evaporated to dryness. A purified yield of 104.3 mg (44.9%) was obtained. The dried product was dissolved in dichloromethane. This solution was filtered into the bottom of an outer diameter of 5 mm glass tube, a few drops of dichloromethane was layered over that solution and then diethyl ether was layered over the mixture. As the solutions diffused together, crystalline yellow blocks with green luminescence were isolated.

Infrared spectrum: 3271(w), 3034(w), 2958(w), 2824(m), 2852(m), 1692(m), 1648 (m), 1636 (m), 1545 (m), 1437(s), 1396(w), 1304(w), 1172(w), 1160(w), 1100(s), 999(w), 839(vs), 774(m), 738(m),689(vs), 849(w), 780(m), 738(s), 720(s), 687 (vs) cm^{-1}

UV-Vis: 354 nm, 0.791 abs, 1973.48 L/mol/cm; 385nm, 0.468 abs, 1167.62 L/mol/cm

$^{31}P\{^1H\}$ Nuclear Magnetic Resonance: the phosphorus atoms of the dppm; singlet at 27.95 ppm and the phosphiorus atom of the PF_6 anion a multiplet at -144.65 ppm in acetonitrile-d_3 at 290 K.

^1H Nuclear Magnetic Resonance: complex multiplets for the aromatic resonances at 7.77, 7.76, 7.75, 7.74, 7.73, 7.72, 7.48, 7.47, 7.45, 7.38, 7.37, and 7.35 ppm (40 protons); methylene resonance, broad quintett, 4.63 ppm (4 protons) in acetonitrile-d_3 at 290 K.

Preparation of $[Au_2(\mu\text{-dppm})_2](AsF_6)_2 \bullet CH_2Cl_2$ (4)

A 78.9 mg (0.205 mmol) portion of dppm was dissolved in 5 ml of dichloromethane, and an equivalent amount of thtAuCl (65.8mg, 0.205 mmol) dissolved in 4mL of dichloromethane was added to the dppm solution under agitation. The solution was stirred for 5 minutes followed by the addition of $AgAsF_6$ (58.9 mg, 0.198 mmol) dissolved in 4 mL of dichloromethane and 1 mL of methanol. The colorless solution was stirred for 3 hours and the crude mixture was air dried. The resulting colorless solid was dissolved in a minimum amount of dichloromethane. The solution was filtered using a filter pipet, and the filtrate was evaporated to dryness. A purified yield of 11.0 mg (3.6%) was obtained. The dried product was dissolved in dichloromethane. This solution was filtered into the bottom of an outer diameter of 5 mm glass tube, a few drops of dichloromethane was layered over that solution and then diethyl ether was layered over the mixture. As the solutions diffused together, colorless block crystals and green luminescence were isolated.

Infrared spectrum: 3034(w), 2924(w), 2852(w), 2360(m), 2358(m), 2340(m), 2156(w), 2159(w), 2029(w), 2028(w), 1966(w), 1559(w), 1540(w), 1489(w), 1484(w), 1444(w), 1437(s), 1101(m), 1072(w), 1004(w), 1000(m), 780(m), 739(s), 701(vs), 694(s), 668(m), 616(s), 605(m) cm^{-1}

UV-Vis: 298 nm, 0.355 abs, 359.88 L/mol/cm; 338 nm, 0.281 abs, 284.86 L/mol/cm

$^{31}P\{^1H\}$ Nuclear Magnetic Resonance: 35.58 ppm in acetonitrile-d_3 at 295 K.

^1H Nuclear Magnetic Resonance: complex multiplets for the aromatic resonances at 7.74, 7.73, 7.72, 7.71, 7.55, 7.53, 7.52, 7.45, 7.43, and 7.41 ppm (40 protons); methylene resonance, quintet, 4.43 ppm (4 protons) in acetonitrile-d_3 at 295 K.

X-ray Crystallography and Data Collection. The crystals were removed from the glass tubes in which they were grown together with a small amount of mother liquor and immediately coated with a hydrocarbon oil on a microscope slide. Suitable crystals of $[Au_2(\mu\text{-}dppm)_2I][Au_2(\mu\text{-}dppm)_2(\mu\text{-}I)](AsF_6)_4\bullet 4CH_2Cl_2$ (**1**) and $[Au_2(\mu\text{-}dppm)_2](AsF_6)_2\bullet CH_2Cl_2$ (**4**) were mounted on a microloop with hydrocarbon oil and placed in the liquid nitrogen cold stream of a Bruker APEX-II CCD with graphite monochromated Mo Kα radiation at 90(2) K. Suitable crystals of $[[Au_2(\mu\text{-}dppm)_2(\mu\text{-}I)]I\bullet 2CH_2Cl_2$ (**2**) and $[Au_2(\mu\text{-}dppm)_2(\mu\text{-}I)](PF_6)\bullet CH_2Cl_2$ (**3**) were mounted on a dual-thickness microloop with hydrocarbon oil and placed in the liquid nitrogen cold stream of a Bruker Kappa DUO with graphite monochromated Mo Kα radiation at 90(2) K. Crystal data are given in Table S1.

Data collected were corrected for Lorentz and polarization effects with Saint and for absorption using Blessing's method[42] and merged as incorporated with the program Sadabs. The SHELXTL program package was implemented to determine the probable space group and set up the initial files based upon system symmetry, systematic absences and intensity statistics. The structures were determined by SHELXT and structural refinements were performed with SHELXL.[43,44]

Table 1. Crystal Data for Gold(I) Complexes

	$[Au_2(\mu\text{-dppm})_2I][Au_2(\mu\text{-dppm})_2(\mu\text{-I})](AsF_6)_4\bullet 4CH_2Cl_2$ (**1**)	$[Au_2(\mu\text{-dppm})_2(\mu\text{-I})]I\bullet 2CH_2Cl_2$ (**2**)	$[Au_2(\mu\text{-dppm})_2(\mu\text{-I})](PF_6)\bullet CH_2Cl_2$ (**3**)	$[Au_2(\mu\text{-dppm})_2](AsF_6)_2\bullet CH_2Cl_2$ (**4**)
color/habit	Yellow Block	Yellow Irregular Plate	Yellow Block	Colorless Block
chemical formula	$C_{51}H_{46}AsAu_2Cl_2F_6IP_4$	$C_{52}H_{46}Au_2Cl_3I_2P_4$	$C_{50}H_{44}Au_2F_6I\ P_5$ [+ solvent]	$C_{52}H_{48}As_2Au_2Cl_4F_{12}P_4$
formula weight	1563.42	1548.85	1434.54	1710.36
crystal system	triclinic	orthorhombic	monoclinic	orthorhombic
space group	$P\bar{1}$	$P2_12_12_1$	C2/c	Pnma
a (Å)	15.8401(5)	13.6768(6)	42.063(3)	20.6227(17)
b (Å)	18.4089(6)	14.8760(8)	11.7847(8)	20.6478(18)
c (Å)	19.5383(6)	26.1893(14)	22.0854(15)	13.1233(11)
α (deg)	91.437(2)	90	90	90
β (deg)	112.451(2)	90	103.495(4)	90
γ (deg)	91.727(2)	90	90	90
V (Å^3)	5259.0(3)	5328.4(5)	10645.5(13)	5588.1(8)
Z	4	4	8	4
T (K)	90(2)	90(2)	90(2)	90(2)
λ (Å)	0.71073	0.71073	0.71073	0.71073
ρ (g/cm^3)	1.975	1.931	1.790	2.033
μ (mm^{-1})	7.064	6.963	6.289	6.803
R_1 (obsd data)[a]	0.0538	0.0373	0.0226	0.0286
wR_2 (all data, F^2 refinement)[b]	0.1509	0.0909	0.0593	0.0617

[a] $R_1 = (\Sigma||F_o| - |F_c||)/\Sigma|F_o|$
[b] $wR_2 = ((\Sigma[w(F_o^2 - F_c^2)^2])/\Sigma[w(F_o^2)^2])^{1/2}$

Physical Measurements. Infrared spectra were recorded on a Bruker ALPHA FT-IR spectrometer. Excitation and emission spectra were recorded on a Perkin-Elmer LS50B luminescence spectrophotometer.

Associated Content

Supporting Information Available: CCDC 2419015-2419018 contain the supplementary crystallographic data for this paper. These data can be obtained free of charge via www.ccdc.cam.ac.uk/data_request/cif, by emailing data_request@ccdc.cam.ac.uk, or by contacting The Cambridge Crystallographic Data Centre, 12 Union Road, Cambridge CB2 1EZ, U.K.; fax: +44 1223 336033.

Corresponding Author

Alan. L. Balch − *Department of Chemistry, University of California-Davis, Davis, California 95616, United States;* orcid.org/0000-0002-8813-6281; Email: albalch@ ucdavis.edu

Authors

Sarah Costa − *Department of Chemistry, University of California-Davis, Davis, California 95616, United States:* orcid.org/0000-0002-1498-0762

Sarah M. Chui, *Department of Chemistry, University of California-Davis, Davis, California 95616, United States*

Katelyn A. Espinoza *Department of Chemistry, University of California-Davis, Davis, California 95616, United States*

James C. Fettinger − *Department of Chemistry, University of California-Davis, Davis, California 95616, United States*

Notes

The authors declare no competing financial interest.

Acknowledgments. We thank the U. S. National Science Foundation [Grant CHE-1807637] for support.

References

(1) Hristova, Y. R.; Kemper, B.; Besenius, P. Water-Soluble Au(I) Complexes, Their Synthesis and Applications. *Tetrahedron* **2013**, *69*, 10525–10533.

(2) He, X.; Yam, V. W. W. Luminescent Gold(I) Complexes for Chemosensing. *Coord. Chem. Rev.* **2011**, *255*, 2111–2123.

(3) Yam, V.W.-W.; Au, V. K.-M.; Leung, S. Y.-L. Light-Emitting Self-Assembled Materials Based on d^8 and d^{10} Transition Metal Complexes. *Chem. Rev*. **2015**, *115*, 7589−7728.

(4) Schmidbaur, H.; Raubenheimer, H. G. Excimer and Exciplex Formation in Gold(I) Complexes Preconditioned by Aurophilic Interactions *Angew. Chem. Int. Ed*. **2020**, *59*, 14748–14771.

(5) Pyykkö, P. Theoretical Chemistry of Gold. *Angew. Chem. Int. Ed. Engl.* **2004**, *43*, 4412–4456.

(6) Pyykkö. P. Strong Closed-Shell Interactions in Inorganic Chemistry. *Chem. Rev*. **1997**, *97*, 597-636.

(7) Mirzadeh, N.; Privér, S. H.; Blake, A. J.; Schmidbaur, H.; Bhargava, S. K. Innovative Molecular Design Strategies in Materials Science Following the Aurophilicity Concept. *Chem. Rev*. **2020**, *120*, 7551−7591.

(8) Toronto, D. V.; Weissbart, B.; Tinti, D. S.; Balch, A. L. Solid State Structures and Gold–Gold Bonding in Luminescent Halo(dimethylphenylphosphine)gold(I) Complexes. *Inorg*. *Chem*. **1996**, *35*, 2484-2489.

(9) White-Morris, R. L.; Olmstead, M. M.; Attar, S.; Balch, A. L. Intermolecular Interactions in Polymorphs of Trinuclear Gold(I) Complexes: Insight into the Solvoluminescence of $Au^{I}_3(MeN{=}COMe)_3$**.** *Inorg. Chem*. **2005**, *44*, 5021-5029.

(10) White-Morris, R. L.; Olmstead, M. M.; Balch, A. L. Aurophilic Interactions in Cationic Gold Complexes with Two Isocyanide Ligands. Polymorphic Yellow and Colorless Forms of [(Cyclohexyl Isocyanide)$_2$Au^{I}](PF$_6$) with Distinct Luminescence. *J. Am. Chem. Soc*. **2003**, *125*, 1033-1040.

(11) Luong, L. M. C.; Olmstead, M. M.; Balch, A. L. A Non-Luminescent Polymorph of [(Cyclohexyl Isocyanide)$_2$Au]PF_6 that Becomes Luminescent Upon Grinding or Exposure to Dichloromethane Vapor. *Chem. Commun*. **2021**, *57*, 793-796.

(12) Seki, T.; Sakurada, K.; Muromoto, M.; Seki, S.; Ito, H. Detailed Investigation of the Structural, Thermal, and Electronic Properties of Gold Isocyanide Complexes with Mechano-Triggered Single-Crystal-to-Single-Crystal Phase Transitions. *Chem. Eur. J*. **2016**, *22*, 1968 – 1978.

(13) Seki, T.; Tokodai, N.; Omagari, S.; Nakanishi,T.; Hasegawa,Y.; Iwasa, T.; Taketsugu, T.; Ito, H. Luminescent Mechonochromic 9-Anthryl Gold(I) Isocyanide Complex with an Emission Maximum at 900 nm after Mechanical Stimulation. *J. Am. Chem. Soc*. **2017**, *139*, 6514−6517.

(14) Lasanta, T.; Olmos, M. E.; Laguna, A.; López-de-Luzuriaga, J. M.; Naumov, P. Making the Golden Connection: Reversible Mechanochemical and Vapochemical Switching of Luminescence from Bimetallic Gold_Silver Clusters Associated through Aurophilic Interactions. *J. Am. Chem. Soc.* **2011**, *133*, 16358–16361.

(15) Ito, H.; Muromoto, M.; Kurenuma, S.; Ishizaka, S.; Kitamura, N.; Sato, H.; Seki, T. Mechanical stimulation and solid seeding trigger single-crystal-to-single-crystal molecular domino transformations. *Nat. Commun*. **2013**, *4*, 2009.

(16) Streitberger, M.; Schmied, A.; Hey-Hawkins, E. Selective Formation of Gold(I) Bis-Phospholane Macrocycles, Polymeric Chains, and Nanotubes. *Inorg. Chem*. **2014**, *53*, 6794−6804.

(17) Lim, S. H.; Schmitt, J. C.; Shearer, J.; Jia, J.; Olmstead, M. M.; Fettinger, J. C.; Balch, A. L. Crystallographic and Computational Studies of Luminescent, Binuclear Gold(I) Complexes, $Au^{I}_2(Ph_2P(CH_2)_nPPh_2)_2I_2$ (n = 3−6). *Inorg. Chem*. **2013**, *52*, 823−831.

(18) Boar, P.; Streitberger, M.; Lönnecke, P.; Hey-Hawkins, E. Copper(I) Complexes of a Flexible Bis-phospholane Ligand: Route to Paddle-Wheel- and Box-Type Macrocycles. *Inorg. Chem*. **2017**, *56*, 7285−7291.

(19) Balch, A. L.; Tulyathan, B. Interactions between Rhodium(I) Centers in Dimeric Complexes. *Inorg. Chem*. **1977**, *16*, 2840−2845.

(20) Costa, S.; Walters, D. T.; McNamara, L. E.; Olmstead, M. M.; Fettinger, J. C.; Balch, A. L. Structure and Luminescence Studies of Salts of the Helical Dication, $[Au_2(\mu$-bis(diphenylphosphine)ethane$)_2]^{2+}$ and Comparison with Salts of $[Au_2(\mu$-bis(diphenylphosphine)propane$)_2]^{2+}$. *Inorg. Chem.* **2023**, *62*, 15902−15911.

(21) Lim, S. H.; Olmstead, M. M.; Balch, A. L. Molecular Accordion: Vapoluminescence and Molecular Flexibility in the Orange and Green Luminescent Crystals of the Dimer, Au_2(μ-bis-(diphenylphosphino)ethane$)_2Br_2$. *J. Am. Chem. Soc*. **2011**, *133*, 10229-10238.

(22) Lim, S. H.; Olmstead, M. M.; Balch, A. L. Inorganic topochemistry. Vapor-induced solid state transformations of luminescent, three-coordinate gold(I) complexes. *Chem. Sci*. **2013**, *4*, 311–318.

(23) Costa, S.; Aristov, M. M.; Lim, S. H.; Chui, S. M.; Espinoza, K. A.; Olmstead, M. M.; Fettinger, J. C.; Berry, J. F.; Balch, A. L. Molecular Flexibility in Solvated Crystals of the Dimer, $Au_2(\mu$-1,2- bis(diphenylphosphino)ethane$)_2I_2$, with Three-Coordinate Gold(I). *Inorg. Chem.* **2024**, *63*, 12752−12763.

(24) Walters, D. T.; Aristov, M. M.; Babadi Aghakhanpour, R.; SantaLucia, D. J.; Costa, S.; McNamara, L. E.; Olmstead, M. M.; Berry, J. F.; Balch, A. L. Self-Assembled Encapsulation of CuX_2- (X = Br, Cl) in a Gold Phosphine Box-like Cavity with Metallophilic Au-Cu Interactions. *Inorg. Chem.* **2023**, *62*, 4467–4475.

(25) Walters, D. T.; Costa, S.; Babadi Aghakhanpour, R.; Olmstead, M. M.; Balch, A. L. Aurophilic Interactions in Luminescent, Box-Like or Partial Helical Cations Formed from Bis(2-diphenylphosphinoethyl)phenylphosphine (Triphos) and Gold(I) Ions. *Polyhedron* **2024**, *261*, 117140. https://doi.org/10.1016/j.poly.2024.117140.

(26) Costa, S.; Chui, S. M.; Espinoza, K. A.; Fettinger, J. C.; Balch, A. L. Bridging 1,2-Bis(diphenylphosphino)methane Ligands Facilitate the Formation of Binuclear Complexes with Both Two-Coordinate and Three-Coordinate Gold(I) Ions. *Inorg. Chem.* **2024**, *63*, 24563−24572

(27) Lin, I. J. B.; Hwang, J. M.; Feng, D.-F.; Cheng, M. C.; Yu Wang, Y. New Aspect on Di-μ-[bis(diphenylphosphino)methane]dichlorotrigold(I) Chloride, Including It Crystal and Molecular Structure. *Inorg. Chem*. **1994**, *33*, 3467-3472.

(28) Shain, J.; Fackler, Jr., J. P. The First Example of a Gold Bis(diphenylphosphino)-methane Cationic Dimer with a Bridging Iodide. The X-ray Crystal Structures of (μ-I)[Au(dppm)]$_2$ [I] and [Au(dppm)Br]$_2$. *Inorg. Chim. Acta* **1987**, *131*, 157-158.

(29) Khan, M. N. I.; King, C.; Heinrich, D. D.; Fackler, J. P.; Porter, L. C. Syntheses and Crystal Structures (No Au-H Interactions) of Luminescent [Au$_2$(Dppm)$_2$][BH$_3$CN]$_2$ and of [Au$_2$(Dppm)$_2$(I)][Au(CN)$_2$] and [Au$_2$(Dppm)$_2$(S$_2$CNEt$_2$)][BH$_3$CN]. *Inorg. Chem.* **1989**, *28*, 2150–2154.

(30) Bruce, M. I.; Jevric, M.; Skelton, B. W.; Smith, M. E.; White, A. H.; Zaitseva, N. N. Syntheses and Molecular Structures of Some Phosphine–Gold(I) Derivatives of 1,3-Diynes. *J. Organomet. Chem.* **2006**, *691*, 361–370.

(31) Schmidbaur, H.; Wohlleben, A.; Schubert, U.; Frank, A.; Huttner, G. Gold-Komplexe von Diphosphinomethanen, II. Synthese und Kristallstruktur achtgliedriger Ringverbindungen von Gold(I) mit Au–Au-Wechselwirkung. *Chem. Ber*. **1977**, *110*, 2751-2757.

(32) de Jongh, L.-A.; Strasser, C. E.; Cronje, S.; Raubenheimer, H. G. Bis[μ-bis(diphenylphosphino)methane-κ^{2}P:P']digold(I)(*Au*—*Au*) dinitrate perdeuteromethanol solvate. *Acta Crystallogr., Sect. E: Struct. Rep. Online* **2007**, *E63*, m2137–m2138.

(33) Cao, Q.-Y.; Yin, B.; Liu, J.-H. Bis[μ-bis(diphenylphosphino)methane-κ^{2}P:P']digold(I)(bis(perchlorate). *Acta Crystallogr., Sect. E: Struct. Rep. Online* **2006**, *E62*, m2730–m2731.

(34) Porter, L. C.; Khan, Md. N. I.; King, C.; Fackler, Jr., J. P. Structure of the Bis[bis(diphenylphosphino)methane]digold(I) Cation in [Au$_2$(dppm)$_2$](BF$_4$)$_2$. *Acta Crystallogr., Sect. C: Struct. Chem*. **1989**, *C45*, 947-949.

(35) Wu, M.; Zhang, L.; Chen, Z. Bis[l-bis(diphenylphosphino)methane]-digold(I) bis(hexafluorophosphate) dichloromethane disolvate. *Acta Crystallogr., Sect. E: Struct. Rep. Online* **2003**, *E59*, m72-m73.

(36) Hunt, C. T.; Balch, A. L. Halogen Additions to Bis(diphenylphosphino) methane Complexes of Palladium. Interrelationships of Monomeric and Dimeric Complexes of Pd(II), Pd(I), and Pd(0). *Inorg. Chem*. **1981**, *20*, 2267-2270.

(37) Lee, C.-L.; Hunt, C. T.; Balch, A. L. Addition of Carbon Monoxide and Methyl Isocyanide to Methylpalladlum A-Frame Complexes and Some Reactions of the Product Acyl Complexes. *Organometallics* **1982**, *1*, 824-829.

(38) Fu, W.-F.; Chan, K.-C.; Cheung, K.-K.; Che, C.-M. Substrate-Binding Reactions of the $^3[d\sigma^*p\sigma]$ Excited State of Binuclear Gold(I) Complexes with Bridging Bis(dicyclohexylphosphino)methane Ligands: Emission and Time-Resolved Absorption Spectroscopic Studies. *Chem. Eur. J.* **2001**, *7*, 4656-4664.

(39) King, C.; Wang, J.-C.; Khan, M. N. I.; Fackler, Jr., J. P. Luminescence and Metal-Metal Interactions in Binuclear Gold(I) Compounds. *Inorg. Chem*. **1989**, *28*, 2145-2149.

(40) Che, C.-M.; Kwong, H.-L.; Yam, V. W.-W.: Cho, K.-C. Spectroscopic Properties and Redox Chemistry of the Phosphorescent Excited State of $[Au_2(dppm)_2]^{2+}$ [dppm = bis(diphenylphosphino)methane]. *J . Chem. Soc., Chem. Commun*., **1989**, 585-586.

(41) Fu, W.-F.; Chan, K.-C.; Cheung, K.-K.; Che, C.-M. Substrate-Binding Reactions of the $^3[d\sigma^*p\sigma]$ Excited State of Binuclear Gold(I) Complexes with Bridging Bis(dicyclohexylphosphino)methane Ligands: Emission and Time-Resolved Absorption Spectroscopic Studies. *Chem. Eur. J.* **2001**, *7*, 4656-4664.

(42) Blessing, R. H. An Empirical Correction for Absorption Anisotropy. *Acta Crystallogr. Sec. A.* **1995**, *A51*, 33-38.

(43) Sheldrick, G. M. SHELXT - Integrated space-group and crystal-structure determination. *Acta Crystallogr. Sec. A.* **2015**, *A71*, 3-8.

(44) Sheldrick, G. M. Crystal structure refinement with *SHELXL*. *Acta Crystallogr. Sec. C* **2015**, *71*, 3-8.

TOC Text: The NMR spectra of solutions of the iodide complexes, $[Au_2(\mu\text{-dppm})_2I][Au_2(\mu\text{-dppm})_2(\mu\text{-I})](AsF_6)_4\bullet 4CH_2Cl_2$, $[Au_2(\mu\text{-dppm})_2(\mu\text{-I})]I\bullet 2CH_2Cl_2$ and $[Au_2(\mu\text{-dppm})_2(\mu\text{-I})](PF_6)\bullet CH_2Cl_2$, suggest that the iodide ion is bound to the $[Au_2(\mu\text{-dppm})_2]^{2+}$ core but is able to circulate around that core.

TOC Figure:

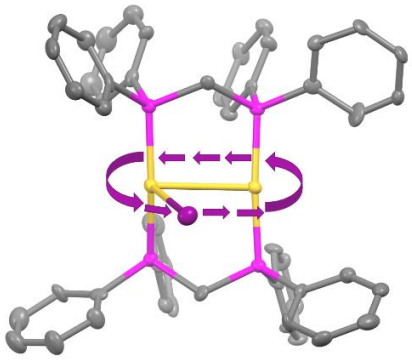

Appendix: List of Publications

Graduate Career:

1. **Costa, S.**; Walters, D.; McNamara, L.; Olmstead, M.; Fettinger, J.; Balch, A. Structure and Luminescence Studies of Salts of the Helical Dication, $[Au_2(\mu\text{-Bis(Diphenylphosphine)Ethane})_2]^{2+}$ and Comparison with Salts of $[Au_2(\mu\text{-Bis(Diphenylphosphine)Propane})_2]^{2+}$. **2023**, *Inorg. Chem. 62* (39), 15902–15911.
2. **Costa, S.**; Aristov, M. M.; Lim, S. H.; Chui, S. M.; Espinoza, K. A.; Olmstead, M. M.; Fettinger, J. C.; Berry, J. F.; Balch, A. L. Molecular Flexibility in Solvated Crystals of the Dimer, $Au_2(\mu\text{-1,2-Bis(Diphenylphosphino)Ethane})_2I_2$, with Three-Coordinate Gold(I). *Inorg. Chem.* **2024**, *21*, 4.
3. **Costa, S**.; Chui, S. M.; Espinoza, K. A.; Olmstead, M. M.; Fettinger, J. C.; Balch, A. L. Bridging 1,2-Bis-(diphenylphosphino)methane Ligands Facilitate the Formation of Binuclear Complexes with Both Two-Coordinate and Three-Coordinate Gold(I) Ions. *Inorg. Chem.* **2024**, *63* (52), 24563–24572.
4. **Costa, S.**; Chui, S. M.; Espinoza, K. A.; Olmstead, M. M.; Fettinger, J. C.; Balch, A. L. A Molecular Planetarium: Evidence for an Iodide Ligand Orbiting two Gold (I) Ions in $[Au_2(\mu\text{-1,2 Bis-(diphenylphosphino)methane})_2I]^+$. *In Submission.* **2025,**
5. Gralinski, S. R.; **Costa, S.;** Fettinger, J. C.; Balch, A. L. Mechanochromic Behavior or a Rhodium A-Frame Complex: Release of Gaseous Sulfur Dioxide from a Crystalline Solid. *Manuscript in Process*. **2025**,
6. Walters, D. T.; **Costa, S**.; Aghakhanpour, R. B.; Olmstead, M. M.; Balch, A. L. Aurophilic Interactions in Luminescent, Box-like or Partial Helical Cations Formed from Bis(2-Diphenylphosphinoethyl)Phenylphosphine (Triphos) and Gold(I) Ions. *Polyhedron.* **2024**, *261*, 117140.
7. Walters, D.; Aristov, M.; Babadi Aghakhanpour, R.; SantaLucia, D.; **Costa, S**.; McNamara, L. E.; Olmstead, M.; Berry, J.; Balch, A. Self-Assembled Encapsulation of CuX_2^- (X = Br, Cl) in a Gold Phosphine Box-like Cavity with Metallophilic Au–Cu Interactions. *Inorg. Chem.* **2023,** *62* (11), 4467–4475.
8. Cena, N.; Peloquin, A. J.; Boatz, J. A.; **Costa, S.**; Gralinski, S. R.; Balch, A. L.; Ghiassi, K. B. Metal-Mediated Rearrangement of 1,2-Diphenylhydrazine to Ortho-Semidine upon Reaction with Dichlorotris(Triphenylphosphine)Ruthenium(Ii). *Chem. Commun.* **2022**, *58* (83), 11673–11676.

Contributions:

1. First author- SC performed all reactions, performed all characterization (FTIR, NMR, luminescence, etc.), collected all crystal data, refined preliminary crystal solutions, and made the figures + experimental section. SC edited the manuscript.
2. First author- SC performed all reactions, performed characterization of luminescence and lifetimes, completed Cifs of crystal solutions, and made the figures + experimental section. SC edited the manuscript.
3. First author- SC preformed all reactions, performed most characterization (FTIR, NMR, luminescence, etc.), collected most crystal data, refined preliminary crystal solutions, and made the figures + experimental section. SC wrote part of the manuscript and conducted edits.
4. First author- SC preformed all reactions, performed most characterization (FTIR, NMR, luminescence, etc.), collected all crystal data, refined preliminary crystal solutions, and made the figures + experimental section. SC wrote part of the manuscript and conducted edits.
5. Second author- SC analyzed crystals with SC- and PXRD, made TOC figures, gave insight on how to analyze products, and edited manuscript.
6. Second author- SC synthesized a main product, made figures and tables, and edited manuscript.
7. Fifth author- SC found new synthetic pathways and processed luminescence and lifetime data. Additionally, made figures, tables, and edits to manuscript.
8. Fourth author- SC found first crystal of a main complexes and ran PXRD. Conducted minor edits on manuscript.